Evaluating the role of groundwater to Yellowstone cutthroat trout in the upper Snake River Watershed, Wyoming

Jeffrey R. Baldock[1] and Annika Walters[2]

[1]Wyoming Cooperative Fish and Wildlife Research Unit, Department of Zoology and Physiology and Program in Ecology and Evolution, University of Wyoming, Laramie, WY; [2]United States Geological Survey, Wyoming Cooperative Fish and Wildlife Research Unit, Department of Zoology and Physiology and Program in Ecology and Evolution, University of Wyoming, Laramie, WY.

A report to fulfill conditions as stipulated by contractual agreements with the Jackson Hole One Fly Foundation (grant no. 2021-050), Wyoming Wildlife and Natural Resource Trust (award no. 03-21-023), and Grand Teton Association Boyd Evison Fellowship program.

June 2024
Laramie, Wyoming

WYOMING COOPERATIVE
FISH & WILDLIFE RESEARCH UNIT
UNIVERSITY OF WYOMING

ACKNOWLEDGEMENTS

The research presented in this report is a testament to the importance of broad coalitions of stakeholders for ensuring the success of science to support conservation and management needs for vulnerable species. Many more individuals than who are listed below contributed to this work in important ways. This research has benefited from countless streamside and parking lot conversations with conservation professionals, anglers and recreationists, landowners, and other members of the public. We are grateful to the Jackson community for their endless support.

We thank Quincy Harris, Nate Heili, Sasha Pereira, and Joe Reinhofer for aiding with fieldwork and data management. Diana Miller, Clark Johnson, Darren Rhea, Rob Gipson, and Mark Smith of the Wyoming Game and Fish Department provided expert advice regarding the initial study design and broader implications and helped to coordinate field assistance. Chad Whaley of the National Park Service helped to coordinate field assistance. Leslie Steen of Trout Unlimited, Simeon Caskey of the National Park Service, and Patrick Barry, Chance Roberts, Justin Peterson, and Kelly Owens of the US Forest Service provided insight on the broader implications of this research. We thank the Harrington, Morgan, Overlock, Petersen, Resor, and Ford families, Teton Science Schools, and Crescent H Ranch for allowing access to private properties. Benjamin Letcher (USGS), Yoichiro Kanno (CSU), and Mark Rains (USF) provided insight on the statistical analysis for Chapter 1; Eric Ward and Ole Shelton (NOAA) provided insight on the statistical analysis for Chapter 2. Katharine Coykendall and John Hargrove of the Eagle Fish Genetics Laboratory provided advice on the suitability of existing DNA sequencing methods for Chapter 2. Jesse McCane, Angie Chia, and Lynn Schrader of the Eagle Fish Genetics Laboratory provided logistical support and assisted with DNA extraction for Chapter 2. The Walters Lab at the University of Wyoming provided helpful comments on the development of this research as well as on the statistical analyses and interpretation of results.

We acknowledge that the University of Wyoming occupies the ancestral and traditional lands of the Cheyenne, Arapaho, Crow, and Shoshone Indigenous peoples along with other Native tribes who call the Great Basin and Rocky Mountain region home. We recognize, support, and advocate alongside Indigenous individuals and communities who live here now, and with those forcibly removed from their Homelands. We also acknowledge the historical and contemporary importance of fish and fisheries to Native peoples, particularly those who once resided within the Jackson Hole region. We hope our research builds upon the great wealth of knowledge that Native peoples hold regarding the function and management of ecosystems. (Adapted from ASUW Senate Bill #2699).

This work was funded by the Jackson Hole One Fly Foundation (grant no. 2021-050), Wyoming Wildlife and Natural Resource Trust (award no. 03-21-023), Grand Teton Association Boyd Evison Fellowship, University of Wyoming Biodiversity Institute, UW-NPS AMK Ranch Small Grants Program, University of Wyoming Department of Zoology and Physiology, and the Wyoming Anticipating Climate-Water Transitions (WyACT) project at the University of Wyoming (National Science Foundation award no. OIA-2149105). All animals were treated humanely, and the methods were approved by the University of Wyoming Institutional Animal Care and Use Committee protocol no. 20200507AW00423-01. Any use of trade, firm, or product names is for descriptive purposes only and does not imply endorsement by the U.S. Government.

TABLE OF CONTENTS

EXECUTIVE SUMMARY

Riverine ecosystems of the western United States are characterized by habitat conditions that limit fish growth and survival (e.g., extreme temperatures, flooding, drought, and ice formation). However, groundwater input buffers against seasonal fluctuations in water temperature and discharge, such that suitable fish habitat may persist year-round. How groundwater regulates the importance of different streams to fish populations at broad spatial scales has not been evaluated despite the critical role that groundwater-fed habitats are expected to play under future climate scenarios.

Both within the upper Snake River watershed (USRW) and across the Greater Yellowstone Area, Yellowstone cutthroat trout (*Oncorhynchus virginalis bouvieri*; YCT) are an integral component of aquatic and terrestrial food webs and support economically and culturally valuable recreational fisheries. Habitat degradation and hybridization and competition with non-native species has led to widespread declines and anticipated climate warming further threatens many extant populations. However, YCT in the USRW display successful natural reproduction, negligible genetic introgression by non-natives, and stable or increasing trends in population abundance. These features, in combination with high habitat connectivity and life-history diversity, make the USRW a high priority for YCT conservation efforts. Groundwater is a key component of the hydrologic budget in the USRW, and many groundwater-dominated streams are considered to be important YCT habitat. However, the role of groundwater to YCT has not been systematically evaluated, particularly within the context of the much larger river network, for which streamflow is overwhelmingly dominated by snowmelt.

Here, we report on findings from two studies that sought to understand the role of groundwater to YCT across the USRW. In Chapter 1, we combined machine learning and remote sensing techniques, mechanistic field studies, and Bayesian hierarchical models to describe how spatial variation in groundwater discharge to streams structures spatiotemporal variation in juvenile YCT growth and production. Our results demonstrate how groundwater, an important driver of aquatic ecosystem heterogeneity, structures key organismal and population-level processes for YCT across a riverscape. Chapter 1 has been submitted for consideration as a research article in *Ecological Monographs* with Jeffrey Baldock, Robert Al-Chokhachy, and Annika Walters as authors. In Chapter 2, we used genetic stock identification to understand the effect of tributaries on metapopulation structure for YCT occupying the mainstem Snake River. We found near complete reliance of the mainstem metapopulation on demographic support from tributaries, where distance between habitats, catchment area, and groundwater input acted in concert to determine tributary contribution to the mainstem metapopulation. We also found evidence for carry-over effects of tributaries on growth, where metapopulation size structure was a function of natal tributary characteristics and life stage. Chapter 2 is being prepared for submission to *Ecology Letters* with Jeffrey Baldock, William Rosenthal, Robert Al-Chokhachy, Matthew Campbell, Catherine Wagner, and Annika Walters as authors. In Chapter 3, we discuss how the results of our research can be used to guide the of conservation and management of YCT in the USRW. Specifically, our results can be used to prioritize the implementation of stream habitat protection and restoration projects at broad spatial scales. Our results also provide insight into how existing YCT population monitoring programs may be interpreted to understand the drivers of population change.

DATA AVAILABILITY STATEMENT

All data and code will be permanently archived on GitHub and made freely available for public use. At the time of writing (June 2024), data and code are undergoing quality assurance and quality control checks and have not yet been uploaded. GitHub repositories will be attached to Jeff Baldock's GitHub profile, which can be found here: https://github.com/j-baldock

CHAPTER 1

Groundwater structures fish growth and production across a riverscape

Jeffrey R. Baldock[1], Robert K. Al-Chokhachy[2], and Annika Walters[3]

[1]Wyoming Cooperative Fish and Wildlife Research Unit, Department of Zoology and Physiology and Program in Ecology and Evolution, University of Wyoming, Laramie, Wyoming, USA. [2]Northern Rocky Mountain Science Center, U.S. Geological Survey, Bozeman, Montana, USA. [3]U.S. Geological Survey, Wyoming Cooperative Fish and Wildlife Research Unit, Department of Zoology and Physiology and Program in Ecology and Evolution, University of Wyoming, Laramie, Wyoming, USA.

This chapter is in review at Ecological Monographs.

Abstract

Landscapes are composed of habitat patches and conditions that vary across space and time. While habitat variability and complexity can support important ecological processes and ecosystem services, the dynamic nature of habitats can also constrain organismal and population processes as optimal conditions are fleeting. In riverine ecosystems, groundwater discharge to streams stabilizes water temperature and flow regimes, thus mediating how habitat complexity is expressed across space and time. Yet, how stable habitats structure ecological processes within the broader landscape matrix is not well understood. In this study, we combine machine learning and remote sensing techniques, mechanistic field studies, and Bayesian hierarchical models to describe how spatial variation in groundwater discharge to streams structures spatiotemporal variation in growth and production for juvenile Yellowstone Cutthroat Trout (*Oncorhynchus virginalis bouvieri*) across the upper Snake River watershed, Wyoming, USA. We found that geologic and topographic variables explained spatial heterogeneity in groundwater influence in streams, which was linked to spatial variation in water temperature regimes and conspecific density. Temperature and density, in turn, interacted to influence growth rates: growth increased strongly with temperature, but this effect was reduced when density was high. Accordingly, variation in groundwater influence among stream reaches was associated with diversity in both growth and production regimes. At the riverscape scale, asynchrony in growth reduced spatial variation in growth capacity, but – when combined with density – led to the formation of distinct hotspots of biomass production. Our results demonstrate how groundwater, an important driver of aquatic ecosystem heterogeneity, structures key organismal and population-level processes for fish across space and time. Importantly, rare, but stable groundwater-fed habitats disproportionately affect ecological processes and serve as important sources of population diversity across large river networks. The distribution of groundwater and links to fish growth and production can be used to identify and prioritize protection and conservation of critical recruitment habitat. Our study demonstrates how patterns at broad spatial extents arise from processes acting at fine spatial and temporal resolutions, highlighting the importance of integrated approaches to both ecological research and conservation planning, particularly under climate change.

Introduction

Spatial and temporal variation in habitat conditions across landscapes (e.g., Stanford et al. 2005) can promote species, food web, genetic, and life-history diversity that stabilize ecological processes and ecosystem services (Oliver et al. 2010, Schindler et al. 2010, 2015, Scholl et al. 2023). But habitat variability can also impose constraints on organisms as optimal conditions and resources are fleeting (Davidson and Andrewartha 1948, MacArthur 1958). Therefore, landscape features that create patches of stability may constitute hotspots of biological activity as environmental constraints on organisms are relaxed (Scholl et al. 2023). While stable habitats are often rare relative to other habitat types, they may be disproportionately important to ecological processes at broader spatial and temporal scales given their resistance to change (e.g., climate refugia; *sensu* Keppel et al. 2012). The role of stable habitats represents a critical knowledge gap in our understanding of landscape complexity and heterogeneity.

In riverine ecosystems, spatiotemporal variation in water temperature and flow result from complex interactions among the physical and biological habitat template, prevailing climate, and water source (e.g., rain, snow, or groundwater; Brown 1969, Poff et al. 1997, Webb et al. 2008). Critically, groundwater discharge to streams stabilizes water temperature and flow regimes: attenuating high flows, increasing water availability during dry periods, and buffering against high temperatures during summer and low temperatures overwinter (Ward 1985, Poff et al. 1997, Constantz 1998, Caissie 2006). However, the location of groundwater discharge to streams is unevenly distributed across stream networks (Winter 2001, Dugdale et al. 2015), resulting in discontinuities in water temperature, flow, and biological activity (Fullerton et al. 2015, Briggs and Hare 2018). Therefore, groundwater mediates how habitat heterogeneity is expressed across space and time by creating patches of stability nested within otherwise dynamic riverscapes.

Variation in habitat conditions associated with groundwater has implications for the growth and production of riverine taxa, such as salmonid fishes. Understanding how growth is expressed across riverscapes is important as body size is associated with life-history expression (Hutchings 1993), competitive ability (Cutts et al. 1999), fecundity (Meyer et al. 2003), survival (Quinn and Peterson 1996), and dispersal (Comte and Olden 2018). Growth is driven by density-independent factors such as water temperature (Brett 1971, Elliott 1976) and density dependence, which modifies the effect of density-independent factors by affecting competition for limited trophic resources (Imre et al. 2005, Myrvold and Kennedy 2015). Growth ultimately sums across individuals within a patch to determine production (O'Gorman et al. 2016, Kaylor et al. 2021). Highly productive patches subsidize connected habitats through density-dependent dispersal (Tsuboi et al. 2022), which can stabilize total recruitment via portfolio effects and allow for demographic rescue (Hanski 1998, Harrison et al. 2020). Previous work indicates that the effects of groundwater on salmonid growth may be highly context dependent (Mejia et al. 2016, Gallagher and Fraser 2023). However, our understanding of how density dependence moderates the importance of groundwater is limited, particularly when considering growth and production across large spatial extents.

The drivers of fish growth and production are often explored at relatively fine spatial resolutions (O'Gorman et al. 2016, Letcher et al. 2022), but these efforts are difficult to apply over the spatial extents at which fish complete their life-history and populations interact (i.e., across

riverscapes; Fausch et al. 2002). While researchers have begun to consider how these processes vary at broad spatial extents (Falke et al. 2019, Armstrong et al. 2021), this often comes at a cost to spatial and/or temporal resolution. Kaylor et al. (2021) demonstrated how site-specific studies can be used to understand seasonality in riverscape patterns by generating season-specific predictions of growth and production from spatially continuous habitat data. But the drivers of growth may also change within seasons (Rossi et al. 2022). For example, groundwater regulates habitat conditions at very fine spatial and temporal resolutions (Roy et al. 2011) and may affect when and where individuals accrue growth and how productivity is distributed across riverscapes (*sensu* Brennan et al. 2019), but this is not well understood.

Understanding patterns of growth and production at fine spatial and temporal resolutions is particularly important for early life stages (i.e., young-of-year, YOY), which have limited swimming ability and are highly susceptible to local environmental conditions (Einum et al. 2006). Growth conditions early in life have also been shown to strongly influence lifetime body size trajectories (Vincenzi et al. 2008), which can ultimately determine key life-history characteristics such as age-at-maturity and lifetime reproductive success (Hutchings 1993, Vincenzi et al. 2010). Therefore, the effect of groundwater on YOY growth and production at fine spatial and temporal resolutions and across broad spatial extents may underlie the generation and maintenance of life-history diversity across riverscapes. Life-history diversity associated with YOY growth and production may promote population stability in the face of environmental stochasticity and may play an important role in maximizing adaptive capacity in the face of climate change (Bellmore et al. 2022, Campana et al. 2023).

How groundwater structures YOY growth and production across riverscapes is critically important given global climate change. Groundwater-fed stream ecosystems are expected to be more resistant to climate warming as groundwater input buffers against physiologically stressful water temperatures and hydrologic variability that can limit YOY recruitment (Power et al. 1999, Burns et al. 2017, Sweka and Wagner 2022). Groundwater-fed habitats are thus expected to serve as refugia for salmonids under future climate scenarios (Larsen and Woelfle-Erskine 2018, Sullivan et al. 2021). Accordingly, calls for identification and protection of groundwater-based climate refugia (Cartwright et al. 2020, Casas-Mulet et al. 2020) require data products that map groundwater influence at spatial scales relevant to habitat and fisheries management: fine resolutions and broad extents (i.e., riverscapes; Fausch et al. 2002, Mejia et al. 2023). Remote sensing and associated techniques provide a robust approach to generate such data products (*sensu* Carbonneau et al. 2012). Gerlach et al. (2022) illustrated how remote sensing and machine learning can be used to locate groundwater discharge to streams across riverscapes. Integrating this information with an understanding of how groundwater affects fish growth and production will aid fisheries management and conservation under global climate change.

In this study, we assessed the drivers of growth and production for YOY (i.e., age-0) Yellowstone cutthroat trout (*Oncorhynchus virginalis bouvieri*) among streams spanning a gradient of groundwater influence and describe how spatial variation in groundwater yields distinct growth and production regimes across a riverscape. Specifically, we (1) generated spatially continuous indices of groundwater influence across a river network, (2) explored how groundwater mediates temporal variation in water temperature and conspecific density, (3) quantified the effects temperature and density on YOY growth, (4) quantified the temporal

dynamics of growth and production as mediated by groundwater, and (5) generated spatially and temporally continuous projections of growth and production across the riverscape and throughout the early life period. Our results provide insight into the mechanisms underlying variation in fish growth and production, highlight how groundwater generates diversity in growth and production regimes among habitats, and can be used to identify priority areas for habitat restoration and protection. Ultimately, our study demonstrates the importance of habitat diversity and stability as climate change threatens to destabilize ecosystems.

Methods

Study System and Species

We conducted our study within the upper Snake River watershed (USRW) in northwest Wyoming, USA, an 8943 km^2 region situated between 1708 and 4194 meters elevation (Figure 1). The USRW comprises the core of the Greater Yellowstone Area and is characteristic of many other gravel-bed river systems (Ward et al. 1999, Hauer et al. 2016). Precipitation in the USRW falls primarily as snow (Hostetler et al. 2021). Spring snowmelt results in widespread flooding in streams and rivers, typical of snowmelt-dominated hydrographs of the Rocky Mountain region. A portion of that snowmelt also percolates into surface sediments, recharging the Snake River alluvial aquifer (Nolan and Miller 1995). The USRW has undergone two major Pleistocene glaciations, each of which deposited considerable amounts of glacial outwash in what is now known as Jackson Hole (Pierce et al. 2018). The unconsolidated alluvial and colluvial deposits that fill Jackson Hole and surrounding valleys collectively constitute a large, unconfined alluvial aquifer (Wright 2013). Glacial deposits thin towards their southern (i.e., downstream) extent (Nolan et al. 1998), which likely drives upwelling from the aquifer, forming dense drainage networks in which groundwater appears to comprise the majority of streamflow.

Both within the USRW and across the Greater Yellowstone Area, Yellowstone cutthroat trout (YCT) are an integral component of aquatic and terrestrial food webs (Koel et al. 2019) and support economically and culturally valuable recreational fisheries. Habitat degradation and hybridization and competition with non-native species has led to widespread declines (Gresswell 2011) and anticipated climate warming further threatens extant populations (Wenger et al. 2011). However, YCT in the USRW display successful natural reproduction (Baldock et al. 2023), negligible genetic introgression by non-natives (Kovach et al. 2018), and stable or increasing trends in abundance (Wyoming Game and Fish Department 2019). These features, in combination with high habitat connectivity and life-history diversity, make the USRW a high priority for YCT conservation efforts (Al-Chokhachy et al. 2018). Spawning typically occurs over a 10-week period between May and July with YOY emerging from redds (i.e., nests constructed in gravel substrate) between late July and early September (Kiefling 1997, Baldock et al. 2023).

Approach

We used a multi-faceted approach to explore the degree to which groundwater structures spatiotemporal patterns of YOY growth and production across the USRW. First, we combined

field observations with machine learning techniques and remote sensing data to understand spatial variation in groundwater discharge to streams throughout the USRW. Second, we evaluated the effect of groundwater on water temperature regimes in 32 streams and YOY density estimates from 13 focal streams to understand how groundwater affects growing conditions. Third, between August and November of 2021 and 2022, we monitored changes in YOY body size in the same 13 focal streams to quantify the effects of temperature and density on growth. Fourth, we used statistical models fit to empirical data to evaluate the ultimate role of groundwater in shaping trends in YOY growth and production. Fifth, and finally, we projected growth and production at a daily time step across the entire stream network to understand how spatial variation in groundwater activity generates spatiotemporal variation in growth and production at the riverscape scale.

Stream Network Delineation

To model groundwater influence in streams and subsequently project growth and production continuously across the riverscape, we required a stream network spatial object that accurately represented flowlines in the USRW, particularly in areas where groundwater upwelling creates dense drainage networks. We used the WhiteboxTools library implemented in R (Lindsay 2016, Wu and Brown 2022) to delineate a stream network from a 1/3 arc-second (*ca.* 10 m) bare-earth digital elevation model (DEM; accessed 15 November 2023, https://apps.nationalmap.gov/downloader/). We used a threshold flow accumulation value of 25,000 cells (2.5 km^2) as this yielded a network in which headwater flowlines typically initiated at the onset of surface flow, as determined from visual analysis of satellite imagery (Google Earth Pro 7.3.6. 2023). This approach, however, tended to omit flowlines for streams originating from high-volume groundwater springs and seeps, as catchments for groundwater-fed streams are often very small and poorly defined (Whiting and Moog 2001). To account for this, we used our knowledge of the study area, discussions with local experts, and extensive visual inspection of satellite imagery to locate streams that were not mapped using the automated process but are otherwise high-volume and likely or known to be fish-bearing. We delineated flowlines for these streams by hand and merged these features to the stream network using ArcMap ver. 10.8 (ESRI, Redlands, CA). This approach proved necessary to generate a stream network that accurately represents the complex hydrology of groundwater-dominated riverscapes.

Modeling Groundwater Influence in Streams

Field observations suggested that the location of groundwater discharge to streams (i.e., springs) could be predicted based on geology and topography alone (Pourtaghi and Pourghasemi 2014, Leach et al. 2017). We therefore used MaxEnt version 3.4.4 (Phillips and Dudík 2008, Elith et al. 2011; https://biodiversityinformatics.amnh.org/open_source/maxent/, accessed on 17 July 2023), a presence-only machine learning technique, to predict the prevalence of springs throughout the USRW (Gerlach et al. 2022). Between 2019 and 2023, we opportunistically collected 105 GPS locations of springs. We identified springs as either (1) areas where water actively upwelled from surface substratum within riparian and floodplain areas or (2) locations where water flowed laterally out of a hillside, typically at valley-bottom toeslopes (floodplain and upland hillslope springs, respectively, *sensu* Stevens et al. 2021). We combined field observations with 77 additional locations downloaded from the Groundwater Atlas of Wyoming

(https://portal.wsgs.wyo.gov/arcgis/apps/webappviewer/index.html?id=181c32a872a346bfae3579a62230a65a, accessed on 15 July 2023), filtered to remove hot springs as geothermal activity likely exerts different controls on stream ecosystems than "cold" groundwater inputs that were the focus of this study. Spring locations downloaded from the Groundwater Atlas of Wyoming were previously digitized from U.S. Geological Survey 1:100,000 scale topographic maps covering the state of Wyoming.

Following Gerlach et al. (2022), we modeled the prevalence of groundwater springs across the USRW using the 182 spring locations as presence points and 11 geologic and topographic layers as predictors. Geologic layers included bedrock and surficial geology (Love and Christiansen 1985), which are known to control both deep and shallow groundwater storage capacity (Tague et al. 2007, O'Sullivan et al. 2020, Dralle et al. 2023), and distance to geologic lineaments (i.e., bedrock fractures), which are known to affect groundwater flow paths (Mallast et al. 2011). Underlying geology interacts with topographic features to determine locations of groundwater discharge to streams. We used the DEM to extract elevation, slope, profile curvature, profile curvature range, planform curvature, planform curvature range, and terrain ruggedness index for the USRW (Gerlach et al. 2022). Steep slopes may represent steep hydraulic gradients driving shallow groundwater flow (Haitjema and Mitchell-Bruker 2005). Profile curvature measures surface curvature parallel to the slope, while planform curvature measures surface curvature perpendicular to the slope. We calculated the range of profile and planform curvature and terrain ruggedness index within a 3 x 3 cell (*ca.* 30 x 30 m) window to measure variation in curvature over short distances and topographic heterogeneity, respectively. Curvature, curvature range, and terrain ruggedness index may indicate slope failures induced by groundwater discharge (Reid and Iverson 1992), stream headwaters formed by groundwater discharge (Jaeger et al. 2007), and abrupt changes in slope where the water table may be close to the ground surface (Winter 2001, Detty and McGuire 2010). We used the curvature and tri functions in the R package spatialEco (Evans and Murphy 2023) to calculate curvature and terrain ruggedness and the focal function in the R package terra (Hijmans 2023) to calculate curvature range. Finally, we calculated distance to flowlines using the gDistance function in the R package rgeos (Bivand and Rundel 2023). Flowlines represent areas where the water table is near or above the ground surface (Winter 1999) and the upstream extent of flowlines is associated with stream headwaters formed by groundwater discharge (Jaeger et al. 2007). Geologic layers and the DEM used to prepare topographic layers were accessed from the Wyoming Geospatial Hub on 17 July 2023 (https://data.geospatialhub.org/).

We modeled the prevalence of groundwater springs using a logistic model with the default parameters, except for a default prevalence value of 0.1, as we expected springs to be uncommon at the landscape scale. Of the 182 spring locations, 70% (n = 128) were used for model training and 30% (n = 54) were used for model testing. We did not test for or exclude predictor variables that were correlated as our primary goal was to build a model with high predictive accuracy, rather than to make inference on the effect of any single variable. We assessed model performance by calculating the area under the receiver operating curve (AUC): the probability that a randomly chosen presence point will be ranked above a randomly chosen background location (Phillips and Dudík 2008).

While accounting for spatial bias in search effort can help increase the accuracy of MaxEnt modeling (Kramer-Schadt et al. 2013), we did not consider this necessary for three reasons. First, fieldwork over five years brought us to most areas within the USRW and we therefore did not think search effort was systematically biased towards certain locations. Second, combining field observations with the Groundwater Atlas of Wyoming increased our sample size of spring locations in high elevation, headwater areas that were difficult to access on foot. Third, the model output describing spring prevalence aligned well with our *a priori* understanding of groundwater activity in the region (see *Study System and Species*). Therefore, we considered the spatial clustering of spring locations to be a real pattern (*sensu* Winter 2001), rather than an artifact of unequal search effort.

From the MaxEnt model output (a raster of spring prevalence, where the value for each *ca.* 10 x 10 m cell represents the probability of the cell containing a groundwater spring), we derived a metric describing groundwater influence on stream conditions. We buffered (100 m radius) the prevalence raster to the stream network as we assumed only groundwater discharging from springs adjacent to flowlines exert influence on stream conditions, such as temperature. We then used WhiteboxTools to delineate catchments for 13,083 locations spaced every 300 m (the distance between study reaches) across the stream network (hereafter, network locations), 32 stream temperature monitoring locations, and 52 study reaches (the downstream extent of four reaches within each of the 13 focal streams). Deriving a metric of groundwater influence across the entire stream network was necessary to allow for projections of growth and production at this scale. We restricted network locations to those with catchments <500 km^2 as we assumed groundwater effects on ecosystem processes likely differ between large rivers and smaller tributary streams that were the focus of our study. For each watershed corresponding to either a network, temperature, or study location, we calculated a distance-weighted mean prevalence from the buffered spring prevalence raster. Our weighting scheme used inverse exponential weights with an *e*-folding distance (the distance at which the weight is 1/*e*) of 5 km (Isaak et al. 2010). This approach assumes that springs located immediately upstream of a given point exert the greatest influence on local stream conditions, while springs located further upstream are exponentially less likely to affect conditions at the location of interest. To aid interpretation, we normalized the metric of groundwater influence to 0-1 based on the minimum and maximum values calculated for the 13,083 network locations. We used the normalized, distance-weighted mean spring prevalence within the contributing catchment to describe relative groundwater influence at each network, temperature, or study location (hereafter, groundwater index or GWI).

Association Between Groundwater and Temperature

We used Hobo temperature sensors (Onset Corp.) to monitor stream temperature because groundwater inflow is known to affect temperature regimes (Caissie 2006) and temperature is a proximate driver of growth rates in fish (Brett 1971, Letcher et al. 2022). We placed temperature sensors within PVC housing to limit the effects of solar radiation on sensor readings and attached these to pieces of rebar anchored to the stream bed to ensure sensors would not be lost during high flow events (Heck et al. 2018). Within streams selected for fish sampling, we deployed two sensors (at the downstream and upstream extents of fish sampling, thus spanning 1.05 stream kms) to account for longitudinal lapse in stream temperature. Inspection of time series data indicated little to no difference in stream temperature at this scale. We therefore used data from

the downstream site to characterize thermal conditions within each of the four sections, for each focal stream, summarized as daily means. Stream temperature monitoring within the 13 focal streams supplemented longer-term monitoring efforts at an additional 19 sites. None of the 32 stream temperature monitoring locations had overlapping catchments (i.e., data were entirely non-nested).

We used a hierarchical stream temperature model (*sensu* Letcher et al. 2016) to assess the influence of basin characteristics, including GWI, on temperature sensitivity: stream temperature response to modeled mean daily air temperature (Daymet; Thornton et al. 2021). Note that we use the prime symbol $'$ to distinguish similar parameters in different models. We modeled daily mean stream water temperature $T^W_{s,d,y}$ (°C) at site s, on day d, and in year y, as a normally distributed random variable $\mu_{s,d,y}$ with standard deviation σ:

$$T^W_{s,d,y} \sim N(\mu'_{s,d,y}, \sigma') \quad (1)$$

$$\mu'_{s,d,y} = \boldsymbol{\alpha'_s} + \beta'_1 Y_y + \boldsymbol{\beta'_{2,s}} T^A_{s,d,y} \quad (2)$$

Where, $\boldsymbol{\alpha'_s}$ is a vector of site-specific intercepts, β'_1 is the year effect and Y_y is a binary variable denoting year (*0* for 2021 and *1* or 2022), and $\boldsymbol{\beta'_{2,s}}$ is a vector of slopes describing site-level sensitivity to air temperature $T^A_{s,d,y}$. Site-level temperature sensitivity $\boldsymbol{\beta'_{2,s}}$ was then modeled as a normally distributed random variable ν_s with standard deviation ω:

$$\boldsymbol{\beta'_{2,s}} \sim N(\nu_s, \omega) \quad (3)$$

$$\nu_s = \varphi + \Sigma \boldsymbol{\gamma} \boldsymbol{X'_s} \quad (4)$$

Where, φ is an intercept, $\boldsymbol{\gamma}$ is a vector of coefficients, and $\boldsymbol{X'_s}$ is a matrix of centered and scaled basin characteristics. We fit a single model to describe the effects of basin characteristics on temperature sensitivity. Covariates included GWI, mean basin slope, basin area (logged), lake area (logged), percent riparian forest cover, and two-way interactions between groundwater index and each of the four other basin characteristics (Appendix S1: Table S1; Lisi et al. 2015, Beaufort et al. 2020). Basin slope and area were calculated from the DEM. Lake area was calculated by intersecting site-specific catchments with a polygon layer of lentic waterbodies (accessed from the Wyoming Geospatial Hub on 17 July 2023). Percent riparian forest cover was calculated by first buffering the LANDFIRE Percent Canopy Cover dataset (accessed on 15 Dec 2023 via the rlandfire package in R; Buckner 2023) to the stream network (100 m buffer radius) and then calculating the mean canopy cover value for each catchment. We restricted analyses to our study period (1 August – 5 November) as this was the temporal scale of interest for YOY growth and given hysteresis and non-linearities in stream-air temperature relationships during other times of year (Mohseni et al. 1998). Because our goal was to assess the effect of basin characteristics on temperature sensitivity rather than predict stream temperature itself, we considered a highly parameterized model unnecessary (e.g., one accounting for spatial and temporal autocorrelation; *sensu* Letcher et al. 2016).

Fish Sampling and Association Between Groundwater and Fish Density

Our investigation of the effect of groundwater on YOY growth and production was based on data collected from 13 focal streams, which we selected to span a gradient of GWI, inferred *a priori* based on the presence of groundwater springs and stream channel geomorphology. Within each focal stream, we conducted fish sampling across four 150 m reaches, each separated by 150 m, to capture local variation in GWI, water temperature, and fish density (n = 52 study reaches). We placed sampling reaches within stream sections in which we found both redds and newly emerged YOY during stream surveys conducted in previous years. Through field observations and discussions with local biologists, we considered the selected study reaches to be representative of the spawning and YOY rearing habitat within each focal stream.

We used single-pass backpack electrofishing (pulsed DC current) to monitor the density and body size distribution of YOY within each reach. We sampled fish once every three weeks, on average, for a total of five sampling events per reach per year. Electrofishing of this frequency has no known effects on salmonid growth (Clancy et al. 2022). Single-pass electrofishing has been shown to as effective as multi-pass sampling for monitoring spatial and temporal patterns of fish density (Bateman et al. 2005, Hanks et al. 2018). Given our protocol, we were able to sample two streams (8 reaches) per day; thus, we typically sampled all 13 focal streams within one week. We enumerated, measured (total body length), and then released all captured fish unharmed back into the middle of each reach.

We summarized YOY density per sampling event as the number of fish captured per meter of stream. This measure was found to be highly correlated and linearly related (on log-log scales) to other metrics of density, such as catch-per-unit-effort (number captured per minute of sampling, Pearson's r = 0.97) and effective density (sum of squared body lengths, *sensu* Post et al. 1999; Pearson's r = 0.91), but was more interpretable and explained more of the variation in growth rates than these other metrics (in this study and others; *e.g.,* Imre et al. 2005). Preliminary data exploration suggested a non-linear relationship between GWI and YOY density that was poorly described by polynomial regression. Accordingly, and because quantifying the groundwater-density relationship was not a primary goal of this study, we used locally estimated scatterplot smoothing (LOESS) to explore the relationship between GWI and peak YOY densities (logged to account for heteroscedasticity). We used annual maximum density per reach to avoid pseudo-replication (multiple sampling events per reach).

We used changes in mean body size and density to calculate YOY growth and production between each pair of consecutive sampling events (Kaylor et al. 2021). As YOY captured during our study were smaller than the recommended minimum size for tagging (69 mm; Vollset et al. 2020), we had to assume that the individuals sampled within each reach were similar among sampling events. This is reasonable given that the distance between reaches (300 m) approximated median YOY dispersal distance (Einum et al. 2011, Eisenhauer et al. 2021). Kaylor et al. (2021) found a strong positive relationship between growth rates calculated from changes in mean body size (as we do in this study) and growth rates assessed from individually tagged juvenile salmonids, supporting the assumption above and our approach generally.

Modeling the Drivers of Growth

We used a Bayesian hierarchical model within a model-selection framework to understand the effects of temperature and density on growth. Following Letcher et al. (2022), we modeled observed mean body size $L_{t,y,s,r}$ (total length in mm) at sampling event *t*, in year *y*, stream *s*, and reach *r*, as a normally distributed random variable $\mu''_{t,y,s,r}$, which itself was defined as the previously observed mean length $L_{t-1,y,s,r}$ plus the daily growth rate $\delta''_{t,y,s,r}$ (mm day^{-1}) multiplied by the number of days between sampling events $T_{t,y,s,r}$:

$$L_{t,y,s,r} \sim N\left(\mu''_{t,y,s,r}, \sigma''_{t,y,s,r} * T_{t,y,s,r}\right) \quad (5)$$

$$\mu''_{t,y,s,r} = L_{t-1,y,s,r} + \delta''_{t,y,s,r} * T_{t,y,s,r} \quad (6)$$

Where, $\sigma''_{t,y,s,r}$ is the standard deviation of estimated length, which we multiplied by $T_{t,y,s,r}$ to account for unequal intervals among sampling events. We modeled the standard deviation of estimated length $\sigma''_{t,y,s,r}$ as a linear function of GWI $G_{s,r}$ to evaluate the effect of groundwater on variation in the response of body size to density-dependent and density-independent variables:

$$\ln(\sigma''_{t,y,s,r}) = \rho'' + \theta'' G_{s,r} \quad (7)$$

Where, ρ'' is an intercept and θ'' is the coefficient for $G_{s,r}$. We modeled daily growth rate as a function of covariates and random effects:

$$\delta''_{t,y,s,r} = \alpha'' + \alpha''_y + \alpha''_s + \alpha''_{s_r} + \Sigma \boldsymbol{\beta}'' \boldsymbol{X}''_{\boldsymbol{t,y,s,r}} \quad (8)$$

Where, α'' is the global intercept, α''_y is the year-specific offset to α'', α''_s is the stream-specific offset to α'', α''_{s_r} is the reach-specific offset to α'', $\boldsymbol{\beta}''$ is a vector of coefficients, and $\boldsymbol{X}''_{\boldsymbol{t,y,s,r}}$ is a matrix of centered and scaled covariate data. The parameters α''_y and α''_s were drawn from normal distributions with a mean of 0 (i.e., crossed random effects), whereas α''_{s_r} was drawn from a normal distribution with a mean of α''_s as specific reaches were nested within streams (i.e., nested random effects). Candidate models (Appendix S1: Table S2) included both individual and interactive effects of temperature (mean temperature between sampling events, °C) and density (density at the time of sampling, fish per meter, logged given the log-linear relationship between growth and density; Imre et al. 2005). We included a squared temperature term to allow for non-linearities in the growth-temperature relationship (Brett 1971). All candidate models included prior mean total length ($L_{t-1,y,s,r}$) as a covariate to account for metabolic scaling (Elliott 1976). Although we were primarily interested in growth rates (e.g., specific growth), we did not model growth rate directly as prior length would then appear on both sides of the equation and this is known to induce spurious correlations between response and predictor variables (Kenney 1982, *sensu* Kanno et al. 2022). Prior to model fitting, we removed all sampling events during which we caught <5 individuals to avoid misrepresenting mean body size. A sensitivity analysis indicated that removing sampling events during which we caught <10 and <15 individuals produced similar results.

Modeling Temporal Trends in Growth and Production

Given the hypothesized role of groundwater in structuring spatiotemporal patterns of temperature and density and the associated effects of temperature and density on growth, we considered it reasonable that spatial variation in the temporal dynamics of growth could be explained by groundwater alone. We therefore used a model like that described above (eqs. 5-8) to understand how groundwater mediates temporal trends in growth (Bacon et al. 2005):

$$L_{t,y,s,r} \sim N\left(\mu'''_{t,y,s,r}, \sigma'''_{t,y,s,r} * T_{t,y,s,r}\right) \quad (9)$$

$$\mu'''_{t,y,s,r} = L_{t-1,y,s,r} + \delta'''_{t,y,s,r} * T_{t,y,s,r} \quad (10)$$

$$\ln(\sigma'''_{t,y,s,r}) = \rho''' + \theta''' G_{s,r} \quad (11)$$

$$\delta'''_{t,y,s,r} = \alpha''' + \alpha'''_{y} + \alpha'''_{s} + \alpha'''_{s_r} + \beta'''_1 J_{t,y,s,r} + \beta'''_2 J^2_{t,y,s,r} + \beta'''_3 G_{s,r} + \beta'''_4 J_{t,y,s,r} G_{s,r} + \beta'''_5 J^2_{t,y,s,r} G_{s,r} \quad (12)$$

Where, $J_{t,y,s,r}$ is the Julian date (numeric day of year) of sampling, and all other terms are defined as above. The $J_{t,y,s,r}$ and $J^2_{t,y,s,r}$ terms allow for linear and non-linear trends in growth rates (Bacon et al. 2005), respectively, while interactions with $G_{s,r}$ allow trends to vary according to GWI. We did not include higher order $J_{t,y,s,r}$ terms as we did not expect growth rates to peak more than once during the study period (Rossi et al. 2022). We did not include prior body size ($L_{t-1,y,s,r}$) in this model (compare to eq. 8) as day of year and prior body size were strongly correlated (Pearson's r = 0.81). We therefore assumed that metabolic scaling would be accounted for by including day of year, the primary variable of interest. This assumption was supported by preliminary analysis which revealed that body size trajectories (see below) derived from models with and without prior body size were virtually identical. Ultimately, day of year is a surrogate for a suite of unmeasured covariates (e.g., temperature, discharge, and food availability in addition to prior body size; *sensu* Bacon et al. 2005) and interactions between day of year and GWI represent how groundwater mediates seasonality in growing conditions.

We used the fitted model to understand the effect of GWI on growth capacity: total growth accrued between emergence and the onset of winter (i.e., end of season body size; Sloat et al. 2005). Because emergence timing differed among streams and final sampling events were conducted over a 10-day period across all streams, we could not simply regress observed end of season body size against GWI. Instead, we used the fitted model to project mean body size over the course of the study period (*sensu* Letcher et al. 2022), starting from a common date (20 August, the earliest measured growth rate) and initial size (35 mm, the mean body size in late August). From these starting conditions, we calculated body size at daily time-steps through 5 November (the final sampling date across all sampling events). We generated body size trajectories for 100 values of GWI ranging from 0 to 1.

While modeling average body size provides insight into the constraints on and dynamics of individual growth, it does not provide information on total biomass production. We therefore used a similar approach to understand the role of groundwater in structuring spatiotemporal patterns of production (Kaylor et al. 2021). We estimated production between each consecutive pair of sampling events using the increment summation method (Hayes et al. 2007) and divided

by the number of days between sampling events (T_{tysr}) to yield daily productivity rate (P_{tysr}; mm m^{-1} day^{-1}):

$$P_{t,y,s,r} = \frac{(L_{t,y,s,r} - L_{t-1,y,s,r}) * D_{t,y,s,r}}{T_{t,y,s,r}} \quad (13)$$

Where, $D_{t,y,s,r}$ is YOY density (fish m^{-1}) during sampling event *t* in year *y*, stream *s*, and reach *r*; and all other variables are defined as above. We acknowledge that length-based estimates of production are less common than estimates based on mass; however, given well-established power relationships between length and mass for fish (Pope and Kruse 2007), we posit that length-based production can be interpreted similarly. We modeled $P_{t,y,s,r}$ as a log-normally distributed random variable (to satisfy assumptions of homoscedasticity):

$$\ln(P_{t,y,s,r}) \sim N\left(\mu'''_{t,y,s,r}, \sigma'''_{t,y,s,r} * T_{t,y,s,r}\right) \quad (14)$$

$$\ln(\sigma'''_{t,y,s,r}) = \rho'''' + \theta'''' G_{s,r} \quad (15)$$

$$\mu'''_{t,y,s,r} = \alpha'''' + \alpha''''_{y} + \alpha''''_{s} + \alpha''''_{s_r} + +\beta''''_1 J_{t,y,s,r} + \beta''''_2 J^2_{t,y,s,r} + \beta''''_3 G_{s,r} + \beta''''_4 J_{t,y,s,r} G_{s,r} + \beta''''_5 J^2_{t,y,s,r} G_{s,r} \quad (16)$$

Prior to model fitting, we removed four outliers ($P_{t,y,s,r}$ < -0.013) as these data points violated multiple assumptions of linear regression (removing outliers had no effect on the model output). As with body size, we used the fitted model to understand the effect of groundwater on biomass accrual through time. Beginning on 20 August, we projected daily production (*P*, mm m^{-1} day^{-1}) on a daily time-strep through 5 November and then calculated cumulative production (mm m^{-1}) for each day by summing *P* across all prior days. We generated time series of cumulative production for 100 values of GWI ranging from 0 to 1. This approach allowed us to reconcile similarities in growth capacity among streams despite differences in density (see Results).

Riverscape Patterns of Growth and Production

To understand how groundwater structures spatiotemporal patterns of growth and production across the riverscape, we mapped projected body size and cumulative production to the entire stream network based on network wide GWI. Riverscape projections provide insight into how the relative importance of reaches changes through time as groundwater affects the timing and pace of growth and production. This allowed us to identify stream reaches that likely make disproportionate contributions to growth and production and explore how "hotspots" growth and production shift across space and time. We restricted projections to stream reaches with gradients <10% given known geomorphic limitations on YCT distribution (Kruse et al. 1997). We present network-scale projections of growth capacity and cumulative production for three points in time spanning the range of the early rearing period: 1 September, 1 October, and 1 November.

Model Fitting, Selection, and Evaluation

All models were analyzed in a Bayesian framework in the Just Another Gibbs Sampler MCMC sampling environment (JAGS; Plummer 2003), implemented through R (R Core Team 2023) using the R2jags (Su and Yajima 2021), tidyverse (Wickham et al. 2019), HDInterval

(Meredith and Kruschke 2022), and MCMCvis (Youngflesh 2018) packages. We ran models with three MCMC chains, each with 50,000 burn-in and 150,000 evaluation iterations. Chains were thinned to retain every 20th iteration. We assessed model convergence based on large effective sample sizes, Gelman-Rubin diagnostic values (R-hat) <1.01, and visual inspection of MCMC trace plots and posterior probability distributions (Gelman and Hill 2007). JAGS models were run with parameter and/or hyperparameter prior probability distributions specified in Appendix S1: Table S3. For our analysis of the drivers of growth rates, we compared candidate models using leave-one-out cross-validation (LOO-CV), in which the model with the greatest support is that with the lowest expected log pointwise predictive density (elpdloo; Vehtari et al. 2017). We considered the results of candidate models with similar support (i.e., the standard error of the elpdloo difference was greater than the difference itself); however, for simplicity, we only present graphical results from the single top model.

We used multiple diagnostic tools to evaluate the performance of our final set of Bayesian models. To evaluate goodness of fit, we plotted observed data against predicted data generated during parameter estimation, inspected these plots to ensure linearity, and then used this data to estimate Bayesian p-values (Gelman 2003, Letcher et al. 2022). Bayesian p-values represent the proportion of predicted data that is greater than observed data; where values near 0.5 indicate lack of bias and values approaching 0 or 1 indicate poor model performance. We also derived model residuals, which we inspected to ensure normality around 0, and calculated root mean square error (RMSE) as an index of error in model estimates. Finally, we calculated conditional and marginal Bayesian R^2 values (medians and 95% credible intervals) to evaluate the proportion of variation in observed data explained by the fixed and random effects versus the fixed effects alone, respectively (Nakagawa and Schielzeth 2013, Gelman et al. 2019).

Results

Modeled Groundwater Influence Across the Upper Snake River Watershed

The MaxEnt model describing groundwater spring prevalence performed remarkably well: model AUC values were 0.93 for training data and 0.93 for testing data, signifying exceptional model performance (Gerlach et al. 2022). Distance to flowlines and bedrock geology contributed the most information to the model (permutation importance = 36.8% and 35.3%, respectively). Profile curvature range, surficial geology, elevation, and distance to geologic lineaments contributed modest amounts of information to the model (permutation importance = 11%, 6.6%, 5.4%, and 3.5%, respectively), with all other variables contributing little to no information (permutation importance < 1.0%). Collectively, the model indicated that groundwater springs occurred near flowlines where topography changes abruptly over small distances in valley-bottom areas underlain by coarse glacial deposits (i.e., toe slopes formed by stream channel incision into unconsolidated alluvium and colluvium; Appendix S1: Figure S1). While springs were predicted to be widespread throughout the upper Snake River watershed, they were most heavily concentrated in the southwestern, eastern, and northern portions of the study area (Appendix S1: Figure S2), driving similar spatial patterns in derived GWI (Figure 2a). Network locations with high GWI were rare at the scale of the USRW (Figure 2b): locations with GWI ≥ 0.5 represented just 2.8% of all locations for which the index was derived. Stream temperature

monitoring locations and fish study reaches encompassed nearly the complete range of GWI (Figure 2c,d).

Groundwater Effects on Temperature and Density

Water temperature regimes varied considerably among the 32 stream temperature monitoring locations during the study period (Figure 3a,b): daily mean water temperature varied between 0.01 (minimum) and 18.20 °C (maximum) among sites and across time. Streams with a low GWI tended to be warm in the summer (>15 °C) and cold in the late autumn (<3 °C), whereas streams with high GWI exhibited more constant and moderate water temperatures throughout the study period (*ca.* 8-10 °C; Figure 3a,b). Our temperature model performed well (Appendix S1: Figure S3). A Bayesian p-value of 0.481 indicated no bias in temperature estimates and an RMSE of 1.163 indicated low variation in estimated temperature. A Bayesian R^2 of 0.902 (median, 95% credible interval (CI) = 0.900, 0.903) indicated that air temperature and catchment covariates explained a considerable proportion of the variation in stream temperature. Median temperature sensitivity (i.e., the °C response of stream temperature to each °C change in air temperature; $\boldsymbol{\beta'_{2,s}}$ in eq. 2) ranged from 0.03 to 0.87. Model results indicated temperature sensitivity was strongly related to groundwater activity: increasing GWI (log-scale) was negatively related to temperature sensitivity (median scaled effect size = -0.16, 95% CI = -0.25, -0.08; Figure 3c). Associations between temperature sensitivity and other watershed variables were weak or highly uncertain, indicated by 95% CIs broadly overlapping 0 (Appendix S1: Table S4).

We captured a total of 22,358 YOY over a total of 498 sampling events. Zero YOY were captured during 61 sampling events. Maximum observed density was 6.58 fish per meter. Annual peak YOY density (log-scale) was non-linearly associated with GWI, as indicated by LOESS (Figure 4). At very low values of GWI (<0.2) YOY densities were also low, but YOY densities tended to increase approximately linearly as GWI increased (0.2-0.7), before stabilizing at high values (>0.7). Densities in reaches with intermediate GWI were more variable relative to reaches with either very low or very high GWI, in which variation was most constrained.

Temperature and Density Effects on Growth

Mean YOY total length per sampling event varied between 22 and 76 mm. Model selection using LOO-CV provided the most support for modelling growth rate as a function of temperature, (log) density, and their interaction (in addition to prior length, which was included in all candidate models; Appendix S1: Table S2). Model selection provided equivalent support for a model with a quadratic temperature effect (concave up; Appendix S1: Table S2). However, the squared term was considerably weaker than all other effects and the 95% CI overlapped 0. We therefore present results from the more parsimonious model. The final model describing the interactive effects of temperature and density on growth rates performed well (Appendix S1: Figure S4). A Bayesian p-value of 0.522 suggested no bias in estimated length and a RMSE of 3.93 mm indicated little variation in length estimates. Further, conditional and marginal Bayesian R^2 values of 0.864 (0.802, 0.947) and 0.861 (0.722, 0.953), respectively, suggested that the fixed effects alone explained a considerable proportion of the variation in body size. The final model indicated that when density was low, growth rate increased with temperature; but when density was high, growth rate declined with temperature (Figure 5; although the greatest densities, upper

25th percentile, were only observed in streams and at times when temperature was intermediate, *ca.* 8-12).

The final model did not indicate an effect of GWI on the standard deviation of length (i.e., $\sigma''_{t,y,s,r}$ from eq. 7; median = -0.04 and 95% CI = -0.13, 0.04) nor did we observe any association between GWI and model residuals (Appendix S1: Figure S4d). Collectively, this suggests that the effect of groundwater on growth is fully accounted for by considering temperature and density. Inspection of stream-specific intercepts suggested little residual variation in mean growth rate among streams (Appendix S1: Figure S5); residual variation was not apparent for reaches within streams.

Temporal Trends in Growth and Production

Our model explicitly considering temporal dynamics of growth performed nearly as well as the model described above (Appendix S1: Figure S6). A Bayesian p-value of 0.508 suggested no bias in estimated length and a RMSE of 4.11 mm indicated little variation in length estimates. Conditional and marginal Bayesian R^2 values of 0.872 (0.810, 0.944) and 0.869 (0.722, 0.957), respectively, indicated that body size trajectories were well described by the fixed effects alone. Our model suggested strong non-linear trends in growth through time, mediated by GWI (Appendix S1: Table S4). In streams with low GWI, growth decreased over time: growth was greatest in August immediately following emergence, then declined monotonically to a minimum (*ca.* 0) by early November (Figure 6a). In contrast, in streams with high GWI, temporal trends in growth were hump shaped: growth rates were low in August immediately following emergence, increased to a maximum in early October, then decreased into November. Further, our model suggested strong negative effect of GWI on standard deviation of length (Figure 6b): variation not already explained by time and groundwater. As above, inspection of stream-specific posterior intercepts indicated little residual variation in mean growth among streams (Appendix S1: Figure S7), and effectively no variation among reaches within streams.

Using the fitted model to project length through time illustrated how groundwater generates diversity in body size trajectories (Figure 6c). In support of our previous finding, fish in streams with low GWI experience fast growth in the summer when stream temperatures are higher, but this slows over time as temperatures decline. Conversely, fish in streams with high GWI experienced slow growth in the summer and much faster growth in the early autumn. Despite variation in the pace and timing of growth, fish were projected to grow to approximately the same body size by the end of the study period (65 mm): there was no relationship between end of season length and GWI (Figure 6d).

Our model describing the temporal dynamics of (log) production performed reasonably well but explained less variation in observed data than the models described above (Appendix S1: Figure S8). While a Bayesian p-value of 0.477 suggested minimal bias in estimated production, a RMSE of 0.681 indicated moderate error in production estimates. Conditional and marginal Bayesian R^2 values of 0.645 (0.598, 0.689) and 0.365 (0.108, 0.557), respectively, suggested that the random effects explained nearly as much variation in production as did the fixed effects, which was modest. As above, the model indicated non-linear trends in production were mediated by GWI (Appendix S1: Table S4). While August production was similar among streams,

diverging trends in production were observed for streams with contrasting GWI (Figure 7a). In streams with low GWI, production declined from a summer maximum and was no different from 0 by the end of the study period; whereas in streams with high GWI, production increased to a maximum in early October and remained elevated (although declining slightly) throughout the study period. Unlike growth, estimated mean production was always greater in streams with high GWI relative to streams with a low GWI; this pattern was largely due to greater overall densities in groundwater-dominated reaches. The model suggested no effect of GWI on standard deviation of production (median = -0.001 and 95% CI = -0.09, 0.10; Figure 7b). Unlike growth models, inspection of both stream and reach-specific posterior intercepts indicated considerable residual variation in (log) production (Appendix S1: Figure S9).

Projections of cumulative production over time illustrated how groundwater underlies asymmetry in fish production during the YOY rearing period (Figure 7c). In streams with low GWI, production accrued slowly with diminishing returns moving forward in time. Conversely, in streams with high GWI, rates of production increased between August and October, with relatively high rates sustained through November. Diverging trajectories in cumulative production led to streams with the highest GWI (1) producing 7.7 times more biomass than streams with the lowest GWI (0), on average (Figure 7d).

Riverscape Patterns of Growth and Production

Projecting growth and production across the riverscape illustrated how groundwater structures spatial and temporal patterns of these parameters (Figure 8). While there was some heterogeneity in body size during September and October, by November projected YOY length was mostly homogenous across the riverscape. In contrast, spatial variation in cumulative production increased over the study period, such that by November distinct hotspots of productivity had emerged at the riverscape scale. Hotspots of productivity were consistent with the locations of groundwater activity in the southwestern, western, and northern portions of the study area. The effect of groundwater on reach-scale cumulative production resulted in disproportionate contributions of reaches to basin-wide production (Chi-square test: $\chi^2 = 6383.1$, $p < 0.05$). For example, reaches with low GWI (<0.1) were projected to under-contribute by 15% (relative to their abundance), while reaches with very high GWI (>0.9) were projected to over-contribute by *ca.* 415%. However, because groundwater-dominated reaches were rare at the basin-scale, they contributed substantially less to total basin-wide production.

Discussion

How landscape complexity and heterogeneity structure organismal and population-level processes is critical to our understanding of riverscape ecology. In this study, we demonstrate how spatial heterogeneity in groundwater discharge to streams drives spatiotemporal variation in growth and production of young-of-year Yellowstone cutthroat trout across a riverscape. We found that geologic and topographic variables explained spatial heterogeneity in groundwater discharge to streams, which stabilized temperature regimes and was associated with high YOY densities. Temperature and density, in turn, interacted to influence YOY growth rates: growth increased strongly with temperature, but this effect was reduced when density was high.

Accordingly, variation in groundwater influence among stream reaches diversified trends in growth and production. At the riverscape scale, this diversity tended to reduce spatial variation in growth capacity but led to the formation of distinct hotspots of production. Collectively, our results demonstrate how groundwater, an important factor driving aquatic ecosystem heterogeneity, structures YCT recruitment dynamics across a riverscape. This information can be used to identify and prioritize protection and conservation of critical recruitment habitat at broad spatial scales and provides insight into the role of stable, groundwater-dominated habitats under global climate change.

Growth and Production Across Space and Time

There is increasing interest in how salmonid growth dynamics play out at fine spatial and temporal resolutions and across broad spatial extents (Brennan et al. 2019, Falke et al. 2019, Armstrong et al. 2021, Kaylor et al. 2021). Only by combining spatially explicit estimates of groundwater influence, were we able to uncover key spatial heterogeneity in growth regimes. The results of our temporal model reveal that groundwater underlies diversity in YOY growth regimes, and body size projections show how diverse growth regimes buffer against variation in growth potential among stream reaches (Fig. 6). Because juvenile growth is known to influence life-history expression (Hutchings 1993, Brown et al. 2004) and life-history diversity promotes population stability (Schindler et al. 2010), diverse portfolios of growth opportunities associated with groundwater may provide portfolio effects that buffer salmonid populations against environmental stochasticity (*sensu* Campana et al. 2023).

While diversity in growth trajectories reduced spatial variation in growth capacity, greater overall densities in groundwater-dominated reaches led to diverging trends in production through time (Fig. 7). Differences in true biomass production (i.e., based on mass, rather than length) among habitats spanning the range of GWI are likely underestimated given the power relationship between length and mass for fish. Regardless, highly productive groundwater-dominated habitats may subsidize less productive habitats through density-dependent dispersal (Travis et al. 1999), which can stabilize regional recruitment (Harrison et al. 2020), reduce extinction risk (Hanski and Gilpin 1991), and facilitate metapopulation recovery (Wilson et al. 2023). While production in groundwater-dominated reaches was disproportionately high relative to their abundance, the contribution to basin-wide production was relatively small. Therefore, protecting groundwater-dominated habitats alone may fall short of meeting conservation goals. Instead, protecting the full breadth of habitat diversity will be important for supporting recruitment across entire riverscapes.

Our results describing density-dependent effects of temperature on growth rate largely agree with past work (e.g., Brett 1971, Watson et al. 2022). However, unlike recent studies demonstrating a dome-shaped effect of temperature on growth (Huntsman et al. 2021, Letcher et al. 2022), we found that growth was linearly related to temperature (Fig. 5). One explanation for why we did not observe declines in growth under the warmest conditions is that stream temperatures were cool relative to YCT thermal tolerance. The highest mean temperature between sampling periods (16 °C) was slightly less than the “optimal” growth temperature for juvenile YCT (17.6 °C, fed ad libitum; Rogers et al. 2022). Furthermore, while our study design likely masked the effects of short-term high temperature events, the maximum daily mean temperature (18.2 °C) was far less

than the critical thermal maximum for YCT (28.2 °C; Wagner et al. 2001, Rogers et al. 2022). Alternatively, elevated temperatures may allow for increased food production and consumption, and hence increased growth (Railsback and Rose 1999, Railsback 2021). The positive effect of temperature on growth (at low densities), suggests that YOY growth and production in the USRW are more limited by cold temperatures, rather than by warm temperatures, as is often reported for salmonids occupying high elevation basins (Gallagher et al. 2022).

Advances in Riverscape Approaches

Advances in understanding the ecology of riverscapes are often limited by studies and data that that do not match the scales at which fish complete their life-history and population processes play out (Fausch et al. 2002, Torgersen et al. 2021). This study helps to address that mismatch by providing insight into how groundwater structures fish growth and production at a broad spatial extent (i.e., the USRW) and at fine spatial (i.e., reaches) and temporal (i.e., daily) resolutions. Network projections of growth and production illustrate how seasonal bias in fisheries studies (Brady et al. 2020) can misrepresent key processes. For example, restricting population assessments to the summer may lead to conclusions that groundwater-dominated habitats are of limited importance as cold temperatures constrain growth. In fact, we found that growth in these habitats was primarily achieved in autumn, which in part led to greater end of season production relative to habitats with less groundwater influence. Such inferences would not have been possible without connecting field-based sampling with machine learning techniques that allowed us to extrapolate the output of statistical models to the riverscape. Applying established methods in novel and integrated ways will be key to meeting the call for riverscape approaches to understanding and conserving aquatic ecosystems (Torgersen et al. 2021, Mejia et al. 2023).

Riverscape (i.e., spatially continuous) approaches to understanding groundwater influence in streams has been particularly challenging. Because groundwater inflow decouples stream and air temperature regimes (Caissie 2006), temperature sensitivity is often used as a proxy for groundwater influence (O'Driscoll and DeWalle 2006, Adelfio et al. 2019, Gallagher and Fraser 2023). However, using temperature sensitivity alone to infer groundwater contributions to streams is not recommended at broad spatial extents given the many landscape factors that influence sensitivity (Lisi et al. 2015, Beaufort et al. 2020). Therefore, metrics of groundwater that are independent of stream temperature are needed to inform aquatic ecosystem research (Letcher et al. 2016, Mejia et al. 2023). Recent work demonstrates how bedrock geology, which is linked to groundwater storage capacity, structures stream fish community dynamics (Hitt et al. 2023, Ishiyama et al. 2023). While these studies represent important advances, geology interacts with other landscape features to promote preferential groundwater discharge at much finer spatial scales (Jackson et al. 2024). In this study, we show how high resolution, independent metrics of groundwater influence can be used to model stream temperature and understand fish recruitment across scales. Our approach is relatively simple, requiring easy-to-obtain field observations, publicly available spatial data, and modest computing power, making it tractable to apply to other watersheds where increased understanding of groundwater dynamics is needed. Future research optimizing derived GWI values via comparison with empirical discharge data would increase the accuracy of the index and may help to inform models of riverscape hydrology (e.g., McShane and Eddy-Miller 2021). High-resolution data products describing groundwater activity,

as we provide here, provide much needed guidance for climate adaptation planning (Mejia et al 2023).

Key Uncertainties

While unlikely to affect our primary inferences, our study raises several questions motivating future research. The result that end-of-season cumulative production increased with groundwater index was driven primarily by the strong positive association between groundwater and YOY density. Groundwater was positively associated with adult spawning density (i.e., redd density; Pearson's r = 0.67), which was positively associated with YOY density (Pearson's r = 0.63; Appendix S1: Figure S10). Differences in spawning density may be driven by differences in spawning habitat availability. Groundwater seeps were most likely to occur in areas underlain by colluvial deposits and unconsolidated gravels, likely resulting in greater spawning habitat availability in groundwater-dominated streams. Additionally, stable environmental conditions associated with groundwater may promote homing (i.e., natal and breeding site fidelity) relative to habitats that are more dynamic. Homing is evolutionarily beneficial when high quality spawning habitat is stable through time because fitness gains in these areas are predictable (Quinn and Tallman 1987, Cram et al. 2012). Future work investigating associations between groundwater, spawning habitat availability, reproductive success, and homing rates would provide additional insight into the ecological and evolutionary mechanisms that promote spatial heterogeneity in YOY production.

Unexplained variation in trends in production was linked to high variation in the YOY density-groundwater relationship, suggesting additional factors underlie spatial patterns of density. In particular, food-web productivity (i.e., food quantity and quality) is an important driver of fish growth and density (Railsback and Rose 1999, Saunders et al. 2018) and can vary with landscape factors such as forest type and solar radiation (Lamberti and Steinman 1997). Juvenile habitat availability (e.g., vegetated stream margins) may also underlie patterns of YOY density (Hubert and Joyce 2005, Finstad et al. 2009). Expanding our study to consider food-web productivity, YOY habitat availability, and how these factors interact with groundwater would increase our understanding of the drivers of fish growth and production across riverscapes (*sensu* Saunders et al. 2018).

Variation in emergence timing necessitated evaluating growth capacity by simulating body size trajectories from common starting conditions. As a result, estimates of end of season body size should be interpreted as growth capacity or potential (*sensu* Sloat et al. 2005). Groundwater can reduce the magnitude of spring flooding that constrains the onset of spawning (Montgomery 1999) and influence stream temperature regimes that affect emergence timing (Webb and McLay 1996, Caissie 2006). Therefore, future work investigating riverscape patterns of growth and production will likely benefit from describing how groundwater generates spatial variation in the timing and duration of emergence.

Finally, as our study was restricted to the YOY rearing period, uncertainty remains regarding the role of groundwater-dominated habitats for growth and production of later life stages. Field observations and past work indicate limited YCT occupancy of groundwater-dominated streams beyond YOY stage (Baldock et al. 2023). In groundwater-dominated habitats, late-stage YOY

may disperse to other habitats where growth is less constrained by high densities and increased foraging is possible (*sensu* Fretwell and Lucas 1970, Einum et al. 2006). Further, cold groundwater may limit growth in the spring and summer when warmer temperatures become increasingly available in reaches with less groundwater influence. As fish grow and dispersal abilities increase, tracking growth opportunities as they shift across the riverscape may become an increasingly viable strategy for negotiating habitat heterogeneity (Armstrong et al. 2021, Hahlbeck et al. 2022).

Groundwater-Dominated Habitats Under Climate Change

Groundwater will likely mediate how climate change shapes spatial patterns of recruitment and the distribution of climate refugia across riverscapes (Larsen and Woelfle-Erskine 2018, Ebersole et al. 2020). Our results suggest that YOY growth and production in the USRW is currently limited by cold temperatures. Therefore, near-term stream warming associated with global climate change (Hostetler et al. 2021) may benefit growth and production, as previously reported for YCT in the USRW (Al-Chokhachy et al. 2013). However, the effects of longer-term stream warming will likely differ among habitats if streams receiving less groundwater are closer to upper thermal limits. In these systems, autumn gains in growth and production may be offset by losses earlier in the rearing period as summer temperatures become too warm (*sensu* Armstrong et al. 2021). In contrast, warming in groundwater-dominated habitats may benefit growth over the entire season as thermal constraints are incrementally reduced. Therefore, expected stream warming under climate change may enhance riverscape heterogeneity in end-of-season body size and cumulative production beyond what we describe in this study.

In addition to warming, climate change is expected to increase the magnitude and frequency of extreme flooding (Easterling et al. 2000, Queen et al. 2021). For salmonids, flooding negatively affects YOY recruitment processes (Kanno et al. 2015, Sweka and Wagner 2022). Many of the sampling events during which we captured zero YOY (n = 61) were conducted in 2021 following a major summer precipitation event that led to flooding in streams with minimal groundwater input. As groundwater buffers against extreme flows in small streams (Poff et al. 1997), stable recruitment from groundwater-dominated habitats may subsidize variable recruitment from more dynamic habitats, protecting against widespread cohort failure (*sensu* Homel et al. 2015, Harrison et al. 2020). Long-term studies investigating interannual recruitment dynamics as related to climate variability and hydrology would provide key insight into the role of groundwater-dominated habitats as climate refugia.

While groundwater is a key component of climate refugia for stream fishes (Ebersole et al. 2020, Mejia et al. 2023), adaptation to climate change may be most successful under strategies that protect and maintain habitat heterogeneity (Walsworth et al. 2019, Moore and Schindler 2022). For example, as snowmelt often contributes most to aquifer recharge (Winograd et al. 1998), groundwater contributions to streamflow may decline as snowpack is lost under future climate scenarios (Godsey et al. 2014, Hostetler et al. 2021). Therefore, groundwater habitats may instead act as transient "stepping stones" that temporarily relieve climate impacts, assisting longer term adaptation (Hannah et al. 2014). An improved understanding of subsurface hydrology would enable predictions of where and over what time scales groundwater-dominated habitats will be resistant to climate change. Furthermore, locally adapted populations currently

occupying warm and dynamic riverine habitats may harbor the genetic diversity needed for species-level adaptation to novel climate regimes (Jensen et al. 2008, Walsworth et al. 2019). Conserving habitats that span the complete range of groundwater influence is likely necessary to maximize adaptive capacity of salmonids occupying diverse and complex riverscapes.

Conservation Applications

Predicting the future importance of groundwater habitat for cutthroat trout recruitment is challenging due to potential interactions with other anthropogenic stressors. While our study was conducted in a relatively undeveloped location (97% public land), groundwater depletion is occurring at unprecedented rates globally and is major threat to aquatic ecosystems (Perkin et al. 2017). Our results indicate that hydrologic homogenization due to groundwater depletion would constrain the range of distinct growth opportunities, which could destabilize populations as life-history diversity is eroded (*sensu* Schindler et al. 2010, Bellmore et al. 2022). Additionally, while groundwater-fed habitats may be resistant to climate variability, lack of flow-related disturbance suggests increased sensitivity to other stressors, such as land-use change. In agricultural areas, for example, many streams require repeated dredging and gravel rejuvenation to counteract excess sedimentation (Wyoming Game and Fish Department 2001). Thus, groundwater-fed streams may exist near a tipping point, where small changes in the sediment budget may precipitate population declines via the negative effects sediment on reproductive success (Jensen et al. 2009), further constraining recruitment locally and at broad spatial extents.

In river networks, small tributaries often contribute disproportionately to recruitment relative to larger mainstem rivers (Tsuboi et al. 2022, Bouska et al. 2023), but tributaries differ in their capacity to support early life-history requirements. As a result, and given the multiple interacting stressors faced by riverine fish, there is an urgent need for tools and data that allow for prioritization of conservation actions (Leadley et al. 2022). The results of this study (e.g., maps of groundwater, growth, and production) can be compared to the spatial distribution of known stressors to prioritize locations for habitat restoration and protection and to identify where such efforts may have the greatest impact on conservation outcomes (e.g., increasing recruitment). Data and information produced at spatial scales matching species life-history needs, as described in this study, are critical for efficient and effective conservation and management (Fausch et al. 2002).

Conclusions

It is well appreciated that dynamic landscapes and riverscapes underlie the stability of ecosystems and ecosystem services (Schindler et al. 2015, Brennan et al. 2019). Less appreciated is the extent to which rare, stable habitats may disproportionately affect ecological processes and how these habitats function within the broader habitat matrix. Here, we show how groundwater structures stream habitat conditions and spatiotemporal variation in juvenile trout growth and production across a large riverscape. Variation in groundwater influence among stream reaches is an important source of spatial habitat diversity. Stable groundwater-fed habitats represent one endmember of the habitat gradient and, while rare, appear to play a disproportionate role in structuring riverine ecosystems. Groundwater-fed habitats may ultimately act as “ecosystem control points”, whereby the dynamics and demographics of fish populations across river

networks are a function of processes occurring at much smaller spatial scales, driven by the degree of groundwater influence (*sensu* Bernhardt et al. 2017, Briggs and Hare 2018). Our study highlights the critical need for integrated, multi-scale approaches to both ecological research and conservation planning in riverine ecosystems, particularly under climate change (*sensu* Fausch et al. 2002, Torgersen et al. 2021).

References

Adelfio, L. A., S. M. Wondzell, N. J. Mantua, and G. H. Reeves. 2019. Warm winters reduce landscape-scale variability in the duration of egg incubation for coho salmon (Oncorhynchus kisutch) on the Copper River Delta, Alaska. Canadian Journal of Fisheries and Aquatic Sciences 76:1362–1375.

Al-Chokhachy, R., J. Alder, S. W. Hostetler, R. E. Gresswell, and B. Shepard. 2013. Thermal controls of Yellowstone cutthroat trout and invasive fishes under climate change. Global Change Biology 19:3069–3081.

Al-Chokhachy, R., B. B. Shepard, J. C. Burckhardt, D. Garren, S. Opitz, T. M. Koel, L. Nelson, and R. E. Gresswell. 2018. A portfolio framework for prioritizing conservation efforts for Yellowstone Cutthroat Trout populations. Fisheries 43:485–496.

Armstrong, J. B., A. H. Fullerton, C. E. Jordan, J. L. Ebersole, J. R. Bellmore, I. Arismendi, B. E. Penaluna, and G. H. Reeves. 2021. The importance of warm habitat to the growth regime of cold-water fishes. Nature Climate Change.

Bacon, P. J., W. S. C. Gurney, W. Jones, I. S. Mclaren, and A. F. Youngson. 2005. Seasonal growth patterns of wild juvenile fish: Partitioning variation among explanatory variables, based on individual growth trajectories of Atlantic salmon (Salmo salar) parr. Journal of Animal Ecology 74:1–11.

Baldock, J. R., R. K. Al-Chokhachy, M. R. Campbell, and A. Walters. 2023. Timing of reproduction underlies fitness tradeoffs for a salmonid fish. Oikos:1–13.

Bateman, D. S., R. E. Gresswell, and C. E. Torgersen. 2005. Evaluating single-pass catch as a tool for identifying spatial pattern in fish distribution. Journal of Freshwater Ecology 20:335–345.

Beaufort, A., F. Moatar, E. Sauquet, P. Loicq, and D. M. Hannah. 2020. Influence of landscape and hydrological factors on stream–air temperature relationships at regional scale. Hydrological Processes 34:583–597.

Bellmore, J. R., J. B. Fellman, E. Hood, M. R. Dunkle, and R. T. Edwards. 2022. A melting cryosphere constrains fish growth by synchronizing the seasonal phenology of river food webs. Global Change Biology 28:4807–4818.

Bernhardt, E. S., J. R. Blaszczak, C. D. Ficken, M. L. Fork, K. E. Kaiser, and E. C. Seybold. 2017. Control points in ecosystems: moving beyond the hot spot and hot moment concept. Ecosystems 20:665-682.

Bivand, R., and C. Rundel. 2023. rgeos: Interface to Geometry Engine - Open Source ('GEOS'). R package version 0.6-3, https://CRAN.R-project.org/package=rgeos.

Bouska, K. L., B. D. Healy, M. J. Moore, C. G. Dunn, J. J. Spurgeon, and C. P. Paukert. 2023. Diverse portfolios: Investing in tributaries for restoration of large river fishes in the Anthropocene. Frontiers in Environmental Science.

Brady, M. E., A. M. Chione, and J. B. Armstrong. 2020. Missing pieces in the full annual cycle of fish ecology: A systematic review of the phenology of freshwater fish research. bioRxiv.

Brennan, S. R., D. E. Schindler, T. J. Cline, T. E. Walsworth, G. Buck, and D. P. Fernandez. 2019. Shifting habitat mosaics and fish production across river basins. Science 364:783–786.

Brett, J. R. 1971. Energetic responses of salmon to temperature. A study of some thermal relations in the physiology and freshwater ecology of sockeye salmon (Oncorhynchus nerka). American Zoologist 11:99–113.

Briggs, M. A., and D. K. Hare. 2018. Explicit consideration of preferential groundwater discharges as surface water ecosystem control points. Hydrological Processes 32:2435–2440.

Brown, G. W. 1969. Predicting Temperatures of Small Streams. Water Resources Research 5:68–75.

Brown, J. H., J. F. Gillooly, A. P. Allen, V. M. Savage, and G. B. West. 2004. Towards a metabolic theory of ecology. Ecology 85:1771–1789.

Buckner, M. A. 202. rlandfire: Tools for Accessing and Working with LANDFIRE in R. Version 0.3.0. https://github.com/bcknr/rlandfire.

Burns, E. R., Y. Zhu, H. Zhan, M. Manga, C. F. Williams, S. E. Ingebritsen, and J. B. Dunham. 2017. Thermal effect of climate change on groundwater-fed ecosystems. Water Resources Research 53:3341–3351.

Caissie, D. 2006. The thermal regime of rivers: a review. Freshwater Biology 51:1389–1406.

Campana, S. E., S. Smoliński, B. A. Black, J. R. Morrongiello, S. J. Alexandroff, C. Andersson, B. Bogstad, P. G. Butler, C. Denechaud, D. C. Frank, A. J. Geffen, J. A. Godiksen, P. Grønkjær, E. Hjörleifsson, I. G. Jónsdóttir, M. Meekan, M. Mette, S. E. Tanner, P. van der Sleen, and G. von Leesen. 2023. Growth portfolios buffer climate-linked environmental change in marine systems. Ecology 104:1–16.

Carbonneau, P., M. A. Fonstad, W. A. Marcus, and S. J. Dugdale. 2012. Making riverscapes real. Geomorphology 137:74–86.

Cartwright, J. M., K. A. Dwire, Z. Freed, S. J. Hammer, B. McLaughlin, L. W. Misztal, E. R. Schenk, J. R. Spence, A. E. Springer, and L. E. Stevens. 2020. Oases of the future? Springs as potential hydrologic refugia in drying climates. Frontiers in Ecology and the Environment 18:245–253.

Casas-Mulet, R., J. Pander, D. Ryu, M. J. Stewardson, and J. Geist. 2020. Unmanned Aerial Vehicle (UAV)-Based Thermal Infra-Red (TIR) and Optical Imagery Reveals Multi-Spatial Scale Controls of Cold-Water Areas Over a Groundwater-Dominated Riverscape. Frontiers in Environmental Science 8:1–16.

Clancy, N. G., J. L. Dunnigan, and P. Budy. 2022. Relationship of Trout Growth to Frequent Electrofishing and Diet Collection in a Headwater Stream. North American Journal of Fisheries Management 42:109–114.

Comte, L., and J. D. Olden. 2018. Evidence for dispersal syndromes in freshwater fishes. Proceedings of the Royal Society B: Biological Sciences 285.

Constantz, J. 1998. Interaction between stream temperature, streamflow, and groundwater exchanges in alpine streams. Water Resources Research 34:1609–1615.

Cram, J. M., C. E. Torgersen, R. S. Klett, G. R. Pess, D. May, T. N. Pearsons, and A. H. Dittman. 2012. Tradeoffs between homing and habitat quality for spawning site selection by hatchery-origin Chinook salmon. Environmental Biology of Fishes 96:109–122.

Cutts, C. J., N. B. Metcalfe, and A. C. Taylor. 1999. Competitive Asymmetries in Territorial Juvenile Atlantic Salmon, Salmo salar. Oikos 86:479–486.

Davidson, J., and H. G. Andrewartha. 1948. The influence of rainfall, evaporation and atmospheric temperature on fluctuations in the size of a natural population of Thirps imaginis (Thysanoptera). Journal of Animal Ecology 17:200–222.

Detty, J. M., and K. J. McGuire. 2010. Topographic controls on shallow groundwater dynamics: Implications of hydrologic connectivity between hillslopes and riparian zones in a till mantled catchment. Hydrological Processes 24:2222–2236.

Dralle, D. N., G. Rossi, P. Georgakakos, W. J. Hahm, D. M. Rempe, M. Blanchard, M. E. Power, W. E. Dietrich, and S. M. Carlson. 2023. The salmonid and the subsurface: Hillslope storage capacity determines the quality and distribution of fish habitat. Ecosphere 14:1–23.

Dugdale, S. J., N. E. Bergeron, and A. St-Hilaire. 2015. Spatial distribution of thermal refuges analysed in relation to riverscape hydromorphology using airborne thermal infrared imagery. Remote Sensing of Environment 160:43–55.

Easterling, D. R., G. A. Meehl, C. Parmesan, S. A. Changnon, T. R. Karl, and L. O. Mearns. 2000. Climate Extremes: Observations, Modeling, and Impacts. Science 289:2068–2074.

Ebersole, J. L., R. M. Quiñones, S. Clements, and B. H. Letcher. 2020. Managing climate refugia for freshwater fishes under an expanding human footprint. Frontiers in Ecology and the Environment 18:271–280.

Einum, S., G. Robertsen, K. H. Nislow, S. McKelvey, and J. D. Armstrong. 2011. The spatial scale of density-dependent growth and implications for dispersal from nests in juvenile Atlantic salmon. Oecologia 165:959–969.

Einum, S., L. Sundt-Hansen, and K. H. Nislow. 2006. The partitioning of density-dependent dispersal, growth and survival throughout ontogeny in a highly fecund organism. Oikos 113:489–496.

Eisenhauer, Z. J., P. M. Christman, J. M. Matte, W. R. Ardren, D. J. Fraser, and J. W. A. Grant. 2021. Revisiting the restricted movement paradigm: The dispersal of atlantic salmon fry from artificial redds. Canadian Journal of Fisheries and Aquatic Sciences 78:493–503.

Elith, J., S. J. Phillips, T. Hastie, M. Dudík, Y. E. Chee, and C. J. Yates. 2011. A statistical explanation of MaxEnt for ecologists. Diversity and Distributions 17:43–57.

Elliott, J. M. 1976. The energetics of feeding, metabolism, and growth of brown trout (Salmo trutta L.) in realtion to body weight, water temperature, and ration size. Journal of Animal Ecology 45:923–948.

Evans, J. S., and M. A. Murphy. 2023. spatialEco. R package version 2.0-1, https://github.com/jeffreyevans/spatialEco.

Falke, J. A., B. M. Huntsman, and E. R. Schoen. 2019. Climatic Variation Drives Growth Potential of Juvenile Chinook Salmon along a Subarctic Boreal Riverscape. American Fisheries Society Symposium 90:1–26.

Fausch, K. D., C. E. Torgersen, C. V. Baxter, and H. W. Li. 2002. Landscapes to Riverscapes: Bridging the Gap between Research and Conservation of Stream Fishes. BioScience 52:483.

Finstad, A. G., S. Einum, O. Ugedal, and T. Forseth. 2009. Spatial distribution of limited resources and local density regulation in juvenile Atlantic salmon. Journal of Animal Ecology 78:226–235.

Fretwell, S. D., and H. L. J. Lucas. 1970. On territorial behavior and other factors influencing habitat distribution in birds. Acta Biotheoretica 19:16–36.

Fullerton, A. H., C. E. Torgersen, J. J. Lawler, R. N. Faux, E. A. Steel, T. J. Beechie, J. L. Ebersole, and S. G. Leibowitz. 2015. Rethinking the longitudinal stream temperature paradigm: region-wide comparison of thermal infrared imagery reveals unexpected complexity of river temperatures. Hydrological Processes 29:4719–4737.

Gallagher, B. K., and D. J. Fraser. 2023. Stream groundwater inputs generate fine-scale variation in brook trout phenology and growth across a warming landscape. Freshwater Biology:1–16.

Gallagher, B. K., S. Geargeoura, and D. J. Fraser. 2022. Effects of climate on salmonid productivity: a global meta-analysis across freshwater ecosystems. Global Change Biology:1–20.

Gelman, A. 2003. A Bayesian formulation of exploratory data analysis and goodness-of-fit testing. International Statistical Review 71:369–382.

Gelman, A., B. Goodrich, J. Gabry, and A. Vehtari. 2019. R-squared for Bayesian Regression Models. American Statistician 73:307–309.

Gelman, A. and J. Hill. 2007. Data analysis using regression and multi-level/hierarchical models, vol. 1. – Cambridge Univ. Press.

Gerlach, M. E., K. C. Rains, E. J. Guerrón-Orejuela, W. J. Kleindl, J. Downs, S. M. Landry, and M. C. Rains. 2022. Using remote sensing and machine learning to locate groundwater discharge to salmon-bearing streams. Remote Sensing 14.

Godsey, S. E., J. W. Kirchner, and C. L. Tague. 2014. Effects of changes in winter snowpacks on summer low flows: Case studies in the Sierra Nevada, California, USA. Hydrological Processes 28:5048–5064.

Google Earth Pro 7.3.6. 2023. Teton County, Wyoming, USA. 43.546556, -110.786726. Satellite imagery [accessed 15 July 2023].

Gresswell, R. E. 2011. Biology, status, and management of the Yellowstone cutthroat trout. North American Journal of Fisheries Management 31:782–812.

Hahlbeck, N., W. R. Tinniswood, M. R. Sloat, J. D. Ortega, M. A. Wyatt, M. E. Hereford, B. S. Ramirez, D. A. Crook, K. J. Anlauf-Dunn, and J. B. Armstrong. 2022. Contribution of warm habitat to cold-water fisheries. Conservation Biology 36:1–10.

Haitjema, H. M., and S. Mitchell-Bruker. 2005. Are water tables a subdued replica of the topography? Ground Water 43:781–786.

Hanks, R. D., Y. Kanno, and J. M. Rash. 2018. Can Single-Pass Electrofishing Replace Three-Pass Depletion for Population Trend Detection? Transactions of the American Fisheries Society 147:729–739.

Hannah, L., L. Flint, A. D. Syphard, M. A. Moritz, L. B. Buckley, and I. M. McCullough. 2014. Fine-grain modeling of species' response to climate change: Holdouts, stepping-stones, and microrefugia. Trends in Ecology and Evolution 29:390–397.

Hanski, I. 1998. Metapopulation dynamics. Nature 396:41–49.

Hanski, I., and M. Gilpin. 1991. Metapopulation dynamics: brief history and conceptual domain. Biological Journal of the Linnean Society 42:3–16.

Harrison, H. B., M. Bode, D. H. Williamson, M. L. Berumen, and G. P. Jones. 2020. A connectivity portfolio effect stabilizes marine reserve performance. Proceedings of the National Academy of Sciences 117:25595–25600.

Hauer, F. R., H. Locke, V. J. Dreitz, M. Hebblewhite, W. H. Lowe, C. C. Muhlfeld, C. R. Nelson, M. F. Proctor, and S. B. Rood. 2016. Gravel-bed river floodplains are the ecological nexus of glaciated mountain landscapes. Science Advances 2:e1600026–e1600026.

Hayes, D. B., J. R. Bence, T. J. Kwak, and B. E. Thompson. 2007. Abundance, biomass, and production. Pages 327-374 *in* C. S. Guy and M. L. Brown, editors. Analysis and interpretation of freshwater fisheries data. American Fisheries Society, Bethesda, Maryland, USA.

Heck, M. P., L. D. Schultz, D. Hockman-Wert, E. C. Dinger, and J. B. Dunham. 2018. Monitoring Stream Temperatures — A Guide for Non-Specialists. Page 76 p U.S. Geological Survey Techniques and Methods, book 3.

Hijmans, R. 2023. terra: Spatial Data Analysis. R package version 1.7-39, https://CRAN.R-project.org/package=terra.

Hitt, N. P., K. M. Rogers, K. G. Kessler, M. A. Briggs, and J. H. Fair. 2023. Stabilising effects of karstic groundwater on stream fish communities. Ecology of Freshwater Fish 32:538–551.

Homel, K. M., R. E. Gresswell, and J. L. Kershner. 2015. Life history diversity of Snake River finespotted cutthroat trout: Managing for persistence in a rapidly changing environment. North American Journal of Fisheries Management 35:789–801.

Hostetler, S. W., C. Whitlock, B. Shuman, D. Liefert, C. W. Drimal, and S. Bischke. 2021. Greater Yellowstone climate assessment: past, present, and future climate change in greater Yellowstone watersheds. Bozeman, MT.

Hubert, W. A., and M. P. Joyce. 2005. Habitat associations of age-0 cutthroat trout in a spring stream improved for adult salmonids. Journal of Freshwater Ecology 20:277–286.

Huntsman, B. M., A. J. Lynch, and C. A. Caldwell. 2021. Interacting Effects of Density-Dependent and Density-Independent Factors on Growth Rates in Southwestern Cutthroat Trout Populations. Transactions of the American Fisheries Society.

Hutchings, J. A. 1993. Adaptive life histories effected by age-specific survival and growth rate. Ecology 74:673–684.

Imre, I., J. W. A. Grant, and R. A. Cunjak. 2005. Density-dependent growth of young-of-the-year Atlantic salmon Salmo salar in Catamaran Brook, New Brunswick. Journal of Animal Ecology 74:508–516.

Isaak, D. J., C. H. Luce, B. E. Rieman, D. E. Nagel, E. E. Peterson, D. L. Horan, S. Parkes, and G. L. Chandler. 2010. Effects of climate change and wildfire on stream temperatures and salmonid thermal habitat in a mountain river network. Ecological Applications 20:1350–1371.

Ishiyama, N., M. Sueyoshi, J. García Molinos, K. Iwasaki, J. N. Negishi, I. Koizumi, S. Nagayama, A. Nagasaka, Y. Nagasaka, and F. Nakamura. 2023. Underlying geology and climate interactively shape climate change refugia in mountain streams. Ecological Monographs 93:1–20.

Jackson, K. E., E. M. Moore, A. M. Helton, A. B. Haynes, J. R. Barclay, and M. A. Briggs. 2024. Exploring landscape and geologic controls on spatial patterning of streambank groundwater discharge in a mixed land use watershed. Hydrological Processes 38:1–17.

Jaeger, K. L., D. R. Montgomery, and S. M. Bolton. 2007. Channel and perennial flow initiation in headwater streams: Management implications of variability in source-area size. Environmental Management 40:775–786.

Jensen, D. W., E. A. Steel, A. H. Fullerton, and G. R. Pess. 2009. Impact of fine sediment on egg-to-fry survival of pacific salmon: A meta-analysis of published studies. Reviews in Fisheries Science 17:348–359.

Jensen, L. F., M. M. Hansen, C. Pertoldi, G. Holdensgaard, K. L. D. Mensberg, and V. Loeschcke. 2008. Local adaptation in brown trout early life-history traits: Implications for climate change adaptability. Proceedings of the Royal Society B: Biological Sciences 275:2859–2868.

Kanno, Y., S. Kim, and K. C. Pregler. 2022. Sub-seasonal correlation between growth and survival in three sympatric aquatic ectotherms. Oikos:1–11.

Kanno, Y., B. H. Letcher, N. P. Hitt, D. A. Boughton, J. E. B. Wofford, and E. F. Zipkin. 2015. Seasonal weather patterns drive population vital rates and persistence in a stream fish. Global Change Biology 21:1856–1870.

Kaylor, M. J., C. Justice, J. B. Armstrong, B. A. Staton, L. A. Burns, E. Sedell, and S. M. White. 2021. Temperature, emergence phenology and consumption drive seasonal shifts in fish growth and production across riverscapes. Journal of Animal Ecology 90:1727–1714.

Kenney, B. C. 1982. Beware of spurious self-correlations! Water Resources Research 18:1041–1048.

Keppel, G., K. P. Van Niel, G. W. Wardell-Johnson, C. J. Yates, M. Byrne, L. Mucina, A. G. T. Schut, S. D. Hopper, and S. E. Franklin. 2012. Refugia: Identifying and understanding safe havens for biodiversity under climate change. Global Ecology and Biogeography 21:393–404.

Kiefling, J. 1997. A history of the Snake River spring creek spawning tributaries. Cheyenne, WY.

Koel, T. M., L. M. Tronstad, J. L. Arnold, K. A. Gunther, D. W. Smith, J. M. Syslo, and P. J. White. 2019. Predatory fish invasion induces within and across ecosystem effects in Yellowstone National Park. Science Advances 5:1–11.

Kovach, R. P., R. Al-Chokhachy, and T. Stephens. 2018. Proactive Rainbow Trout Suppression Reduces Threat of Hybridization in the Upper Snake River Basin. North American Journal of Fisheries Management 38:811–819.

Kramer-Schadt, S., J. Niedballa, J. D. Pilgrim, B. Schröder, J. Lindenborn, V. Reinfelder, M. Stillfried, I. Heckmann, A. K. Scharf, D. M. Augeri, S. M. Cheyne, A. J. Hearn, J. Ross, D. W. Macdonald, J. Mathai, J. Eaton, A. J. Marshall, G. Semiadi, R. Rustam, H. Bernard, R. Alfred, H. Samejima, J. W. Duckworth, C. Breitenmoser-Wuersten, J. L. Belant, H. Hofer, and A. Wilting. 2013. The importance of correcting for sampling bias in MaxEnt species distribution models. Diversity and Distributions 19:1366–1379.

Kruse, C. G., W. A. Hubert, and F. J. Rahel. 1997. Geomorphic Influences on the Distribution of Yellowstone Cutthroat Trout in the Absaroka Mountains, Wyoming. Transactions of the American Fisheries Society 126:418–427.

Lamberti, G. A., and A. D. Steinman. 1997. A comparison of primary production in stream ecosystems. Journal of the North American Benthological Society 16:95–104.
Larsen, L. G., and C. Woelfle-Erskine. 2018. Groundwater Is Key to Salmonid Persistence and Recruitment in Intermittent Mediterranean-Climate Streams. Water Resources Research 54:8909–8930.
Leach, J. A., W. Lidberg, L. Kuglerova, A. Peralta-Tapia, A. Agren, and H. Laudon. 2017. Evaluating topography-based predictions of shallow lateral groundwater discharge zones for a boreal lake-stream system. Water Resources Research 53:5420–5437.
Leadley, P., A. Gonzalez, D. Obura, C. B. Krug, M. C. Londono-Murcia, K. L. Millete, A. Radulovici, A. Rankovic, L. J. Shannon, E. Archer, F. A. Armah, N. Bax, L. E. Dee, F. Essl, S. Ferrrier, P. Genovesi, M. R. Guariguata, S. Hashimoto, C. I. Speranza, F. Isbell, M. Kok, S. D. Lavery, D. Leclere, and R. Loyola. 2022. Achieving global biodiversity goals by 2050 requires urgent and integrated actions. One Earth 5:597–603.
Letcher, B. H., D. J. Hocking, K. O'Neil, A. R. Whiteley, K. H. Nislow, and M. J. O'Donnell. 2016. A hierarchical model of daily stream temperature using air-water temperature synchronization, autocorrelation, and time lags. PeerJ 2016:1–26.
Letcher, B. H., K. H. Nislow, M. J. O'Donnell, A. R. Whiteley, J. A. Coombs, T. L. Dubreuil, and D. B. Turek. 2022. Identifying mechanisms underlying individual body size increases in a changing, highly seasonal environment: The growing trout of West Brook. Journal of Animal Ecology:1–19.
Lindsay, J. B. 2016. Whitebox GAT: A case study in geomorphometric analysis. Computers and Geosciences 95:75–84.
Lisi, P. J., D. E. Schindler, T. J. Cline, M. D. Scheuerell, and P. B. Walsh. 2015. Watershed geomorphology and snowmelt control stream thermal sensitivity to air temperature. Geophysical Research Letters 42:3380–3388.
Love, J. D., and A. C. Christiansen. 1985. Geologic map of Wyoming: U.S. Geological Survey Geologic Map, scale 1:500,000, 3 sheets.
MacArthur, R. 1958. Population Ecology of Some Warblers of Northeastern Coniferous Forests. Ecology 39:599–619.
Mallast, U., R. Gloaguen, S. Geyer, T. Rüdiger, and C. Siebert. 2011. Derivation of groundwater flow-paths based on semi-automatic extraction of lineaments from remote sensing data. Hydrology and Earth System Sciences 15:2665–2678.
McShane, R. R., and C. A. Eddy-Miller. 2021. A Machine Learning Approach to Modeling Streamflow with Sparse Data in Ungaged Watersheds on the Wyoming Range, 2012-17:29.
Mejia, F. H., C. V. Baxter, E. K. Berntsen, and A. K. Fremier. 2016. Linking groundwater – surface water exchange to food production and salmonid growth. Canadian Journal of Fisheries and Aquatic Sciences 73:1650–1660.
Mejia, F. H., V. Ouellet, M. A. Briggs, S. M. Carlson, R. Casas-Mulet, M. Chapman, M. J. Collins, S. J. Dugdale, J. L. Ebersole, D. M. Frechette, A. H. Fullerton, A. Carole-Gillis, Z. C. Johnson, C. Kelleher, B. L. Kurylyk, R. Lave, B. H. Letcher, K. M. Myrvold, T.-L. Nadeau, H. Neville, H. Piégay, K. A. Smith, D. Tonolla, and C. E. Torgersen. 2023. Closing the gap between science and management of water refuges in rivers and streams. Global Change Biology:1–27.
Meredith, M., and J. Kruschke. 2022. HDInterval: Highest (Posterior) Density Intervals. R package version 0.2.4, https://CRAN.R-project.org/package=HDInterval.
Meyer, K. A., D. J. Schill, F. S. Elle, and J. A. J. Lamansky. 2003. Reproductive demographics and factors that influence length at sexual maturity of Yellowstone Cutthroat Trout in Idaho. Transactions of the American Fisheries Society 132:183–195.
Mohseni, O., H. G. Stefan, and T. R. Erickson. 1998. A nonlinear regression model for weekly stream temperatures. Water Resources Research 34:2685–2692.
Montgomery, D. R. 1999. Process domains and the river continuum. Journal Of The American Water Resources Association 35:397–410.
Moore, J. W., and D. E. Schindler. 2022. Getting ahead of climate change for ecological adaptation and resilience. Science 376:1421–1426.
Myrvold, K. M., and B. P. Kennedy. 2015. Density dependence and its impact on individual growth rates in an age-structured stream salmonid population. Ecosphere 6:1–16.
Nakagawa, S., and H. Schielzeth. 2013. A general and simple method for obtaining R2 from generalized linear mixed-effects models. Methods in Ecology and Evolution 4:133–142.

Nolan, B. T., D. L. Campbell, and R. M. Senterfit. 1998. Depth of the base of the Jackson aquifer, based on geophysical exploration, southern Jackson Hole, Wyoming, USA. Hydrogeology Journal 6:374–382.
Nolan, B. T., and K. A. Miller. 1995. Water resources of Teton County, Wyoming, exclusive of Yellowstone National Park: U.S. Geological Survey Water-Resources Investigations Report 95–4204.
O'Driscoll, M. A., and D. R. DeWalle. 2006. Stream-air temperature relations to classify stream-ground water interactions in a karst setting, central Pennsylvania, USA. Journal of Hydrology 329:140–153.
O'Gorman, E. J., Ó. P. Ólafsson, B. O. L. Demars, N. Friberg, G. Guðbergsson, E. R. Hannesdóttir, M. C. Jackson, L. S. Johansson, Ó. B. McLaughlin, J. S. Ólafsson, G. Woodward, and G. M. Gíslason. 2016. Temperature effects on fish production across a natural thermal gradient. Global Change Biology 22:3206–3220.
O'Sullivan, A. M., K. J. Devito, J. Ogilvie, T. Linnansaari, T. Pronk, S. Allard, and R. A. Curry. 2020. Effects of Topographic Resolution and Geologic Setting on Spatial Statistical River Temperature Models. Water Resources Research 56:1–23.
Oliver, T., D. B. Roy, J. K. Hill, T. Brereton, and C. D. Thomas. 2010. Heterogeneous landscapes promote population stability. Ecology Letters 13:473–484.
Perkin, J. S., K. B. Gido, J. A. Falke, K. D. Fausch, H. Crockett, E. R. Johnson, and J. Sanderson. 2017. Groundwater declines are linked to changes in Great Plains stream fish assemblages. Proceedings of the National Academy of Sciences 114:7373-7378.
Phillips, S. J., and M. Dudík. 2008. Modeling of species distributions with Maxent: new extensions and a comprehensive evaluation. Ecography 31:161–175.
Pierce, K. L., J. M. Licciardi, J. M. Good, and C. Jaworowski. 2018. Pleistocene Glaciation of the Jackson Hole Area, Wyoming: U.S. Geological Survey Professional Paper 1835.
Plummer, M. 2003. JAGS: a program for analysis of Bayesian graphical models using Gibbs sampling. – In: Hornik, K., Leisch, F. and Zeileis, A. (eds), Proc. 3rd Int. workshop on distributed statistical computing (DSC 2003), Vienna, 20–22 March 2003, pp. 1–10.
Poff, N. L., J. D. Allan, M. B. Bain, J. R. Karr, K. L. Prestegaard, B. D. Richter, R. E. Sparks, and J. C. Stromberg. 1997. The Natural Flow Regime. BioScience 47:769–784.
Pope, K. L., and C. G. Kruse. 2007. Condition. Pages 423–471 *in* M. L. Brown and C. S. Guy, editors. Analysis and interpretation of freshwater fisheries data. American Fisheries Society, Bethesda, Maryland.
Post, J. R., E. A. Parkinson, and N. T. Johnston. 1999. Density-dependent processes in structured fish populations: Interaction strengths in whole-lake experiments. Ecological Monographs 69:155–175.
Pourtaghi, Z. S., and H. R. Pourghasemi. 2014. GIS-based groundwater spring potential assessment and mapping in the Birjand Township, southern Khorasan Province, Iran. Hydrogeology Journal 22:643–662.
Power, G., R. S. Brown, and J. G. Imhof. 1999. Groundwater and fish - Insights from northern North America. Hydrological Processes 13:401–422.
Queen, L. E., P. W. Mote, D. E. Rupp, O. Chegwidden, and B. Nijssen. 2021. Ubiquitous increases in flood magnitude in the Columbia River basin under climate change. Hydrology and Earth System Sciences 25:257–272.
Quinn, T. P., and N. P. Peterson. 1996. The influence of habitat complexity and fish size on over-winter survival and growth of individually marked juvenile coho salmon (Oncorhynchus kisutch) in Big Beef Creek, Washington. Canadian Journal of Fisheries and Aquatic Sciences 53:1555–1564.
Quinn, T. P., and R. F. Tallman. 1987. Seasonal environmental predictability and homing in riverine fishes. Environmental Biology of Fishes 18:155–159.
R Core Team. 2023. R: A language and environment for statistical computing. R Foundation for Statistical Computing, Vienna, Austria. https://www.R-project.org/.
Railsback, S. F. 2021. What We Don't Know About the Effects of Temperature on Salmonid Growth. Transactions of the American Fisheries Society:1–10.
Railsback, S. F., and K. A. Rose. 1999. Bioenergetics Modeling of Stream Trout Growth: Temperature and Food Consumption Effects. Transactions of the American Fisheries Society 128:241–256.
Reid, M. E., and R. M. Iverson. 1992. Gravity-driven groundwater flow and slope failure potential: 2. Effects of slope morphology, material properties, and hydraulic heterogeneity. Water Resources Research 28:939–950.
Rogers, K. B., B. J. Sucher, B. W. Hodge, and C. A. Myrick. 2022. Thermal tolerance in cutthroat trout of the southern Rocky Mountains. Canadian Journal of Fisheries and Aquatic Sciences:1–13.
Rossi, G. J., M. E. Power, S. M. Carlson, and T. E. Grantham. 2022. Seasonal growth potential of Oncorhynchus mykiss in streams with contrasting prey phenology and streamflow. Ecosphere 13:1–16.

Roy, J. W., B. Zaitlin, M. Hayashi, and S. B. Watson. 2011. Influence of groundwater spring discharge on small-scale spatial variation of an alpine stream ecosystem. Ecohydrology 4:661–670.
Saunders, W. C., N. Bouwes, P. McHugh, and C. E. Jordan. 2018. A network model for primary production highlights linkages between salmonid populations and autochthonous resources. Ecosphere 9.
Schindler, D. E., J. B. Armstrong, and T. E. Reed. 2015. The portfolio concept in ecology and evolution. Frontiers in Ecology and the Environment 13:257–263.
Schindler, D. E., R. Hilborn, B. Chasco, C. P. Boatright, T. P. Quinn, L. A. Rogers, and M. S. Webster. 2010. Population diversity and the portfolio effect in an exploited species. Nature 465:609–12.
Scholl, E. A., W. F. Cross, C. S. Guy, A. J. Dutton, and J. R. Junker. 2023. Landscape diversity promotes stable food-web architectures in large rivers. Ecology Letters:1–12.
Sloat, M. R., B. B. Shepard, R. G. White, and S. Carson. 2005. Influence of Stream Temperature on the Spatial Distribution of Westslope Cutthroat Trout Growth Potential within the Madison River Basin, Montana. North American Journal of Fisheries Management 25:225–237.
Stanford, J. A., M. S. Lorang, and F. R. Hauer. 2005. The shifting habitat mosaic of river ecosystems. Internationale Vereinigung für theoretische und angewandte Limnologie: Verhandlungen 29:123–136.
Stevens, L. E., E. R. Schenk, and A. E. Springer. 2021. Springs ecosystem classification. Ecological Applications 31.
Su, Y., and M. Yajima. 2021. R2jags: Using R to Run 'JAGS'. R package version 0.7-1, https://CRAN.R-project.org/package=R2jags.
Sullivan, C. J., J. C. Vokoun, A. M. Helton, M. A. Briggs, and B. L. Kurylyk. 2021. An ecohydrological typology for thermal refuges in streams and rivers. Ecohydrology 14:1–15.
Sweka, J. A., and T. Wagner. 2022. Influence of Seasonal Extreme Flows on Brook Trout Recruitment. Transactions of the American Fisheries Society 151:231–244.
Tague, C., M. Farrell, G. Grant, S. Lewis, and S. Rey. 2007. Hydrogeologic controls on summer stream temperatures in the McKenzie River basin, Oregon. Hydrological Processes 21:3288–3300.
Tague, C., G. Grant, M. Farrell, J. Choate, and A. Jefferson. 2008. Deep groundwater mediates streamflow response to climate warming in the Oregon Cascades. Climatic Change 86:189–210.
Thornton, P. E., R. Shrestha, M. Thornton, S. C. Kao, Y. Wei, and B. E. Wilson. 2021. Gridded daily weather data for North America with comprehensive uncertainty quantification. Scientific Data 8:1–17.
Torgersen, C. E., C. Le Pichon, A. H. Fullerton, S. J. Dugdale, J. J. Duda, F. Giovannini, E. Tales, J. Belliard, P. Branco, N. E. Bergeron, M. L. Roy, D. Tonollo, N. Lamouroux, H. Capra, and C. V. Baxter. 2021. Riverscape approaches in practice: perspectives and applications. Biological Reviews:1–24.
Travis, J. M. J., D. J. Murrell, and C. Dytham. 1999. The evolution of density-dependent dispersal. Proceedings of the Royal Society B: Biological Sciences 266:1837–1842.
Tsuboi, J., K. Morita, Y. Koseki, S. Endo, G. Sahashi, D. Kishi, T. Kikko, D. Ishizaki, M. Nunokawa, and Y. Kanno. 2022. Small giants: tributaries rescue spatially structured populations from extirpation in a highly fragmented stream. Journal of Applied Ecology:1–13.
Vehtari, A., A. Gelman, and J. Gabry. 2017. Practical Bayesian model evaluation using leave-one-out cross-validation and WAIC. Statistics and Computing 27:1413–1432.
Vincenzi, S., A. J. Crivelli, D. Jesensek, and G. A. De Leo. 2008. Total population density during the first year of life as a major determinant of lifetime body-length trajectory in marble trout. Ecology of Freshwater Fish 17:515–519.
Vincenzi, S., A. J. Crivelli, D. Jesensek, and G. A. De Leo. 2010. Individual growth and its implications for the recruitment dynamics of stream-dwelling marble trout (Salmo marmoratus). Ecology of Freshwater Fish 19:477–486.
Vollset, K. W., R. J. Lennox, E. B. Thorstad, S. Auer, K. Bär, M. H. Larsen, S. Mahlum, J. Näslund, H. Stryhn, and I. Dohoo. 2020. Systematic review and meta-analysis of PIT tagging effects on mortality and growth of juvenile salmonids. Reviews in Fish Biology and Fisheries 30:553–568.
Wagner, E. J., R. E. Arndt, and M. Brough. 2001. Comparitive tolerance of four stocks of cutthroat trout to extremes in temperature, salinity, and hypoxia. Western North American Naturalist 61:434–444.
Walsworth, T. E., D. E. Schindler, M. A. Colton, M. S. Webster, S. R. Palumbi, P. J. Mumby, T. E. Essington, and M. L. Pinsky. 2019. Management for network diversity speeds evolutionary adaptation to climate change. Nature Climate Change 9:632–636.
Ward, J. V. 1985. Thermal characteristics of running waters. Hydrobiologia 125:31–46.
Ward, J. V., F. Malard, K. Tockner, and U. Uehlinger. 1999. Influence of ground water on surface water conditions in a glacial flood plain of the Swiss Alps. Hydrological Processes 13:277–293.

Watson, A. S., M. J. H. Hickford, and D. R. Schiel. 2022. Interacting effects of density and temperature on fish growth rates in freshwater protected populations. Proceedings of the Royal Society B: Biological Sciences 289.

Webb, B. W., D. M. Hannah, R. D. Moore, L. E. Brown, and F. Nobilis. 2008. Recent advances in stream and river temperature research. Hydrological Processes 22:902–918.

Webb, J. H., and H. A. McLay. 1996. Variation in the time of spawning of Atlantic salmon (Salmo salar) and its relationship to temperature in the Aberdeenshire Dee, Scotland. Canadian Journal of Fisheries and Aquatic Sciences 53:2739–2744.

Wenger, S. J., D. J. Isaak, C. H. Luce, H. M. Neville, K. D. Fausch, J. B. Dunham, D. C. Dauwalter, M. K. Young, M. M. Elsner, B. E. Rieman, A. F. Hamlet, and J. E. Williams. 2011. Flow regime, temperature, and biotic interactions drive differential declines of trout species under climate change. Proceedings of the National Academy of Sciences 108:14175–14180.

Whiting, P. J., and D. B. Moog. 2001. The geometric, sedimentologic and hydrologic attributes of spring-dominated channels in volcanic areas. Geomorphology 39:131–149.

Wickham, H., M. Averick, J. Bryan, W. Chang, L. D. McGowan, R. François, G. Grolemund, A. Hayes, L. Henry, J. Hester, M. Kuhn, T. L. Pedersen, E. Miller, S. M. Bache, K. Müller, J. Ooms, D. Robinson, D. P. Seidel, V. Spinu, K. Takahashi, D. Vaughan, C. Wilke, K. Woo, and H. Yutani. 2019. Welcome to the tidyverse. Journal of Open Source Software 4:1686. https://doi.org/10.21105/joss.01686.

Wilson, K. L., A. C. Sawyer, A. Potapova, C. J. Bailey, D. LoScerbo, E. K. Sweeney-Bergen, E. E. Hodgson, K. J. Pitman, K. M. Seitz, L. K. Law, L. Warkentin, S. M. Wilson, W. I. Atlas, D. C. Braun, M. R. Sloat, M. T. Tinker, and J. W. Moore. 2023. The role of spatial structure in at-risk metapopulation recoveries. Ecological Applications 33:1–22.

Winograd, I. J., A. C. Riggs, and T. B. Coplen. 1998. The relative contributions of summer and cool-season precipitation to groundwater recharge, Spring Mountains, Nevada, USA. Hydrogeology Journal 6:77–93.

Winter, T. C. 1999. Relation of streams, lakes, and wetlands to groundwater flow systems. Hydrogeology Journal 7:28–45.

Winter, T. C. 2001. The concept of hydrologic landscapes. Journal of the American Water Resources Association 37:335–349.

Wright, P. R. 2013. Hydrogeology and water quality in the Snake River alluvial aquifer at Jackson Hole Airport, Jackson, Wyoming, water years 2011 and 2012: U.S. Geological Survey Scientific Investigations Report 2013-5184.

Wu, Q., and A. Brown. 2022. 'whitebox': 'WhiteboxTools' R Frontend. R package version 2.2.0, https://CRAN.R-project.org/package=whitebox.

Wyoming Game and Fish Department. 2001. Annual Fisheries Progress Report on the 2000 Work Schedule. Cheyenne, WY.

Wyoming Game and Fish Department. 2019. Annual Fisheries Progress Report on the 2019 Work Schedule. Cheyenne, WY.

Youngflesh, C. 2018. MCMCvis: Tools to visualize, manipulate, and summarize MCMC output. Journal of Open Source Software 3:640. https://doi.org/10.21105/joss.00640.

Figures

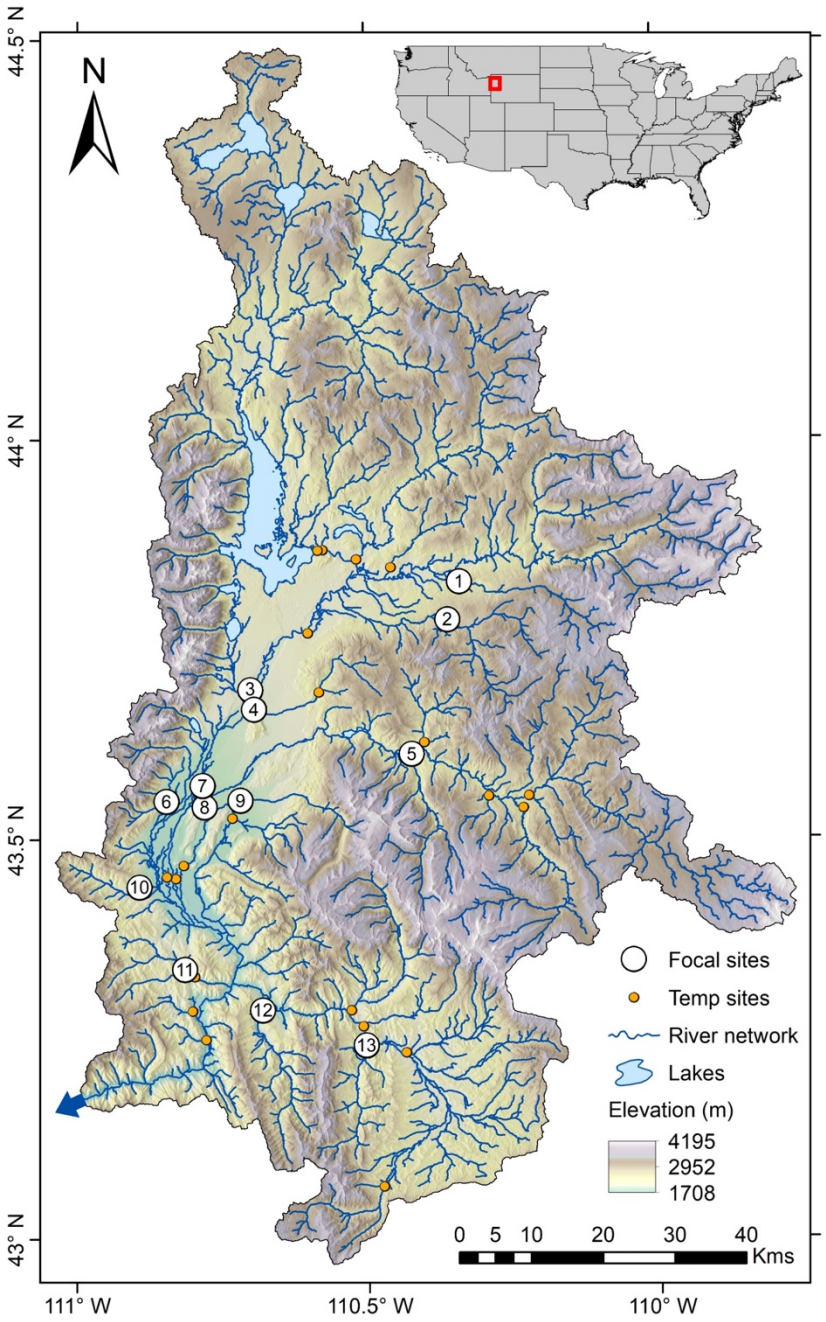

Figure 1 Map of the upper Snake River watershed, Wyoming, USA. White points denote focal streams for study of fish growth and production (numbered as in Appendix S1: Table S1). Orange points denote additional temperature monitoring locations. Basin drains to the southwest; outlet denoted by blue arrow. Blue lines represent the river network and blue polygons represent lentic waterbodies. Area of detail is marked by the red box in the inset map of the U.S.

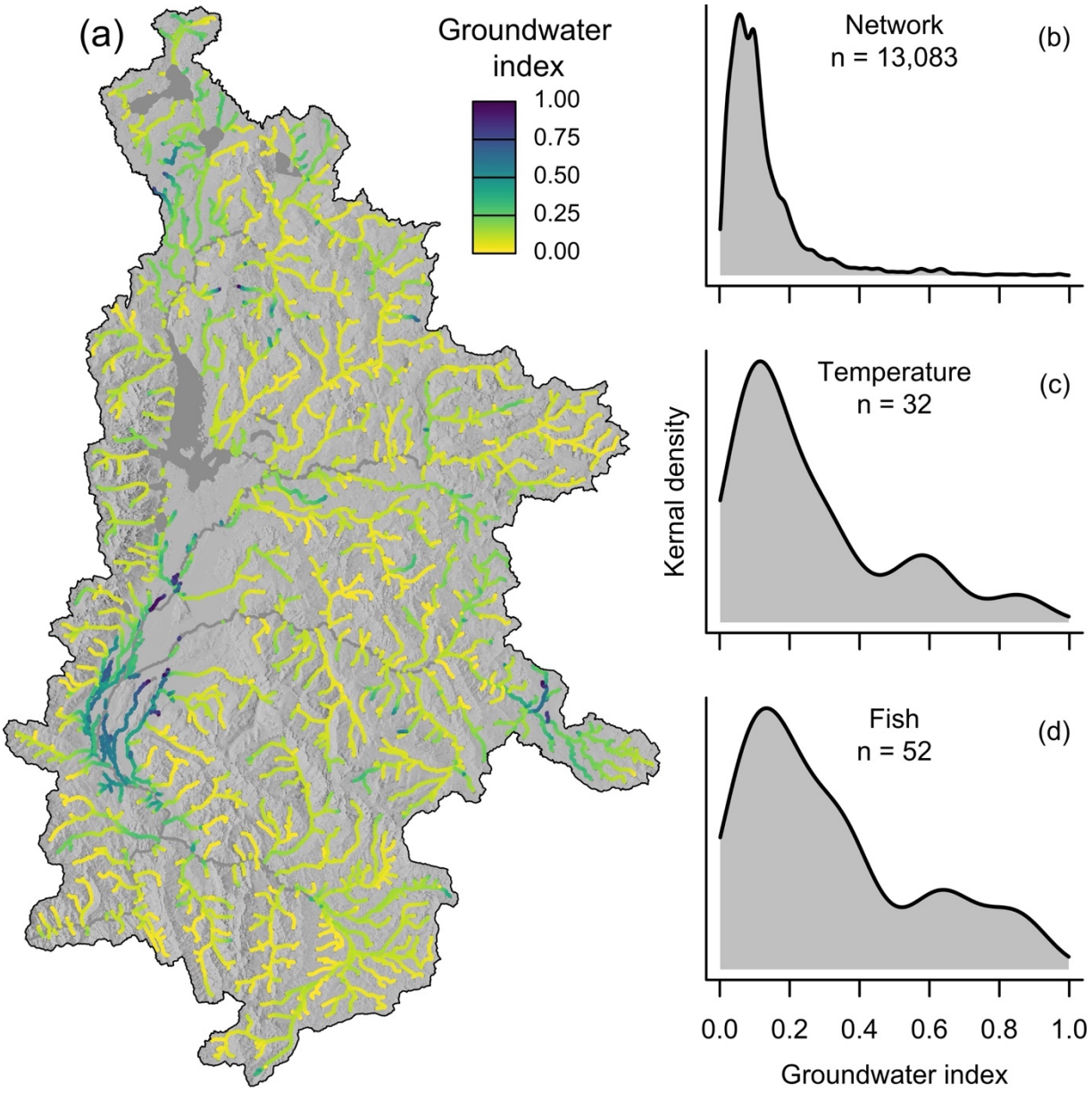

Figure 2 Groundwater is unevenly distributed across the upper Snake River watershed. (a) Index of groundwater influence in stream reaches, derived from the MaxEnt raster of groundwater spring prevalence. Greater index values (darker colors) signify increasing influence of groundwater on stream reach conditions. Dark grey polygons represent lentic waterbodies and dark grey flowlines represent large rivers for which we did not derive groundwater index values. Kernel density plots of groundwater index for (b) network locations, (c) stream temperature monitoring locations, and (d) fish study (focal) reaches.

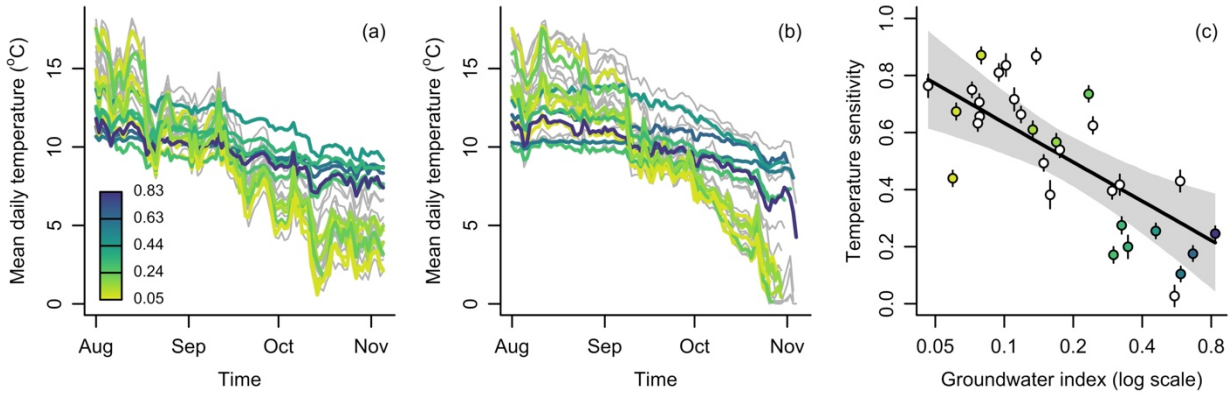

Figure 3 Groundwater structures temperature dynamics in streams: streams with greater groundwater influence are less sensitive to variability in air temperature. Stream water temperature throughout the study period (1 August – 5 November) in (a) 2021 and (b) 2022. (c) Effect of groundwater index on modeled stream temperature sensitivity to air temperature. Line color in (a) and (b) and point color in (c) indicates groundwater index in streams studied for YOY growth and production ("focal streams"). Grey lines in (a) and (b) and white points in (c) represent temperature monitoring at 19 additional locations.

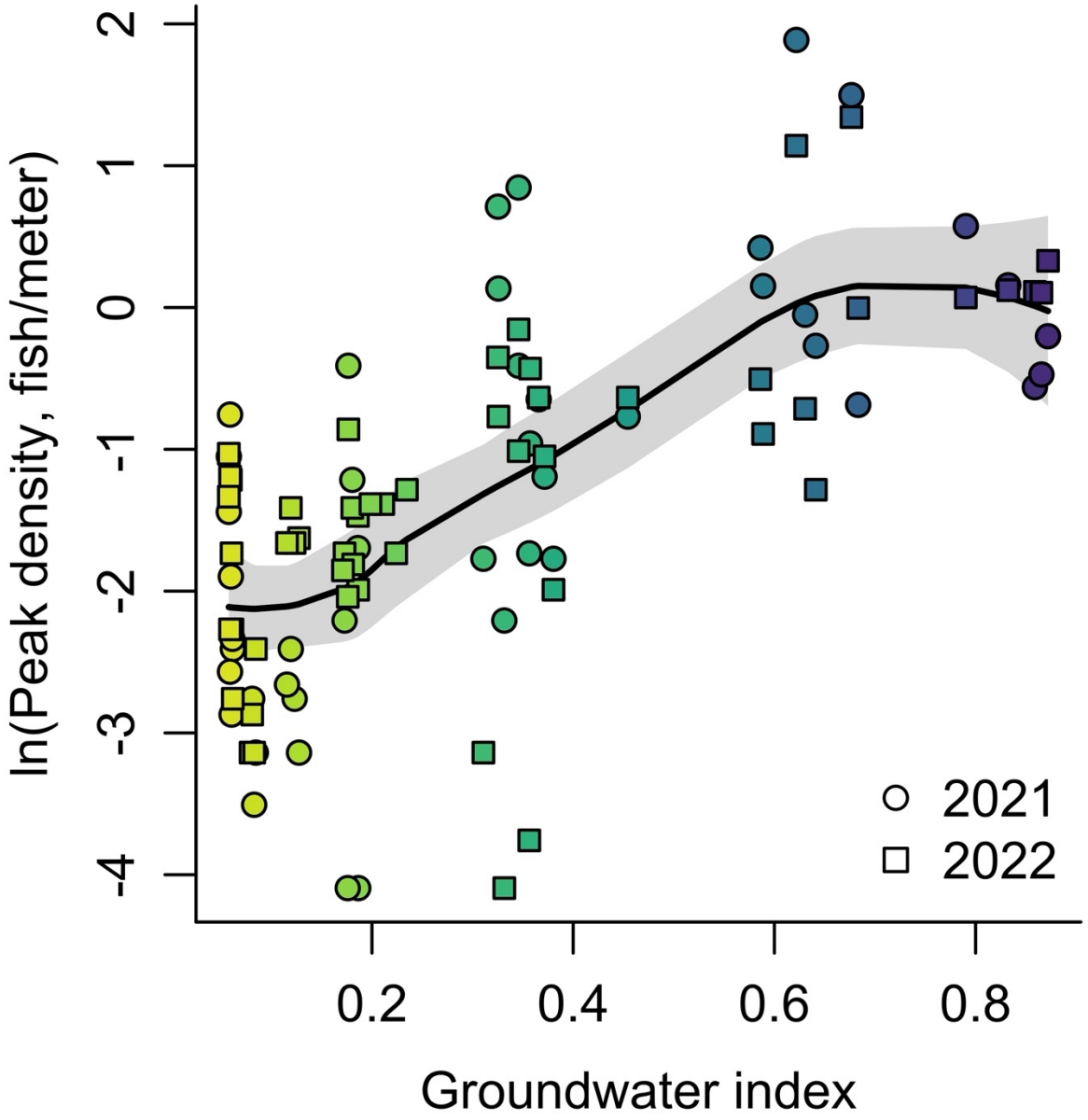

Figure 4 Relationship between groundwater index and (log) peak YOY density: streams with stronger groundwater influence have greater peak YOY densities, on average. Thick black line represents the LOESS smoother (mean); grey polygon represents the 95% confidence interval; point color indicates groundwater index.

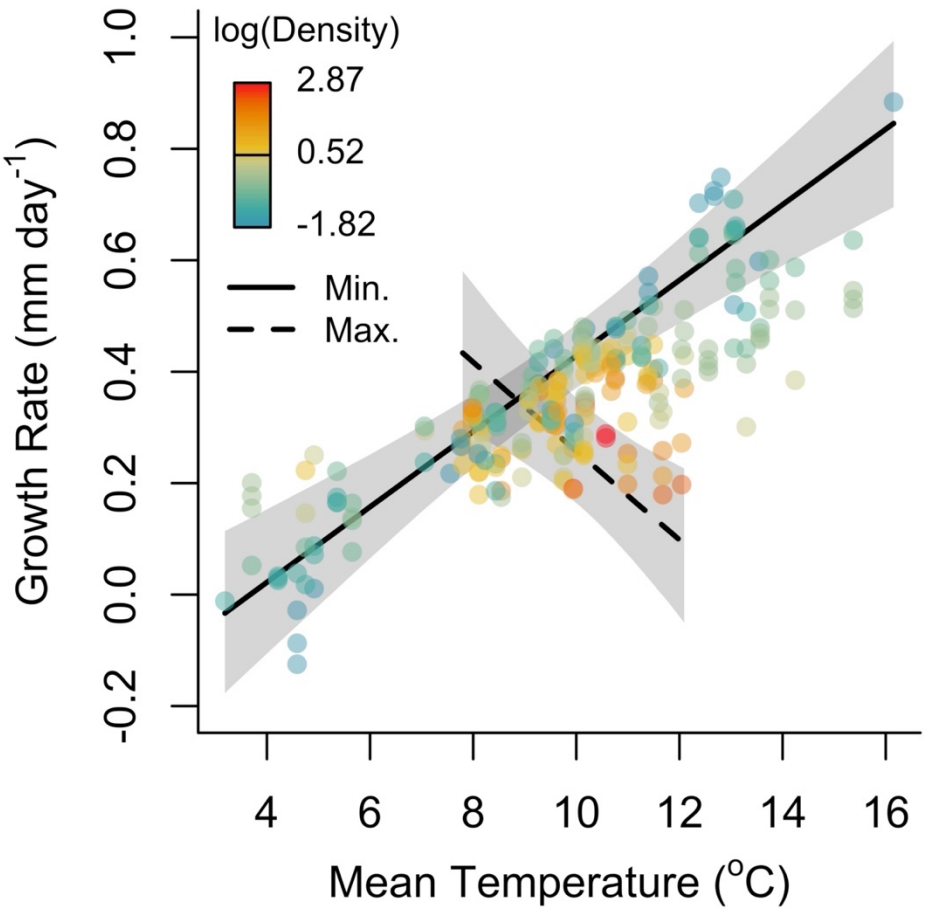

Figure 5 Temperature (°C) and density (fish m^{-1}) interactively affect YOY growth rate (mm day^{-1}). Temperature is the mean stream temperature between sampling events. Points represent model-estimated growth rates and point color denotes (log) YOY density. Solid and dashed regression lines denote the relationship between temperature and growth rate at the minimum (0.03 fish per meter) and maximum observed density (6.58 fish per meter), respectively, where the range of temperature for each regression is limited to the range of temperature observed for the lower and upper 25th percentiles of density. Grey polygons represent 95% credible intervals for each regression.

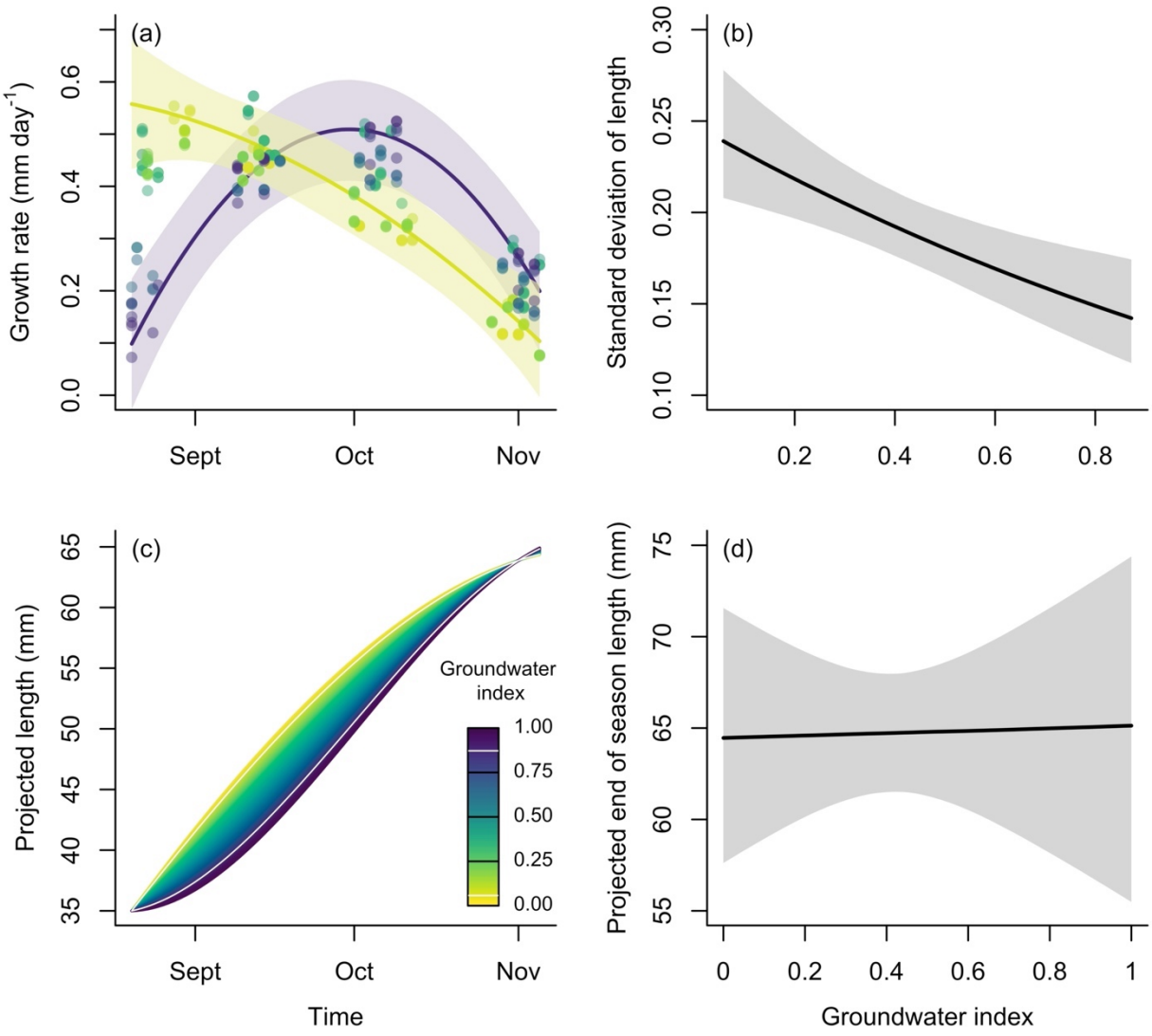

Figure 6 Groundwater mediates the temporal dynamics of YOY growth. (a) Interactive effects of time and groundwater index on growth rate. Regression lines represent growth regimes at the highest (0.87, purple) and lowest (0.06, yellow) observed groundwater index values. Points represent model-estimated growth rates and point color denotes groundwater index. (b) Effect of groundwater index on the standard deviation of estimated length. (c) Projected median YOY total body length from 20 August to 5 November under groundwater index values ranging between 0 and 1 (color). Thin white lines in the plot and color legend represent the range of groundwater index values across the 52 focal stream reaches (0.06-0.87). (d) Effect of groundwater index on projected end of season length. Thick black lines and grey polygons in (b) and (d) represent the median effect and 95% credible interval, respectively.

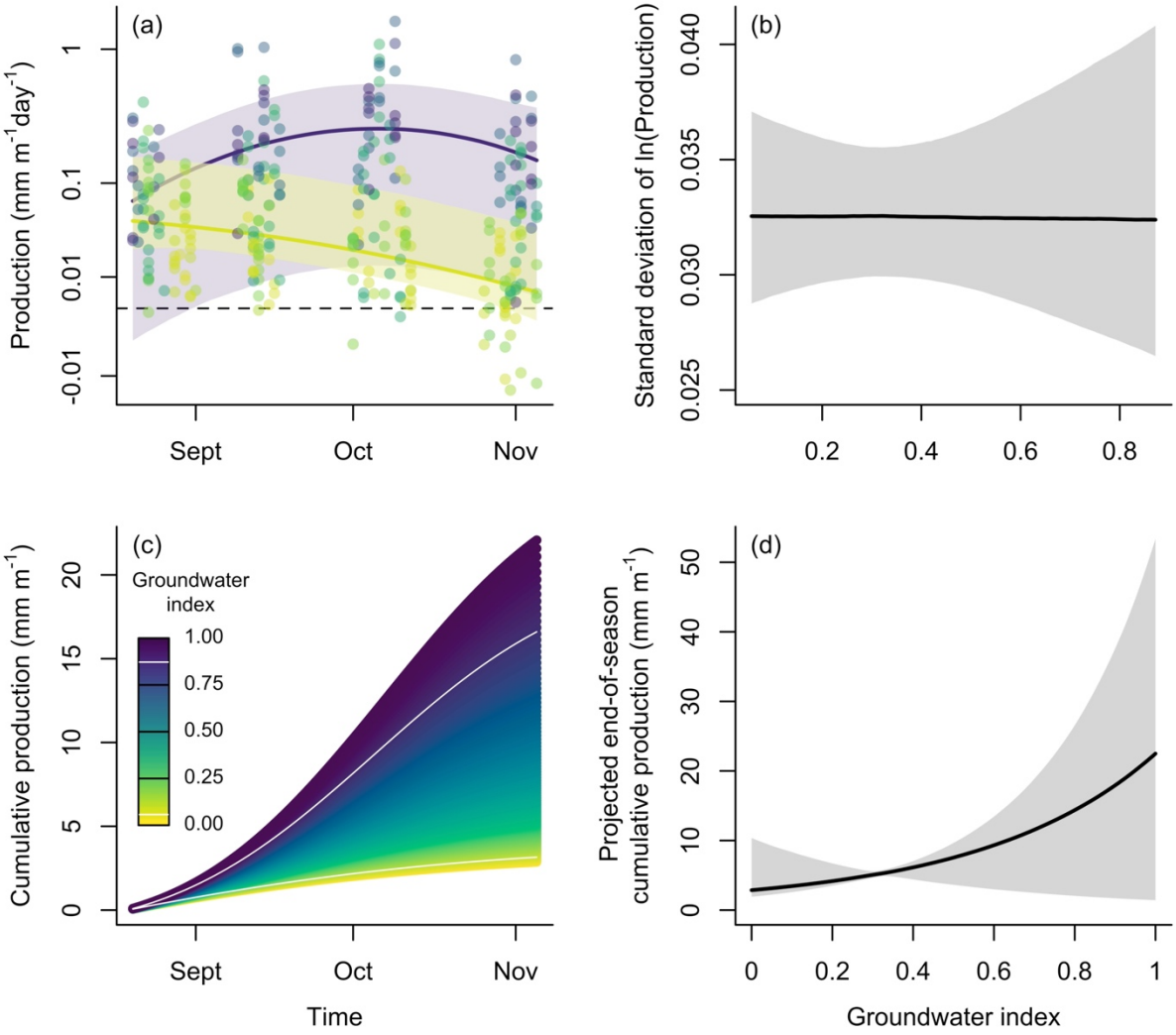

Figure 7 Groundwater mediates the temporal dynamics of YOY production. (a) Interactive effects of time and groundwater index on production, logged to meet assumptions of homoscedasticity. Regression lines represent production regimes at the highest (0.87, purple) and lowest (0.06, yellow) observed groundwater index values. Points represent calculated production (eq. 10) and point color denotes groundwater index. (b) Effect of groundwater index on the standard deviation of production. (c) Projected median cumulative YOY production from 20 August to 5 November under groundwater index values ranging between 0 and 1 (color). Thin white lines in the plot and color legend represent the range of groundwater index values across the 52 focal stream reaches (0.06-0.87). (d) Effect of groundwater index on projected end of season cumulative production. Thick black lines and grey polygons in (b) and (d) represent the median effect and 95% credible interval, respectively.

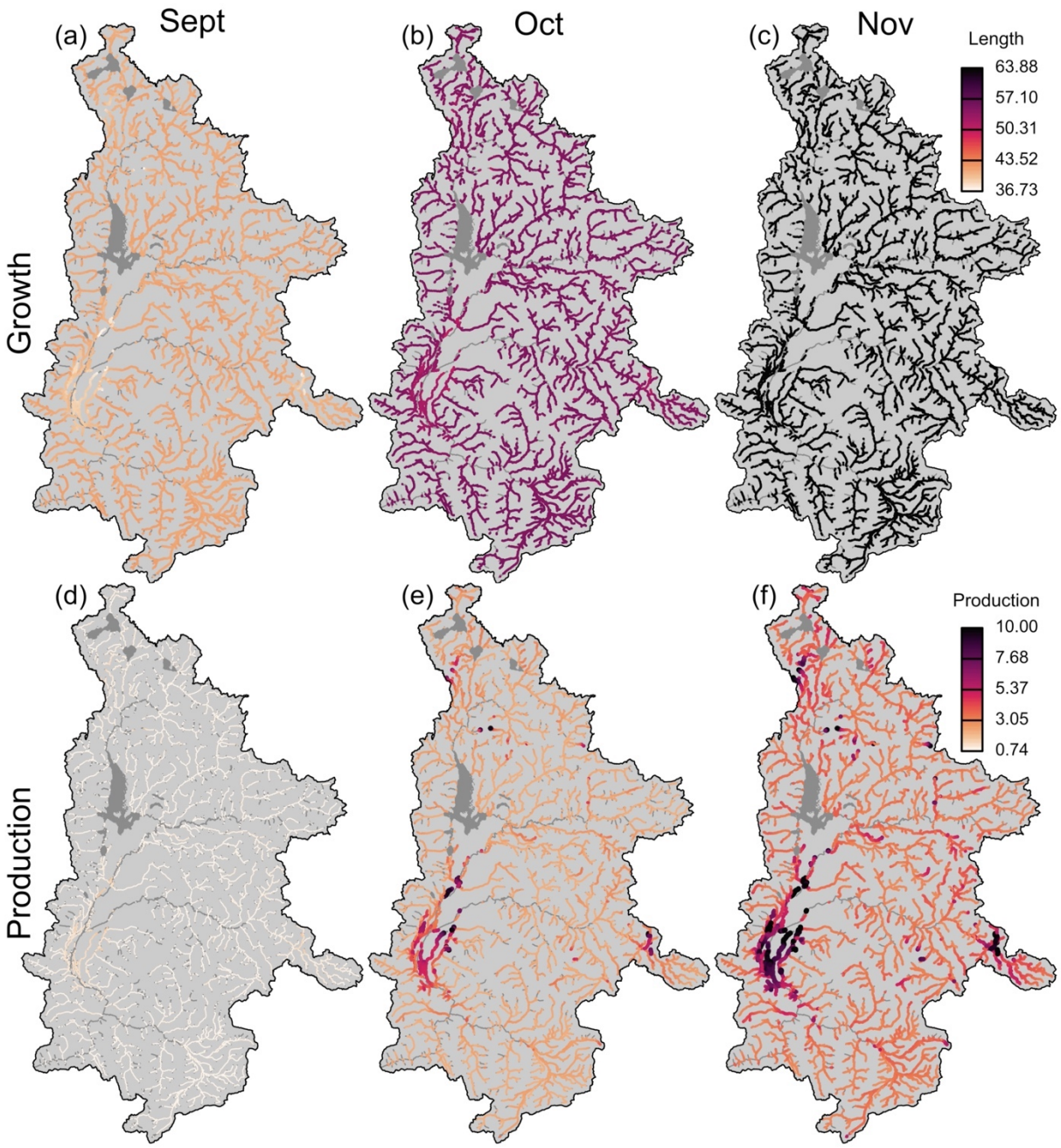

Figure 8 Groundwater structures the temporal dynamics of (a-c) growth and (d-f) production across the upper Snake River watershed. Riverscape projections are shown for (a,d) 1 September, (b,e) 1 October, and (c,f) 1 November. Projections are limited to stream reaches with gradients <10% and watersheds <500 km^2. Projected production is capped at 10 mm m^{-1} to aid visual interpretation (see Figure 7c for complete range).

Supporting Information

Table S1 Catchment characteristics for sites at which temperature monitoring was conducted. Characteristics were used in the temperature model to evaluate individual and interactive drivers of stream temperature response to air temperature. *Site* refers to the site name; *ID* denotes to sites where fish sampling was conducted, numbered as in Figure 1 of the main text (NA if fish monitoring was not conducted); *elev* is mean catchment elevation in meters; *slope* is mean catchment ground surface gradient (%); *forest* is the mean percent forest canopy cover within a 100 m buffer of the flow line; *area* is catchment area in square kilometers; *lake* is upstream lake area in square kilometers; *gw* is the normalized groundwater index calculated from the MaxEnt output raster of groundwater spring prevalence.

site	ID	elev	slope	forest	area	lake	gw
blackrock_1A	1	2739	12.68	0.19	124.82	0.015	0.08
blacktail_1A	4	2138	5.42	0.22	61.08	0.009	0.67
cabin_NA	NA	2213	22.40	0.29	23.51	0.001	0.08
cliff_1A	13	2451	20.57	0.30	158.60	0.048	0.13
cody_Moment	NA	1877	5.82	0.06	2.09	0.016	0.59
cottonwoodNPS	NA	2613	23.94	0.16	187.14	11.350	0.32
crystal_1A	5	2843	18.82	0.26	185.10	0.395	0.06
deadmans_1A	NA	2113	6.52	0.06	11.65	0.865	0.24
dell_NA	NA	2402	14.57	0.17	214.37	0.062	0.15
ditch_upper	NA	2511	13.56	0.28	67.68	0.093	0.09
dog_NA	NA	2245	21.34	0.26	31.11	0.005	0.08
fish_downstream	6	2318	18.59	0.12	38.71	0.002	0.46
flat_4B	9	2684	18.72	0.23	125.89	0.322	0.30
goosewing_NA	NA	2707	13.03	0.25	40.40	0.001	0.11
granite_NA	NA	2598	21.67	0.22	219.91	0.273	0.17
grosventre_upper	NA	2819	14.01	0.16	266.14	0.619	0.10
hoback_upper	NA	2698	19.74	0.19	113.89	0.006	0.12
lava_NA	NA	2457	15.58	0.33	67.66	0.005	0.07
lowerbarbc_SG	8	1952	3.53	0.16	6.40	0.002	0.59
mosquito_1A	10	2348	19.21	0.36	61.63	0.001	0.23
nowlin_NA	NA	2394	14.61	0.26	82.56	0.066	0.30
pacific_NA	NA	2479	12.21	0.20	418.22	9.675	0.08
shoal_NA	NA	2455	17.65	0.16	82.65	0.003	0.14
slate_NA	NA	2539	16.38	0.19	97.24	0.001	0.05
spread_1A	2	2698	15.68	0.23	196.85	0.043	0.06
spring_JLD	NA	2090	1.61	0.18	4.01	0.001	0.16
threechannel_1A	7	1983	3.35	0.18	31.61	0.010	0.33
threechannel_3A	NA	1917	0.85	0.11	0.70	0.005	0.35
unkspring_Ford	NA	1857	0.39	0.32	0.26	0.005	0.55
upperbarbc_SG	3	2031	2.42	0.04	5.74	0.037	0.83
willow_4B	12	2467	23.90	0.31	184.44	0.001	0.17

Table S2 Candidate model statements and leave-one-out cross validation (LOO; Vehtari et al. 2017) diagnostics for the analysis of temperature and density as drivers of fish growth rate. Predictor variables are defined as follows: *log(density)* = logged young-of-year density at the time of sampling (fish per meter of stream), *temp* = mean observed temperature between sampling events (°C), and *priorlen* = prior mean total length (mm). LOO diagnostics are defined as follows: $elpd_{loo}$ = expected log pointwise predictive density, $SE(elpd_{loo})$ = standard error of $elpd_{loo}$, $elpd_{diff}$ = estimated difference of $elpd_{loo}$ of the candidate model and top model, and $SE(elpd_{diff})$ = standard error of $elpd_{diff}$. Candidate models are ordered according to minimum $elpd_{loo}$.

Model Statement	**$elpd_{loo}$**	**$SE(elpd_{loo})$**	**$elpd_{diff}$**	**$SE(elpd_{diff})$**
log(density) + temp + log(density)*temp + priorlen	-733.05	11.89	0.00	0.00
log(density) + temp + $temp^2$ + log(density)*temp + priorlen	-733.13	11.95	-0.08	0.85
log(density) + temp + priorlen	-744.83	12.35	-11.78	4.81
temp + priorlen	-745.02	12.13	-11.97	5.78
temp + $temp^2$ + priorlen	-745.85	12.19	-12.79	5.87
priorlen	-747.81	11.80	-14.75	6.94
log(density) + priorlen	-748.11	11.92	-15.06	6.31

Table S3 Prior probability statements for all Bayesian models. *Model* denotes the model in question, where *Growth (covariates)* represents the model of growth as a function of temperature and density and *Growth (temporal)* represents the model of growth as a function of time and groundwater. Uniform distributions are parameterized in terms of the minimum and maximum, respectively. Normal distributions are parameterized in terms of the mean and standard deviation, respectively. *T(0,)* describes a truncated distribution, where the minimum allowable values is 0 (e.g., truncated to ensure positive values). Parameters in bold face represent vectors of parameters.

Model	**Prior probability specifications**		
Temperature	$\sigma' \sim U(0, 100)$	$\boldsymbol{\alpha_s'} \sim N(0, 30)$	$\beta_1' \sim N(0, 30)$
	$\omega \sim U(0, 100)$	$\varphi \sim N(0, 30)$	$\widehat{\boldsymbol{\gamma}} \sim N(0, 30)$
Growth (covariates)	$\ln(\rho'') \sim N(0, 10)$	$\theta'' \sim N(0, sigma.sb'')$	$sigma.sb'' \sim N(0, 10)\ T(0,)$
	$\alpha'' \sim N(0, 10)$	$\boldsymbol{\beta}'' \sim N(0, 10)$	
	$\alpha_y'' \sim N(0, sigma.yr'')$	$\alpha_s'' \sim N(0, sigma.st'')$	$\alpha_{s_r}'' \sim N(\alpha_s'', sigma.se'')$
	$sigma.yr'' \sim N(0, 10)\ T(0,)$	$sigma.st'' \sim N(0, 10)\ T(0,)$	$sigma.se'' \sim N(0, 10)\ T(0,)$
Growth (temporal)	$\ln(\rho''') \sim N(0, 10)$	$\theta''' \sim N(0, sigma.sb''')$	$sigma.sb''' \sim N(0, 10)\ T(0,)$
	$\alpha''' \sim N(0, 10)$	$\boldsymbol{\beta}''' \sim N(0, 10)$	
	$\alpha_y''' \sim N(0, sigma.yr''')$	$\alpha_s''' \sim N(0, sigma.st''')$	$\alpha_{s_r}''' \sim N(\alpha_s''', sigma.se''')$
	$sigma.yr''' \sim N(0, 10)\ T(0,)$	$sigma.st''' \sim N(0, 10)\ T(0,)$	$sigma.se''' \sim N(0, 10)\ T(0,)$
Production	$\ln(\rho'''') \sim N(0, 10)$	$\theta'''' \sim N(0, sigma.sb'''')$	$sigma.sb'''' \sim N(0, 10)\ T(0,)$
	$\alpha'''' \sim N(0, 10)$	$\boldsymbol{\beta}'''' \sim N(0, 10)$	
	$\alpha_y'''' \sim N(0, sigma.yr'''')$	$\alpha_s'''' \sim N(0, sigma.st'''')$	$\alpha_{s_r}'''' \sim N(\alpha_s'''', sigma.se'''')$
	$sigma.yr'''' \sim N(0, 10)\ T(0,)$	$sigma.st'''' \sim N(0, 10)\ T(0,)$	$sigma.se'''' \sim N(0, 10)\ T(0,)$

Table S4 Fixed effect parameter estimates (*Median*) and 95% credible intervals (*2.5% CI* and *97.5% CI* define the lower and upper bounds, respectively) for each Bayesian model (*Model*). *Growth (covariates)* represents the model of growth as a function of temperature and density and *Growth (temporal)* represents the model of growth as a function of time and groundwater. *Parameter* denotes the parameter as defined in the main text and Appendix 1: Table S3. *Description* describes the fixed effect variable that each parameter represents.

Model	Parameter	Description	Median	2.5% CI	97.5% CI
Temperature	γ_1	slope	-0.013	-0.131	0.106
	γ_2	forest	-0.018	-0.112	0.075
	γ_3	log(catchment area)	0.068	-0.074	0.211
	γ_4	log(lake area)	-0.036	-0.121	0.045
	γ_5	log(gw)	-0.162	-0.247	-0.076
	γ_6	slope * log(gw)	0.060	-0.054	0.182
	γ_7	forest * log(gw)	-0.023	-0.101	0.053
	γ_8	log(catchment area) * log(gw)	-0.041	-0.160	0.075
	γ_9	log(lake area) * log(gw)	0.034	-0.060	0.127
Growth (covariates)	β_1''	log(density)	-0.032	-0.061	-0.001
	β_2''	temperature	0.027	-0.020	0.068
	β_3''	prior length	-0.087	-0.127	-0.052
	β_4''	log(density) * temperature	-0.079	-0.111	-0.047
Growth (temporal)	β_1'''	doy	-0.080	-0.104	-0.054
	β_2'''	doy^2	-0.082	-0.114	-0.052
	β_3'''	gw	0.035	-0.016	0.085
	β_4'''	doy * gw	0.058	0.035	0.082
	β_5'''	doy^2 * gw	-0.041	-0.068	-0.014
Production (temporal)	β_1''''	doy	-0.173	-0.250	-0.096
	β_2''''	doy^2	-0.169	-0.265	-0.072
	β_3''''	gw	0.602	-0.443	0.936
	β_4''''	doy * gw	0.188	0.111	0.267
	β_5''''	doy^2 * gw	-0.087	-0.179	0.003

Table S5 Unique numeric identifier (ID), name, and description of bedrock geological units used in MaxEnt modeling of groundwater spring prevalence. *ID* corresponds to bar labels in Appendix 1: Figure S1j. *Solo* and *Marginal* represent the predicted spring prevalence for each unit in a model fit with bedrock geology as the sole covariate (Appendix 1: Figure S1j) and the full model, respectively.

ID	Name	Description	Solo	Marginal
1	Qa	Alluvium and colluvium	0.18	0.016
2	Qt	Gravel, pediment, and fan deposits	0.2	0.008
3	Qg	Glacial deposits	0.051	0.009
4	Qls	Landslide deposits	0.027	0.005
7	Qu	Undivided surficial deposits	0.013	0.003
8	Qb	Basalt flows, tuff, and intrusive igneous rocks	0.01	0.002
9	Qr	Rhyolite flows, tuff, and intrusive igneous rocks	0.066	0.014
12	QTc	Conglomerate: Jackson Hole (Pleistocene or Pliocene); Med Bow (Pleistocene to Miocene)	0.01	0.002
15	Tte	Teewinot formation, Central Jackson Hole	0.091	0.149
16	Tr	Red Conglomerate on top of Hoback and Wyoming Ranges	0.01	0.002
17	Thr	Huckleberry ridge tuff of Yellowstone group	0.01	0.002
18	Tii	Intrusive and extrusive igneous rocks	0.01	0.002
20	Tsi	Shooting Iron Formation	0.01	0.002
22	Tcd	Camp Davis formation, southernmost Jackson Hole	0.01	0.002
23	Tc	Colter formation, central Jackson Hole	0.01	0.002
34	Twd	Wasatch formation, diamictite and sandstone	0.01	0.002
38	Ti	Intrusive igneous rocks	0.01	0.002
39	Twi	Wiggins Formation	0.01	0.002
40	Ttl	Intrusive Igneous rocks: Thorofare Creek group: Two Ocean and Langford formations, may include Trout Peak Trachyandesite of Sunlight Group	0.01	0.002
42	Ta	Intrusive igneous rocks: Thorofare Creek group: Aycross formation	0.037	0.008
47	Thp	Intrusive Igneous Rocks: Hominy Peak formation	0.01	0.002
50	Tv	Volcanic conglomerate - Jackson Hole	0.01	0.002
51	Twdr	Wind River formation - at base locally includes equivalent of Indian Meadows formation	0.233	0.065
56	Tdb	Devils Basin formation	0.01	0.002
57	TKp	Pinyon conglomerate	0.01	0.002
75	Twlc	Wasatch formation: La Barge and Chappo members	0.01	0.002
78	Tp	Bass Peak formation and equivalents	0.031	0.012
80	Th	Hoback formation	0.01	0.002
102	Kbb	Blind Bull formation	0.01	0.002
104	Kf	Frontier formation	0.08	0.016
107	Ka	Aspen shale	0.01	0.002
108	Kbr	Bear River formation	0.01	0.002
109	Kg	Gannett group	0.01	0.002
110	Jst	Stump formation, Preuss sandstone or redbeds, and Twin Creek limestone	0.01	0.002
111	J@n	Nugget sandstone	0.01	0.002
112	J@nd	Nuggest sandstone and Chugwater and Dinwoody Formations	0.01	0.002
114	Pp	Phosphoria formation and related rocks	0.01	0.002
115	P&Ma	Phosphoria, Wells, and Amsden formations	0.01	0.002
118	MD	Madison limestone and Darby formation	0.009	0.002
120	O_	Bighorn dolomite, Gallatin limestone, GrosVentre formation, and Flathead sandstone	0.044	0.008
123	Kc	Cody shale	0.01	0.002
126	@cd	Chugwater and Dinwoody formations	0.01	0.002
130	Kha	Harebell formation	0.01	0.002
134	Km	Meeteetse formation	0.01	0.002
137	Kmv	Mesaverde group	0.01	0.002
138	Kso	Sohare formation	0.01	0.002
139	Ksb	Sohare formation and Bacon Ridge sandstone	0.032	0.012
140	Kb	Bacon Ridge sandstone	0.039	0.011
147	Kmt	Mowry and Thermoplis shales	0.044	0.01
148	KJ	Clvoerly and Morrison formations	0.01	0.002
150	KJg	Cloverly, Morrison, Sundance and Gypsum Spring formations	0.054	0.028
153	Jsg	Sundance and Gypsum Spring formations	0.01	0.002
165	PM	TenSleep sandstone and Amsden formation	0.01	0.002
199	Wgn	Granite Gneiss	0.01	0.002
200	WVsv	Metasedimentary and Metavolcanic Rocks	0.01	0.002
202	Wmu	Metamorphosed Mafic and Ultramafic Rocks	0.01	0.002
203	Ugn	Oldest Gneiss Complex	0.01	0.002
216	Wg	Granitic Rocks of 2,600Ma Age Group	0.027	0.005
299	H2O	Water	0.01	0.002

Table S6 Unique numeric identifier (ID), name, and description of surficial geological units used in MaxEnt modeling of groundwater spring prevalence. *ID* corresponds to bar labels in Appendix 1: Figure S1k. *Solo* and *Marginal* represent the predicted spring prevalence for each unit in a model fit with surficial geology as the sole covariate (Appendix 1: Figure S1k) and the full model, respectively.

ID	Name	Description	Solo	Marginal
1	Gcsg	glaciated bedrock mixed with colluvium, slopewash and glacial rubble	0.038	0.019
2	Gg	glaciated bedrock mixed with glacial deposits	0.037	0.027
3	Ggc	glaciated bedrock mixed with glacial deposits and colluvium	0.084	0.069
4	Ggcs	glaciated bedrock mixed with glacial deposits, colluvium and slopewash	0.028	0.016
5	Ggs	glaciated bedrock mixed with glacial deposits and slopewash	0.028	0.016
6	Glg	glaciated bedrock mixed with landslide and/or glacial deposits	0.028	0.016
7	Gr	glaciated bedrock mixed with residuum	0.028	0.016
8	Gsu	glaciated bedrock mixed with slopewash and grus	0.028	0.016
9	LAKE	lake - lentic waterbody	0.028	0.016
10	RGc	bedrock and glaciated bedrock covered in places by colluvium	0.028	0.016
11	RGcs	bedrock and glaciated bedrock covered in places by colluvium and slopewash	0.028	0.016
12	RGg	bedrock and glaciated bedrock covered in places by glacial rubble	0.028	0.016
13	RGr	bedrock and glaciated bedrock covered in places by residuum	0.028	0.016
14	Rc	bedrock covered in places by colluvium	0.028	0.016
15	Rcg	bedrock covered in places by colluvium and glacial rubble	0.028	0.016
16	Rcs	bedrock covered in places by colluvium and slopewash	0.021	0.016
17	Rcsg	bedrock covered in places by colluvium, slopewash, and glacial rubble	0.028	0.016
18	Rcsr	bedrock covered in places by colluvium, slopewash, and residuum	0.028	0.016
19	Rcu	bedrock covered in places by colluvium and grus	0.028	0.016
20	Rgc	bedrock covered in places by glacial deposits and colluvium	0.028	0.016
22	Rrcs	bedrock covered in places by residuum, colluvium, and slopewash	0.028	0.016
23	Rrg	bedrock covered in places by residuum and glacial rubble	0.028	0.016
24	Rrs	bedrock covered in places by residuum and slopewash	0.234	0.068
25	Rs	bedrock covered in places by slopewash	0.028	0.016
26	Rsg	bedrock covered in places by slopewash and glacial rubble	0.028	0.016
27	a	alluvium - stream and river deposits	0.196	0.016
28	ag	alluvial deposits mixed with glacial deposits	0.028	0.016
29	ah	alluvial deposits mixed with hot spring deposits	0.028	0.016
30	c	colluvium - loose and incoherent deposits, usually at the foot of a cliff or on the surface of a slope and there chiefly by gravity	0.028	0.016
31	cf	colluvium mixed with alluvial fan deposits	0.028	0.016
32	cs	colluvium mixed with slopewash	0.028	0.016
33	csR	colluvium mixed with and slopewash with bedrock outcrops	0.015	0.012
34	csgG	colluvium mixed with slopewash, glacial rubble and glaciated bedrock	0.028	0.016
35	csgR	colluvium mixed with slopewash, glacial rubble and bedrock outcrops	0.19	0.247
36	e	eolian deposits - wind blown deposits, includes sand, silt, and clay	0.028	0.016
37	f	alluvial fan deposits - a fan shaped deposit made by a stream or a debris flow where they have run out onto a level plain	0.034	0.009
38	fa	alluvial fan deposits that grade into alluvial deposits	0.028	0.016
39	ft	alluvial fan deposits that grade into terrace deposits	0.028	0.016
40	g	glacial deposits - deposits that have been formed through glacial action, such as till and moraine	0.052	0.022
41	gR	glacial deposits mixed with bedrock outcrops	0.028	0.016
42	ge	glacial deposits mixed with eolian (loess) deposits	0.167	0.024
43	grs	glacial deposits mixed with residuum, and slopewash deposits	0.028	0.016
44	l	landslide - earth and rock which became loosened from a hillside and slides, flows, or falls down the slope	0.032	0.016
45	lg	landslide debris and/or glacial/periglacial deposits	0.045	0.022
46	o	glacial outwash - alluvium and drift deposited by meltwater streams beyond active glacier ice	0.328	0.082
47	oe	glacial outwash deposits mixed with scattered eolian deposits	0.457	0.047
48	rRg	residuum mixed with bedrock outcrops and glacial deposits	0.028	0.016
49	raR	residuum mixed with alluvial deposits and bedrock outcrops	0.028	0.016
50	rcs	residuum mixed with colluvium and slopewash	0.028	0.016
51	rs	residuum mixed with slopewash	0.122	0.076
52	rsR	residuum mixed with slopewash and bedrock outcrops	0.02	0.006
53	rsRg	residuum mixed with slopewash, bedrock outcrops, and glacial rubble	0.028	0.016
54	rse	residuum mixed with slopewash and scattered eolian deposits	0.028	0.016
56	rsg	residuum mixed with slopewash and glacial deposits	0.096	0.016
57	rsgR	residuum mixed with slopewash, glacial deposits, and bedrock outcrops	0.028	0.016
60	srR	slopewash mixed with residuum and bedrock outcrops	0.028	0.016
61	t	terrace deposits - relict alluvial deposits on relatively flat, horizontal, or gently inclined surfaces which are bounded by a steeper ascending slope on one side and by a steeper descending slope on the opposite side	0.212	0.016
62	td	dissected terrace deposits	0.028	0.016
63	te	terrace deposits mixed with scattered eolian deposits	0.028	0.016
64	w	lacustrine deposits - deposits associated with lakes	0.028	0.016

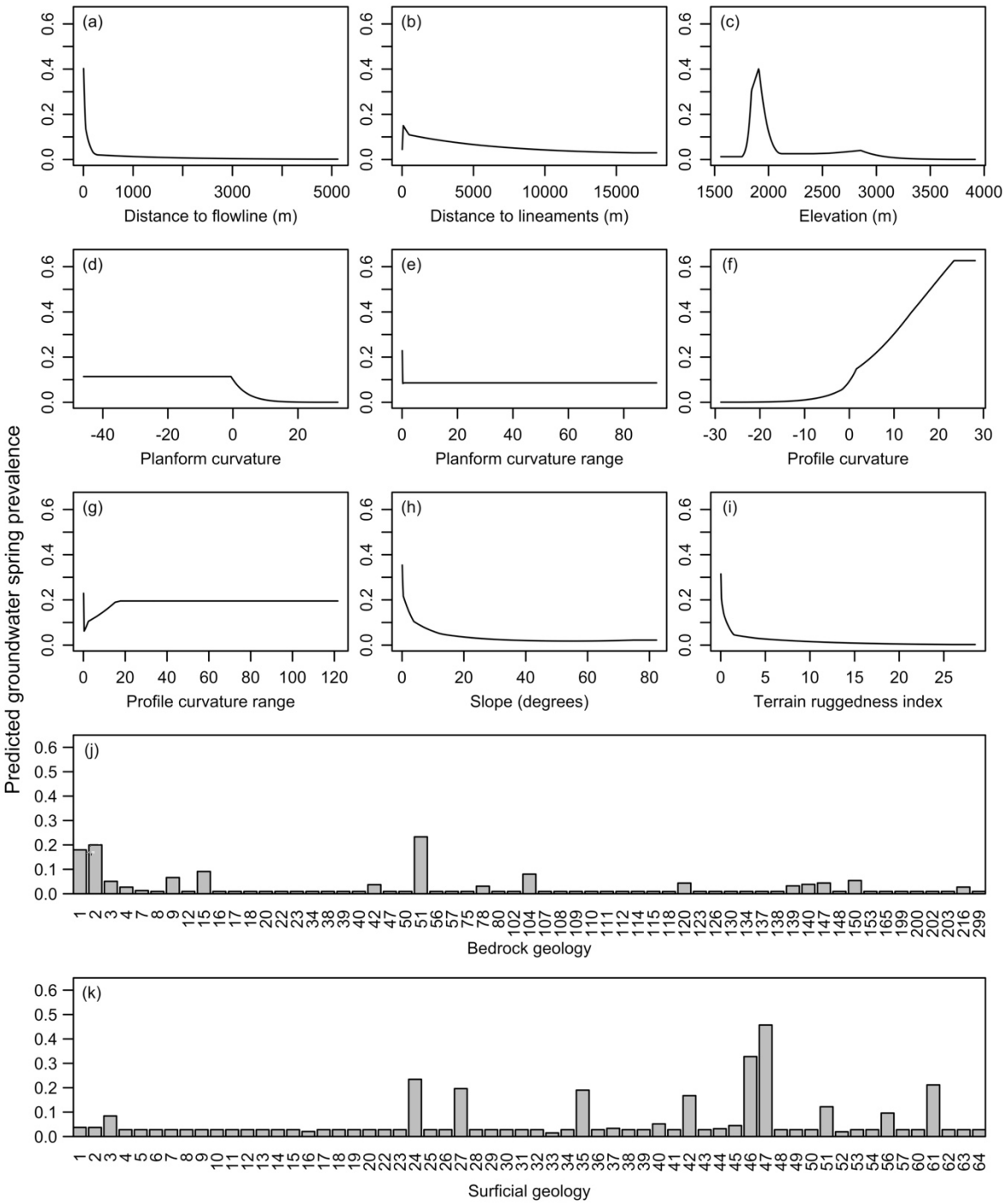

Figure S1 Effects of eleven landscape covariates on predicted probability of groundwater spring prevalence. To aid interpretation, each panel represents a different MaxEnt model created using only the variable in question, thus reflecting the dependence of predicted prevalence both on the variable in question and on dependencies induced by correlations between the variable in question and other variables. Numbered bars in panels (j) and (k) correspond to the ID columns in Appendix 1: Table S5 and Appendix 1: Table S6, respectively (this document).

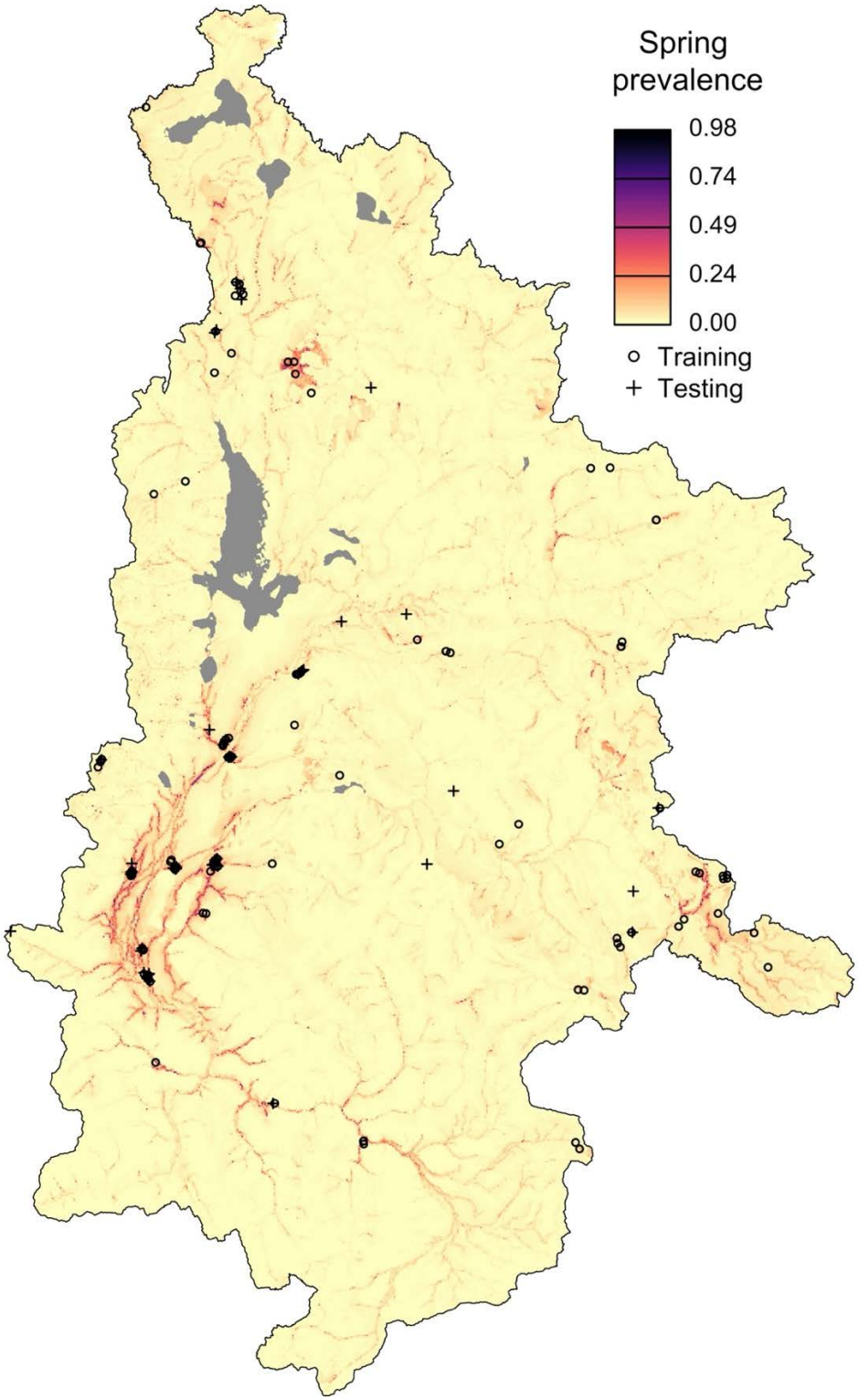

Figure S2 Prevalence of groundwater seeps throughout the upper Snake River watershed, Wyoming, U.S.A., predicted using MaxEnt. Seeps are most likely to occur where prevalence values are highest. Prevalence is predicted continuously across the study area on a *ca.* 10 m x 10 m grid. *Points* represent observed locations of springs used for training (o) and testing (+). *Grey polygons* represent lentic waterbodies (lakes).

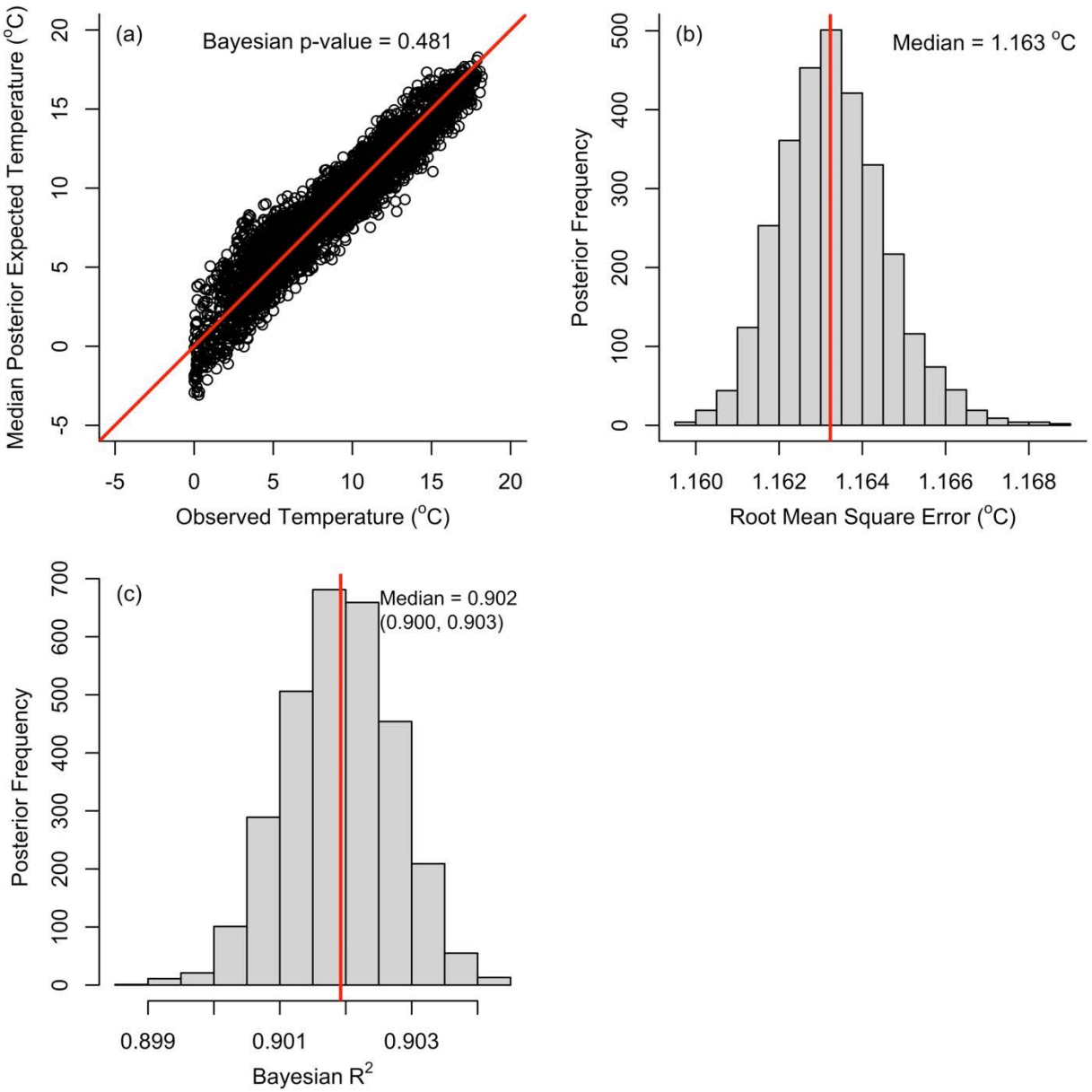

Figure S3 Diagnostic plots for the Bayesian stream temperature model. (a) Posterior predictive check showing the relationship between median posterior expected (i.e., predicted) temperature and observed temperature (°C); *red* line indicates the 1:1 line for visual reference; Bayesian p-value represents the proportion of predicted data that is greater than observed data. (b) Posterior distribution of root mean squared error (RMSE); *red line* denotes the median (1.163 °C). (c) Bayesian R^2 posterior distribution; values in parentheses represent the 95% credible interval.

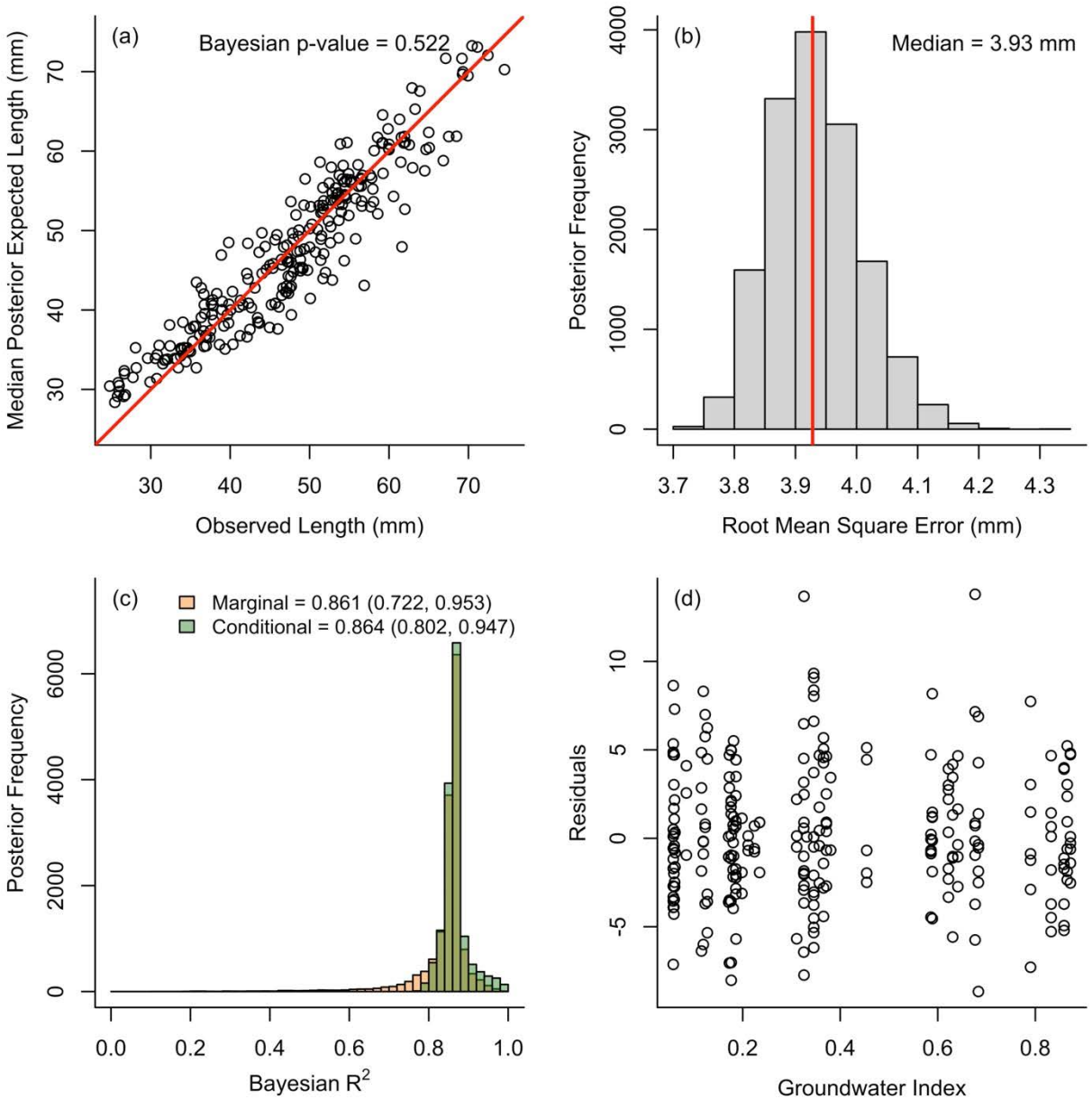

Figure S4 Diagnostic plots for the Bayesian hierarchical model describing the effects of temperature and density on growth. (a) Posterior predictive check showing the relationship between median posterior expected (i.e., predicted) length and observed length (mm); *red* line indicates the 1:1 line for visual reference; Bayesian p-value represents the proportion of predicted data that is greater than observed data. (b) Posterior distribution of root mean squared error (RMSE); *red line* denotes the median (3.93 mm). (c) Posterior distributions for the marginal (proportion of total variance explained by the fixed effects alone; *orange fill*) and conditional (proportion of total variance explained by the fixed and random effects; *green fill*) Bayesian R^2 values; values in legend represent medians and 95% credible intervals. (d) Relationship between model residuals and groundwater index.

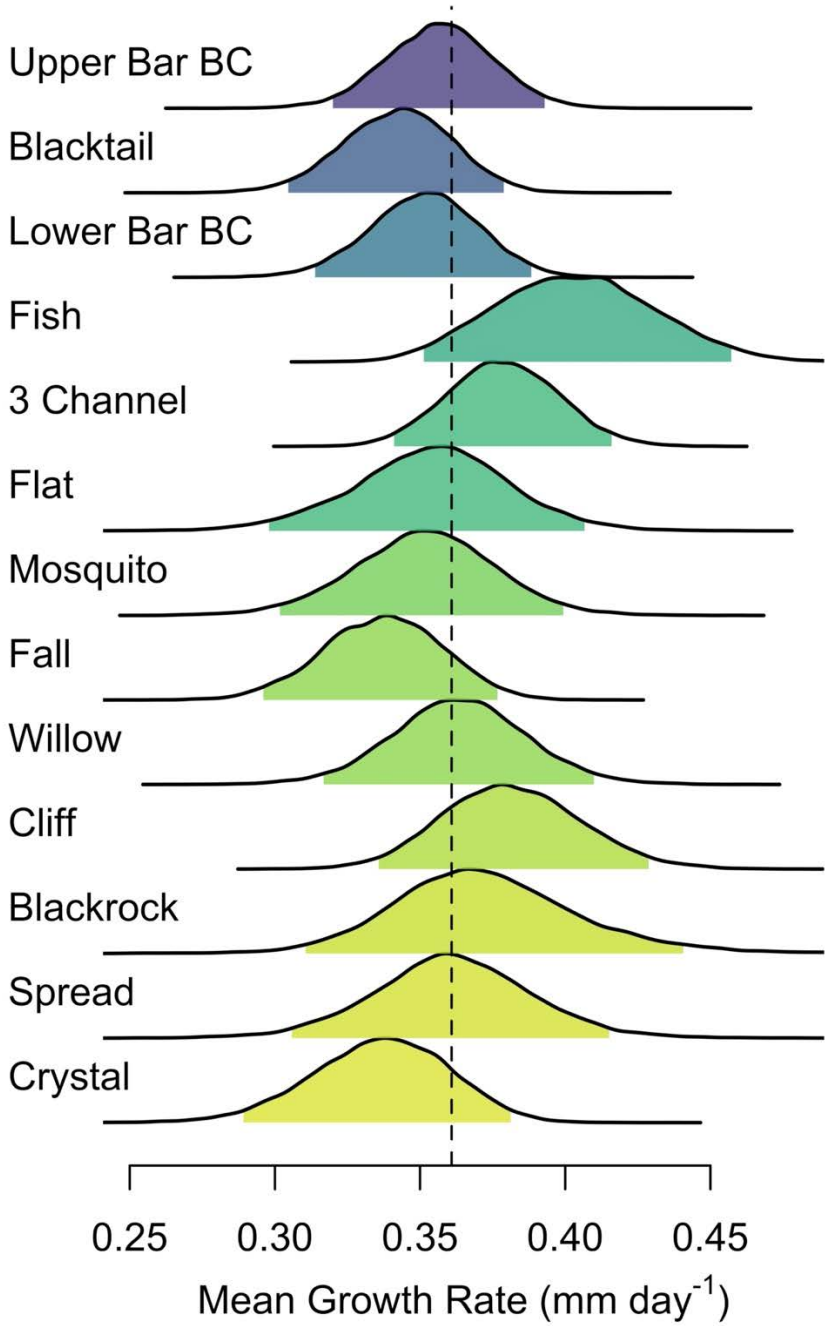

Figure S5 Posterior probability distributions for stream-specific intercepts from the Bayesian hierarchical model describing the effects of temperature and density on growth, where the intercepts describe mean growth rate (mm day^{-1}) in each stream. Streams are ordered from highest (*top*) to lowest (*bottom*) groundwater index. *Vertical dashed line* denotes the global mean growth rate (0.361 mm day^{-1}) for an average sized fish.

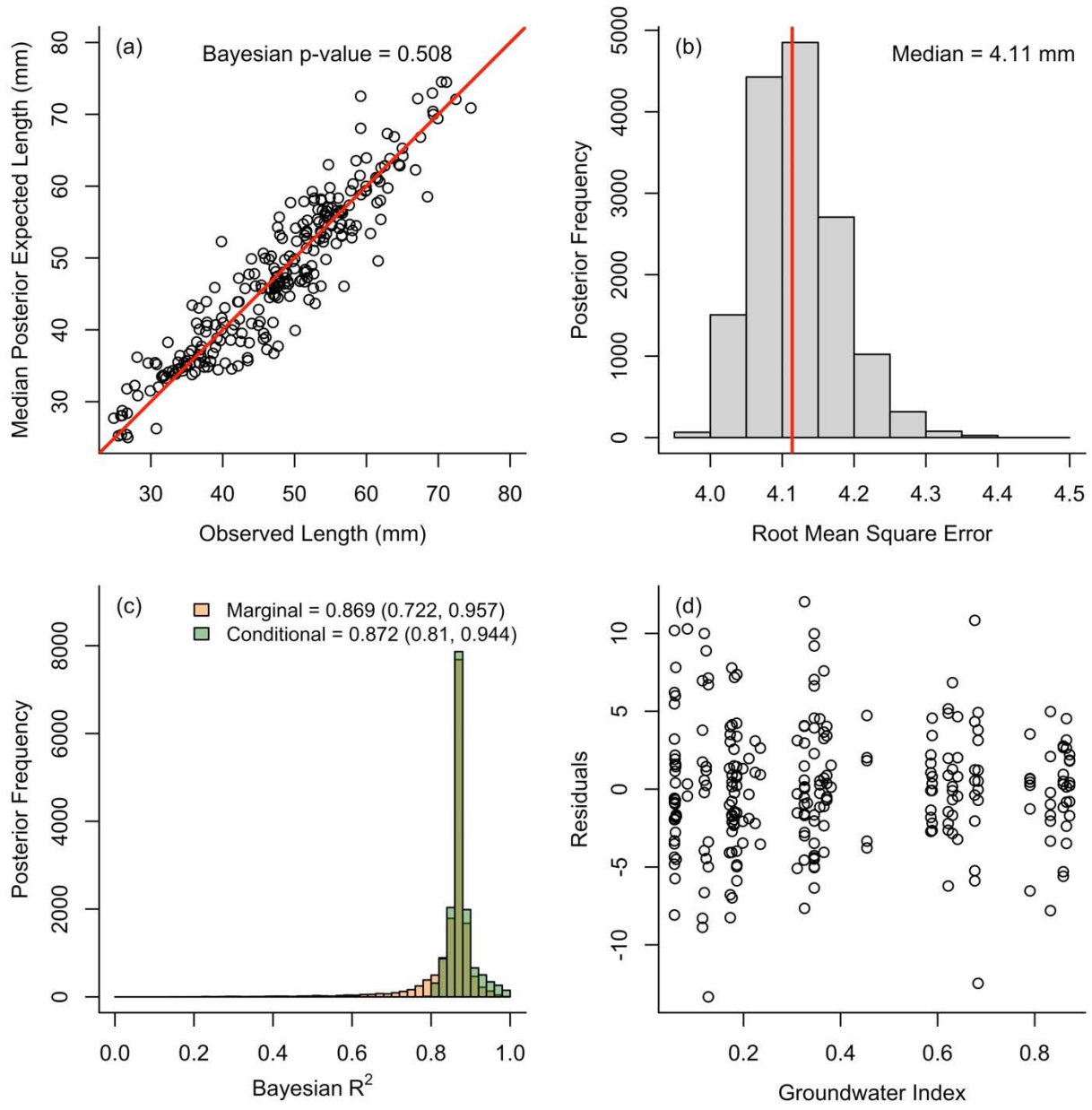

Figure S6 Diagnostic plots for the Bayesian hierarchical model describing the effects of time and groundwater on growth. (a) Posterior predictive check showing the relationship between median posterior expected (i.e., predicted) length and observed length (mm); *red* line indicates the 1:1 line for visual reference; Bayesian p-value represents the proportion of predicted data that is greater than observed data. (b) Posterior distribution of root mean squared error (RMSE); *red line* denotes the median (4.11 mm). (c) Posterior distributions for the marginal (proportion of total variance explained by the fixed effects alone; *orange fill*) and conditional (proportion of total variance explained by the fixed and random effects; *green fill*) Bayesian R^2 values; ; values in legend represent medians and 95% credible intervals. (d) Relationship between model residuals and groundwater index.

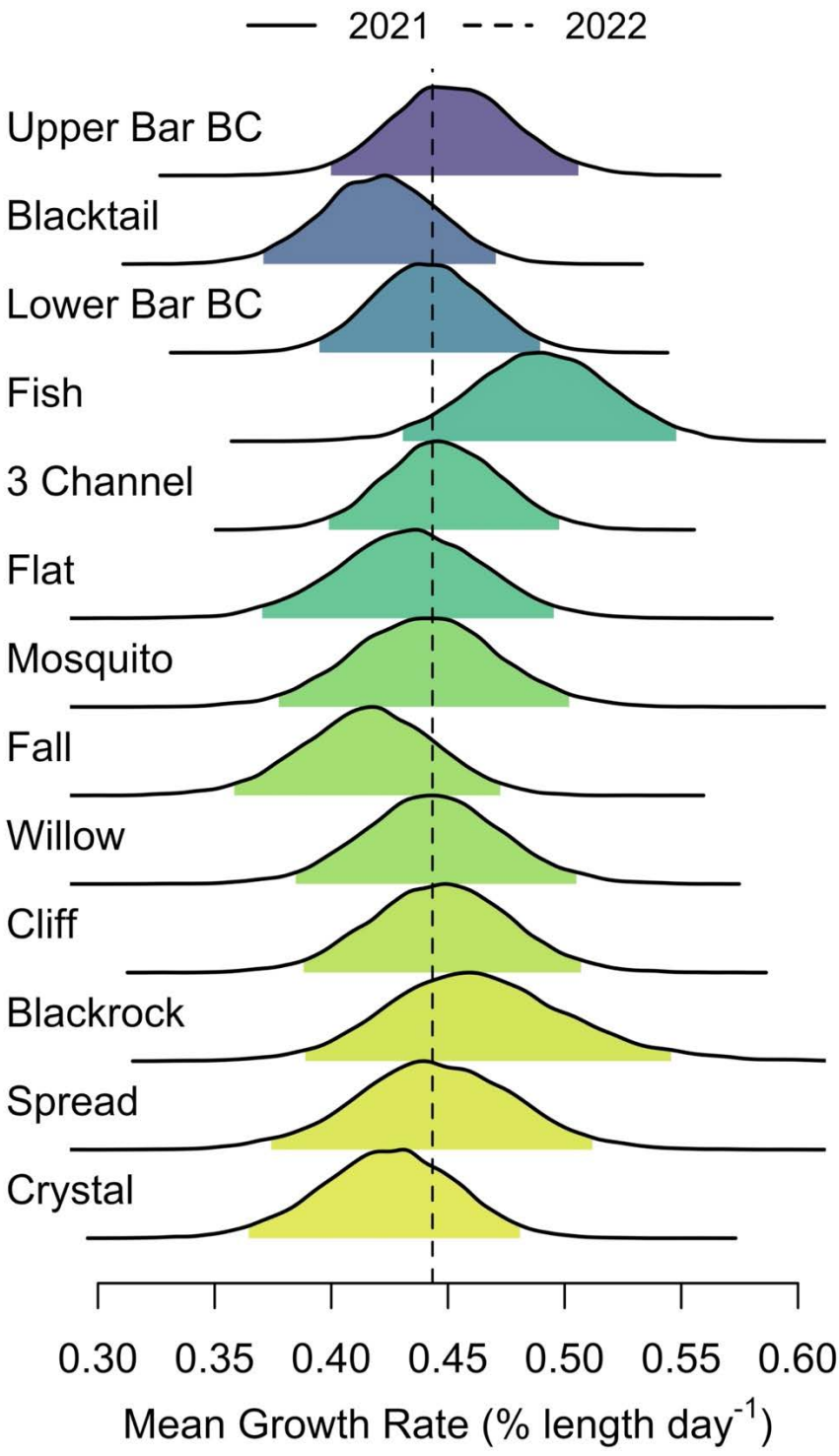

Figure S7 Posterior probability distributions for stream-specific intercepts from the Bayesian hierarchical model describing the effects of time and groundwater on growth, where the intercepts describe mean growth rate (mm day^{-1}) in each stream. Streams are ordered from highest (*top*) to lowest (*bottom*) groundwater index. *Vertical dashed line* denotes the global mean growth rate (0.443 mm day^{-1}) for an average sized fish.

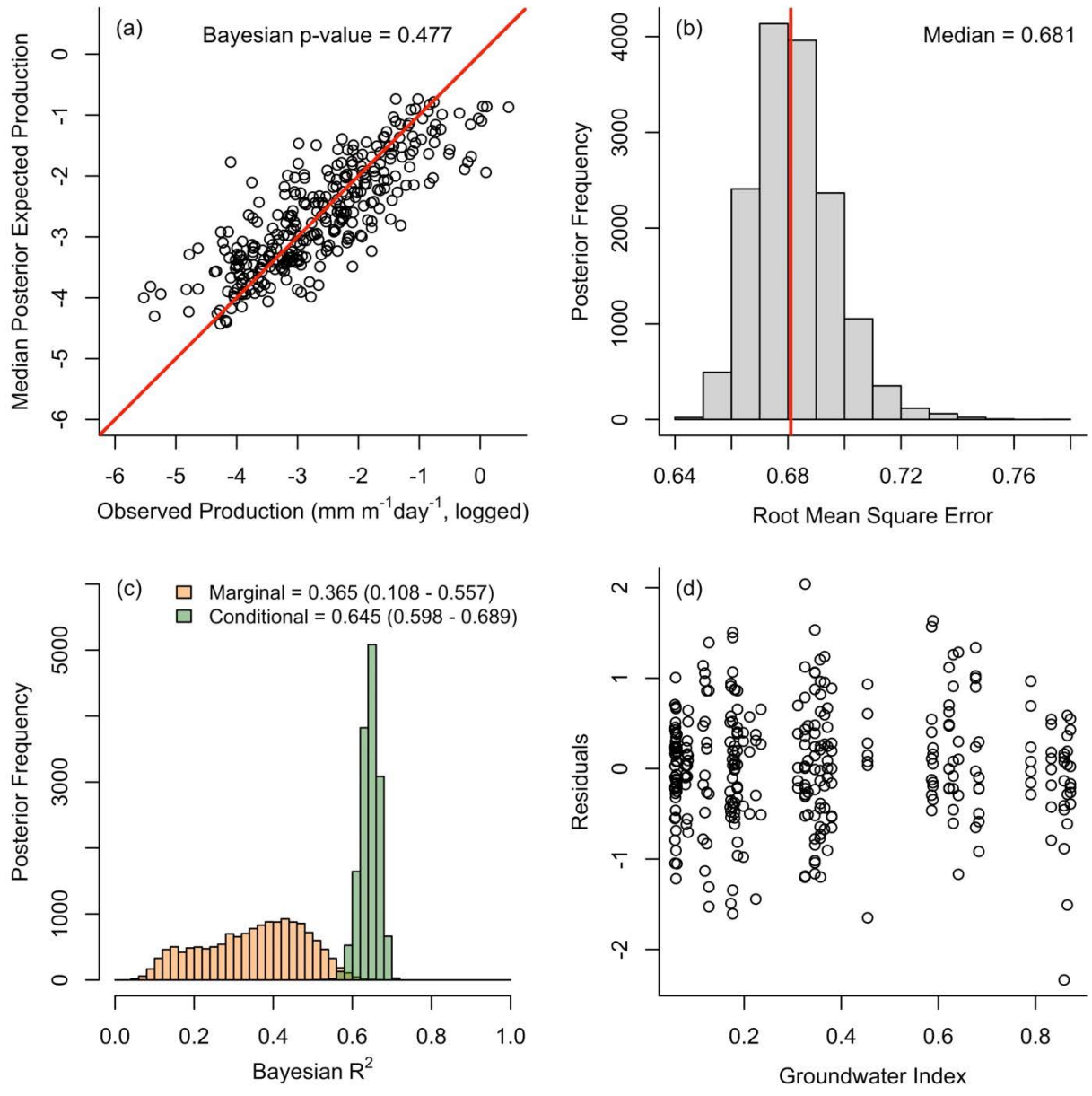

Figure S8 Diagnostic plots for the Bayesian hierarchical model describing the effects of time and groundwater on log(production). (a) Posterior predictive check showing the relationship between median posterior expected (i.e., predicted) production and observed production (mm m^{-1} day^{-1}); *red* line indicates the 1:1 line for visual reference; Bayesian p-value represents the proportion of predicted data that is greater than observed data. (b) Posterior distribution of root mean squared error (RMSE); *red line* denotes the median (0.681). (c) Posterior distributions for the marginal (proportion of total variance explained by the fixed effects alone; *orange fill*) and conditional (proportion of total variance explained by the fixed and random effects; *green fill*) Bayesian R^2 values; values in legend represent medians and 95% credible intervals. (d) Relationship between model residuals and groundwater index.

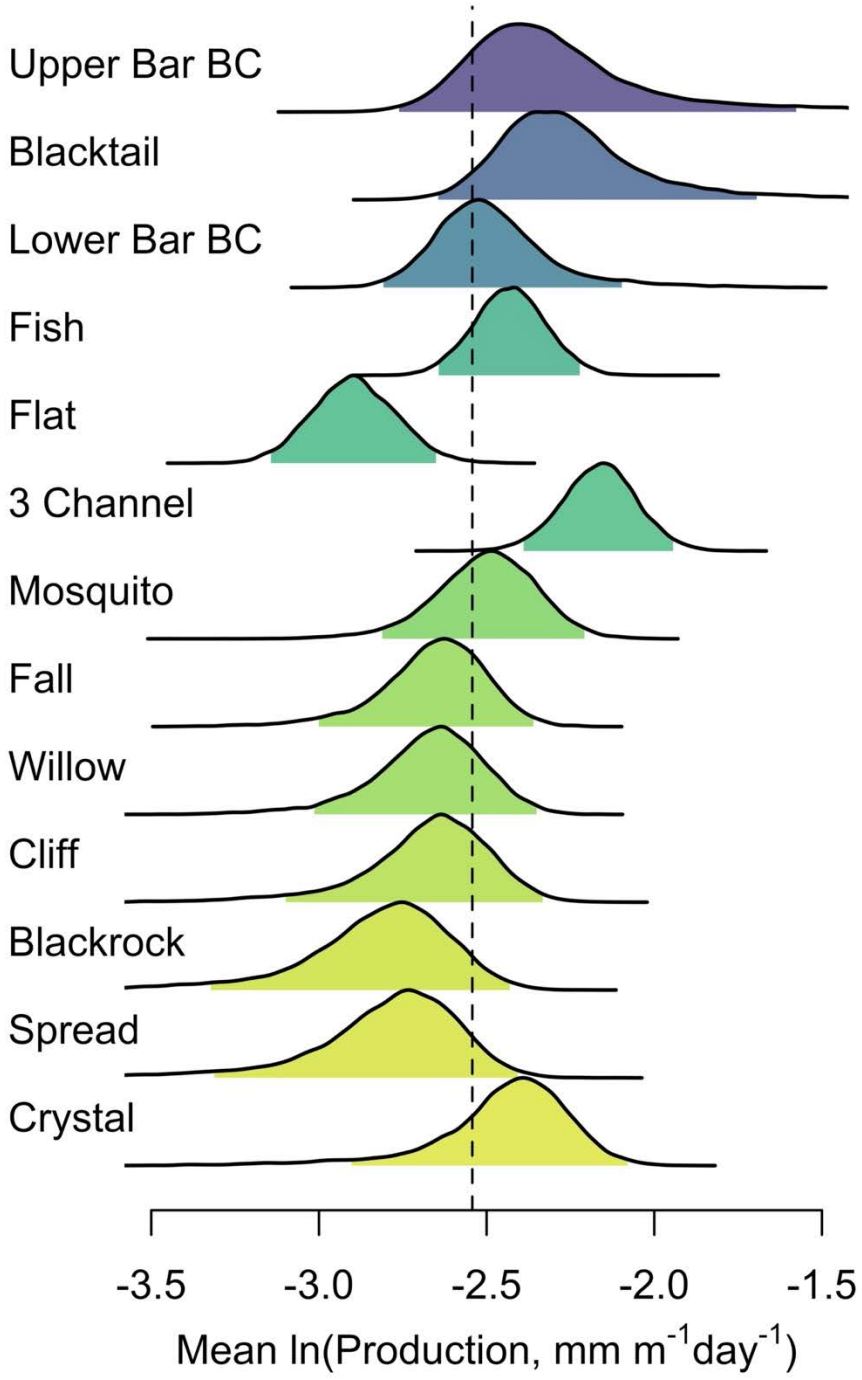

Figure S9 Posterior probability distributions for stream-specific intercepts from the Bayesian hierarchical model describing the effects of time and groundwater on (log) production, where the intercepts describe mean (log) production rate (mm m^{-1} day^{-1}) in each stream. Streams are ordered from highest (*top*) to lowest (*bottom*) groundwater index. *Vertical dashed line* denotes the global mean production rate (0.078 mm m^{-1} day^{-1}).

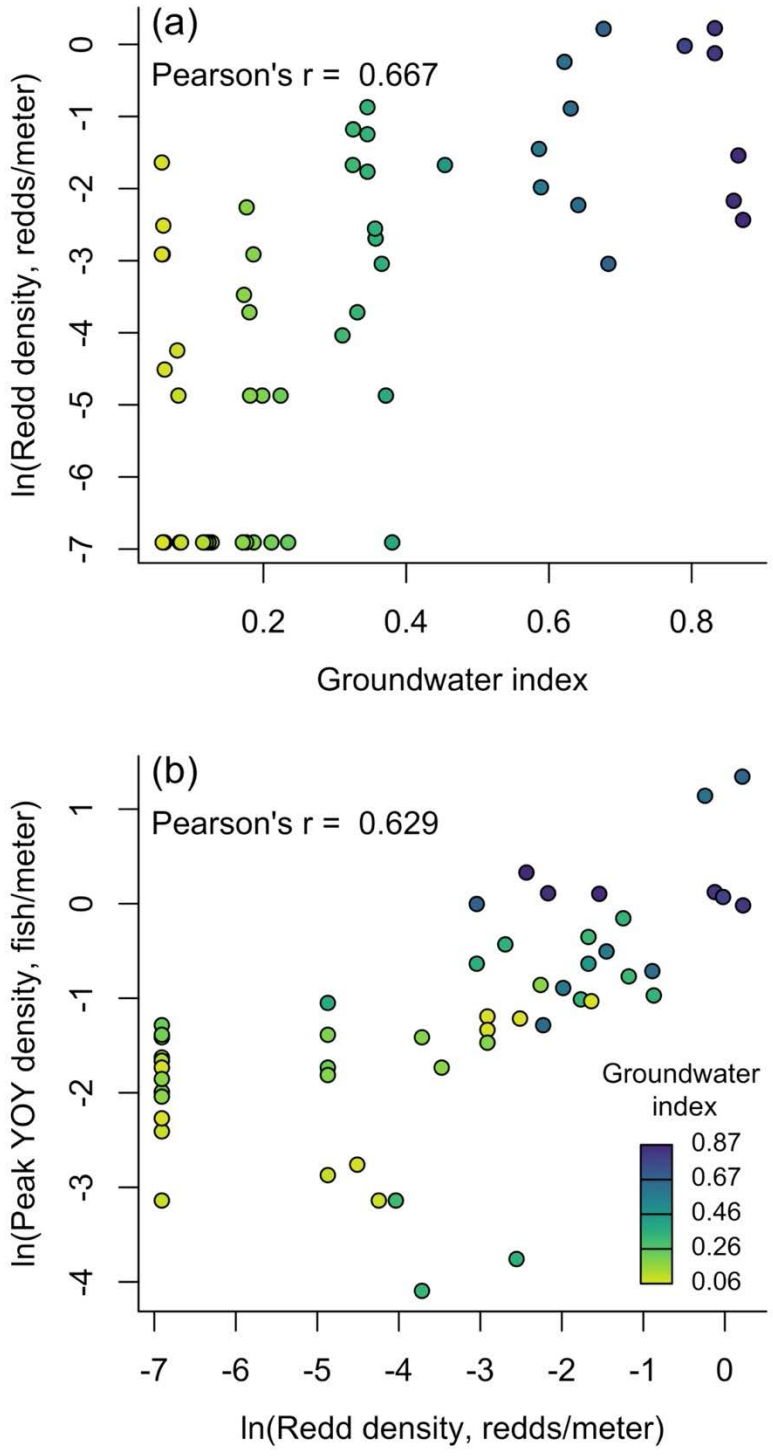

Figure S10 Associations between (a) groundwater index and (log) redd density and (b) (log) redd density and (log) peak young-of-year density. Point color represents groundwater index. Pearson's r correlation coefficients are given for each association (correlations are both significant at alpha = 0.05). Data is from 2022 only as redd counts were not conducted in 2021.

CHAPTER 2

Tributaries structure biocomplexity of a mainstem river metapopulation of native trout

Jeffrey R. Baldock[1], William C. Rosenthal[2], Robert Al-Chokhachy[3], Matthew R. Campbell[4], Catherine E. Wagner[2], and Annika Walters[5]

[1]Wyoming Cooperative Fish and Wildlife Research Unit, Department of Zoology and Physiology and Program in Ecology and Evolution, University of Wyoming, Laramie, Wyoming, USA. Department of Botany and Program in Ecology and Evolution, University of Wyoming, Laramie, Wyoming, USA. [3]Northern Rocky Mountain Science Center, U.S. Geological Survey, Bozeman, Montana, USA. [4]Idaho Department of Fish and Game, Eagle Fish Genetics Laboratory, Eagle, Idaho, USA. [5]U.S. Geological Survey, Wyoming Cooperative Fish and Wildlife Research Unit, Department of Zoology and Physiology and Program in Ecology and Evolution, University of Wyoming, Laramie, Wyoming, USA.

This chapter is formatted for submission to Ecology Letters.

Abstract

The contribution of subpopulations to metapopulations occupying common habitats depends on the spatial arrangement and geometry of source habitats and interactions with intrinsic environmental conditions that independently affect subpopulation productivity. River networks are classic examples of spatially structured environments, where habitat patches are arranged hierarchically from small headwater streams to larger mainstem rivers and habitat diversity is often a function of water source (e.g., snowmelt versus groundwater). For riverine fish, there is increasing evidence that tributaries support mainstem river metapopulations, but how spatially discrete and distributed riverscape attributes influence patterns at broader spatial scales and levels of organization remains unclear. Here, we used genetic stock identification to understand the effect of tributaries on metapopulation structure for Yellowstone cutthroat trout (*Oncorhynchus virginalis bouvieri*) occupying the mainstem Snake River, Wyoming, USA. We found near complete reliance of the mainstem metapopulation on demographic support from tributaries, but metapopulation composition varied from upstream to downstream locations. Distance between habitats, catchment area, and groundwater input acted in concert to determine the contribution of tributaries to the mainstem metapopulation. We also found evidence for carry-over effects of tributaries on growth, where metapopulation size structure was a function of natal tributaries characteristics and life stage. Our results provide insight into the mechanisms that give rise to metapopulation biocomplexity in riverine ecosystems and underscore the importance of protecting and conserving tributaries to ensure the long-term viability of mainstem river ecosystems. Our results have important implications for understanding how habitat fragmentation and the loss of habitat diversity may destabilize ecologically and economically important metapopulations of fish, particularly given global climate change.

Introduction

Populations originating from spatially discrete habitats interact via dispersal, forming metapopulations that often make use of shared habitat patches (Hanski and Gilpin 1991). The contribution of subpopulations to a shared environment depends on both the size of respective habitat patches and on their distances from the receiving patch (Hanski 1999). However, environmental conditions vary across both space and time (Stanford et al. 2005, Dobrowski 2011), such that individuals occupying spatially structured habitats experience dramatically different vital rates (e.g., growth and survival), with implications for local population growth, size, and productivity (Thorson et al. 2014). Therefore, metapopulation dynamics often depend on both habitat geometry and local, spatially distributed processes affecting subpopulation productivity (Moilankn and Hanski 1998, Wilson et al. 2023). The degree to which subpopulations influence metapopulation demography is critically important as this type of biocomplexity provides stability in the face of climate and environmental variability (Hilborn et al. 2003, Schindler et al. 2010).

River networks are classic examples of spatially structured environments, where habitat patches are arranged hierarchically from small headwater streams to larger mainstem rivers (Frissell et al. 1986). Stream ecologists have long recognized that the spatial organization of tributaries within river networks can affect processes downstream (Vannote et al. 1980, Fisher 1997). Specifically, larger tributaries that discharge directly into mainstem river exert greater influence on mainstem rivers than smaller tributaries located further upstream (Peterson et al. 2013). Additionally, asynchrony in biophysical processes among tributaries can stabilize patterns at broad spatial scales, particularly within larger mainstem rivers (Moore et al. 2015, Chezik et al. 2017). Therefore, spatial organization, patch size, and habitat heterogeneity of tributaries may interact to influence riverine ecosystem processes at larger spatial and temporal scales (French et al. 2020, Terui et al. 2021).

For riverine fish, the dendritic structure of river networks can influence metapopulation behavior (Campbell Grant et al. 2007, Terui et al. 2018) and there is increasing evidence that tributaries provide demographic support to mainstem rivers (Tsuboi et al. 2022, Bouska et al. 2023, Healy and Smith 2023). Tributary streams and larger mainstem rivers offer contrasting and often complementary habitat conditions (Bouska et al. 2023). This diversity drives spatiotemporal variation in vital rates and results in distinct dispersal and movement patterns as physiological and habitat requirements change throughout ontogeny (Schlosser 1991, Tsuboi et al. 2022). For example, flooding, sedimentation, and flow regulation can preclude spawning in mainstem rivers as incubating embryos are sensitive to sub-optimal and altered river conditions (Wu 2000, Pollux et al. 2006). Accordingly, tributaries often represent critical spawning and early rearing habitat (Cordoleani et al. 2021). However, the small size and often dynamic environmental conditions limit growth and production, such that fish often disperse to larger mainstem rivers where constraints on foraging are relaxed and larger body sizes can be attained (Petty et al. 2014, Huntsman et al. 2016). Therefore, mainstem river metapopulations are often composed of individuals originating from a network of tributaries (Homel et al. 2015, Budy et al. 2020, Healy and Smith 2023). Maintaining connectivity and allowing for the full expression of life history diversity is critically important for conserving metapopulations of salmonids in large river networks (Moore 2015, Armstrong et al 2021).

The degree to which mainstem river metapopulations reflect component subpopulations may depend on local tributary conditions and subsequent effects on movement (Bouska et al. 2023). Regional climate interacts with landscape features to generate spatiotemporal variation in water temperature and flow among tributaries (Benda et al. 2004, Stanford et al. 2005). As temperature and flow influence nearly every ecological process in stream environments (Magnuson et al. 1979, Poff et al. 1997), vital rates such as individual growth and population productivity vary considerably among tributaries (Letcher et al. 2015, Yamada et al. 2024). Critically, groundwater discharge to streams stabilizes water temperature and flow regimes (Ward 1985, Sear et al. 1999, Lusardi et al. 2021) and is associated with increased growth and production (Mejia et al. 2016; Baldock et al. *in prep*, chapter 3 of this dissertation). Density-dependent resource limitation during the juvenile period can affect the expression of alternative migratory strategies (Forseth et al. 1999, Morita et al. 2014, Sloat and Reeves 2014), whereby individuals disperse to downstream habitats in which constraints on growth and production are relaxed (Fretwell and Lucas 1970, Einum et al. 2006). Therefore, processes that determine juvenile growth and production at the tributary scale, such as groundwater input, are expected to mediate the effects of spatial organization and size of tributaries on contribution to mainstem river metapopulations.

In addition to affecting total contribution, tributary conditions may also influence the demographics of mainstem metapopulations via carry-over effects on growth (*sensu* Griffiths et al. 2013). Ecological carry-over effects occur when an individual's previous experience explains their current performance, particularly when individuals transition between life stages or habitats (Harrison et al. 2011, O'Connor et al. 2014). Growth, expressed as mass-at-age, is important as body size is strongly associated fecundity (Bromage et al. 1990, Meyer et al. 2003), which can affect long-term population dynamics (Vincenzi et al. 2008, 2010). Groundwater input to tributaries may induce carry-over effects on growth via two main pathways. First, during the juvenile period, the stabilizing effect of groundwater on annual variation in temperature can extend growing seasons and enhance growth capacity (Baldock et al. *in prep*). Second, for reproductive adults returning to spawn in natal tributaries (i.e., natal site fidelity or homing; Quinn 1990), groundwater input and associated habitat conditions may affect an individual's ability to recover energetic losses. This is important as depleted nutrition condition after spawning is associated with high overwinter mortality and low probability of future reproduction (maybe Bordeleau et al 2019). Therefore, metapopulation demography (i.e., growth expressed as mass-at-age) may reflect natal habitat conditions rather than those of the shared habitat, and these carry-over effects may be expressed differently across life stages (e.g., juveniles versus reproductive adults).

Evaluating tributary support of mainstem river metapopulations can be challenging due to difficulty associated with sampling at the spatial scale at which coupled habitat use occurs in large river networks (e.g., 100s of kms; Chudnow et al. 2023, Healy and Smith 2023). Tools developed in related fields may help to address this challenge. As commercial fleets exploiting mixed-stock fisheries can inadvertently target vulnerable stocks, threatening metapopulation stability (Hilborn et al. 2003, Hutchinson 2008), fisheries managers require tools to estimate stock-specific exploitation rates and enable sustainable harvest (Crozier et al. 2004). Molecular techniques such as genetic stock identification (GSI) have revolutionized fisheries management in this regard. Genetic stock identification assigns individuals captured in a common

environment to contributing stocks (i.e., subpopulations) based on genetic similarity to groups of individuals captured from known locations (i.e., source habitats), assuming contributing stocks are genetically distinct. While conducting GSI is standard practice in commercial fisheries management, particularly for salmon (e.g., Seeb et al. 2007, Satterthwaite et al. 2015, Bekkevold et al. 2021), it is applied less frequently in non-anadromous fisheries management (but see Taylor et al. 2021), and has not to our knowledge been used to address primarily ecological and/or evolutionary questions.

In this study, we used GSI to understand the role of tributaries to supporting metapopulation of Yellowstone cutthroat trout (*Oncorhynchus virginalis bouvieri*) occupying the upper Snake River, Wyoming, USA. Our primary objectives were three-fold. First, we assessed the degree to which mainstem Snake River metapopulation composition varied across space and time. Second, we quantified the effect of tributary characteristics (distance to the mainstem, catchment size, and groundwater input) on contributions to the mainstem. Third, we evaluated the extent to which tributary characteristics were associated with carry-over effects on growth and whether carry-over effects varied across life stages. Our results provide insight into how intrinsic habitat conditions mediate the effects of size and spatial organization on functional connectivity between tributary and mainstem habitats for a riverine fish. Furthermore, we demonstrate how natal habitats can induce carry-over effects that vary across ontogeny. Our results provide important context for designing conservation and management plans and can be used to prioritize habitat protection and restoration efforts that aim to bolster metapopulation function (Al-Chokhachy et al. 2018, Isaak et al. 2022).

Methods

Study System and Species

We conducted our study within the upper Snake and Greys River watersheds (USRW) in northwest Wyoming, USA, an 10,108 km^2 region situated between 1708 and 4194 meters elevation comprising the core of the Greater Yellowstone Area (Figure 1). Precipitation in the USRW falls primarily as snow (Hostetler et al. 2021). Spring snowmelt results in snowmelt-dominated hydrographs characteristic of the Rocky Mountain region. A portion of that snowmelt percolates into surface sediments, recharging alluvial aquifers (Nolan and Miller 1995). Considerable spatial heterogeneity in groundwater discharge to streams is driven in large part by underlying geology, such that streams within the USRW fall along a hydrologic gradient ranging from flow sourced primarily from snowmelt to exclusively from groundwater (Baldock et al. *in prep*). In general, the USRW represents a relatively intact river network comprised of the large mainstem Snake River, which is fed by tributary streams and rivers that vary widely in hydrogeomorphic characteristics. However, two large dams (Jackson Lake Dam in the north/upstream and Palisades Dam in the south/downstream) form complete barriers to fish passage, thus bounding our study area to the river network between dams.

Both within the USRW and across the Greater Yellowstone Area, Yellowstone cutthroat trout (YCT) are an integral component of aquatic and terrestrial food webs (Koel et al. 2019) and support economically and culturally valuable recreational fisheries. Habitat degradation and

hybridization and competition with non-native species has led to widespread declines (Gresswell 2011) and anticipated climate warming further threatens many extant populations (Wenger et al. 2011). However, YCT in the USRW display successful natural reproduction (Baldock et al. 2023), negligible genetic introgression by non-natives (Kovach et al. 2018), and stable or increasing trends in population abundance (Wyoming Game and Fish Department 2019). These features, in combination with high habitat connectivity and life-history diversity, make the USRW a high priority for YCT conservation efforts (Al-Chokhachy et al. 2018). Like many salmonids, YCT in the USRW display both fluvial migrant and resident life-history forms, where migrants move between tributaries for spawning and larger mainstem rivers for rearing during non-reproductive periods (Novak and Sadak 2003, Sanderson and Hubert 2009, Homel et al. 2015). Homel et al. (2015) documented YCT moving from the mainstem Snake River into a variety of tributary habitats during the summer spawning period, with one individual migrating more than 100 river km. Yellowstone cutthroat trout in the USRW can therefore be described as a metapopulation or stock complex (Hilborn et al. 2003), where individuals originating from discrete tributary streams interact via dispersal and mix in a common rearing environment, the mainstem Snake River.

Fish Sampling

Genetic stock identification requires two types of sample collections: "baseline" samples that describe genetic variation within and among putative source populations (e.g., tributaries) and "mixture" samples collected from a common environment (e.g., the mainstem Snake River). Between 2020 and 2022, we collected YCT tissue samples from tributary streams to establish a baseline of genetic variation (*sensu* Hargrove et al. 2023). We sampled fish using either dip-netting or standard backpack electrofishing. We restricted baseline collections to primarily age-0 individuals (<60 mm total length), which have limited swimming abilities and thus likely represent the population of fish spawning where collections were made (Roff 1991). In cases where age-0 fish were not present, we sampled tissue from larger individuals, but restricted these to <200 mm. At any given sampling location, collections were made at least 50 m apart (approximate flowline distance) to minimize the probability of sampling siblings (*sensu* Vähä et al. 2017). Age-0 sibling groups are often clustered together (Kanno et al. 2011) and including large groups of close relatives can bias downstream genetic analyses, including indices of pairwise genetic differentiation (F_{st}) and GSI (Waples and Anderson 2017, Östergren et al. 2020). We attempted to collect tissue samples from 30-40 individuals per location as relatively small sample sizes allow for accurate GSI when genetic differentiation among source populations is strong ($F_{st} > 0.01$; Beacham et al. 2020), as has been shown in our system (Kovach et al. 2011). However, this was not always possible due to low YCT encounter rates at some locations.

We used raft electrofishing to collect tissue samples from adult YCT in the mainstem Snake River, which served as our mixture samples for GSI. Raft electrofishing was conducted in mid-October following the reduction of flow releases from Jackson Lake Dam (to maximize capture efficiency) and the post-spawn settlement of YCT into winter habitat (Homel et al. 2015). We sampled adult YCT across three years (2020-2022) and six sections of the mainstem Snake River to assess spatiotemporal variability in tributary contributions (Figure 1). Preliminary power analyses indicated that sampling 500 adult YCT per year would allow us to accurately estimate

contributions from tributaries contributing as little as 5% annually. We distributed the target annual sample size (500) evenly across the six sections according to section length (section extents were based on river access points). Additionally, we attempted to distribute collections evenly within each section by electrofishing both intermittently and non-exhaustively. In addition to distributing collections spatially, we also distributed collections evenly by size. Because smaller fish are numerically dominant (Wyoming Game and Fish Department 2019), sampling fish disproportionately relative to their abundance was necessary to accurately estimate proportional contributions for larger size-classes that were less abundant, but nevertheless important to population processes (e.g., spawning and fecundity). Within each section of the Snake River, we distributed collections across 6 size-classes (total length in mm): 201-250, 251-300, 301-350, 351-400, 401-450, and 450+. The minimum size (201 mm) was based on the smallest reproductively mature fish identified in a long-term monitoring program of spawning activity (Wyoming Game and Fish Department, *unpublished data*). We acknowledge that size-classes do not align with average length-at-age. However, as we were interested in capturing fish that were relatively large or small for their age (objective 3), constructing arbitrary size classes forced us to seek out those individuals. Additionally, we acknowledge that our sampling design does not match potential spatial variation in fish abundance or variation in abundance among age-classes. We therefore take care in our inferences to avoid conflating relative contributions with absolute abundance.

Genotyping

We genotyped all baseline and mixture samples following standard protocols. We extracted genomic DNA from fin clip samples using the Nexttec Genomic DNA Isolation Kit (XpressBio, Thurmont, Maryland) following the manufacturer's protocol. We generated genotypes for individual fish using the genotyping-in-thousands by sequencing (GT-seq) protocol which uses multiplexed polymerase chain reactions and amplicon sequencing to characterize hundreds of SNPs for thousands of individuals (Campbell et al. 2015). We then screened samples with a panel of 353 single nucleotide polymorphic (SNP) loci, which included 38 previously developed species-diagnostic SNPs (Pritchard et al. 2013; Idaho Department of Fish and Game, *unpublished data*). We organized genotypes of all individuals using the R package EFGLmh (https://github.com/delomast/EFGLmh/) to create input formats required for the analytical programs used in this study, including producing an input file required for GenAlEx (Peakall and Smouse 2006). Samples we identified as hybrids (n = 7) were removed from analyses. Prior to GSI analyses, we removed species-diagnostic, invariable, and mitochondrial DNA loci; leaving 266 SNP loci. Marker details for these 266 SNP loci, including primer sequences (forward and reverse) are available upon request. Finally, we filtered samples for genotyping completeness, retaining only those loci genotyped at ≥85% success.

Baseline Reporting Units and Assignment Accuracy

To ensure that large groups of highly related individuals were not present in our baseline dataset, we estimated relatedness (Wang 2002) among individuals within collections using the R package *demerelate* (Kraemer and Gerlach 2017). Pairs of individuals were identified as full siblings if the relatedness coefficient was >0.4 (*sensu* Källo et al. 2023). We opted to retain two individuals per full-sibling family following the recommendations of Waples and Anderson (2017) and

Östergren et al. (2020), as a compromise between performance of allele frequency estimates and sample size.

We aggregated baseline tributary collections into reporting units (i.e., putative source populations for genetic assignment) following an iterative process based on assignment accuracy, geographic proximity, and indices of pairwise genetic differentiation (i.e., F_{st}). Grouping of collections into reporting units is often done at large spatial scales (e.g., Bekkevold et al. 2021, Hargrove et al. 2023) to maximize genetic differentiation among units and hence GSI accuracy (Araujo et al 2014). Given that we were interested in evaluating the drivers of contribution and weight-at-age at the scale of individual tributaries, we aimed to combine as few collections as possible to maintain the original character of tributaries in our covariate data, while simultaneously balancing the need to attain reasonable levels of genetic differentiation among reporting units.

To delineate reporting units, we first set out to determine the rate at which individuals correctly assigned to their collection of origin and identify sets of collections for which aggregation into reporting units might increase assignment accuracy. To do so, we conducted preliminary self-assignment tests on individual collections using the leave-one-out procedure as implemented with the "self_assign" function in the R package *rubias* (Moran and Anderson 2019). At the same time, we calculated pairwise F_{st} (Weir and Cockerham 1984) among collections to again identify pairs of collections that could be aggregated, as low levels of differentiation ($F_{st} < 0.01$) can bias GSI (Araujo et al. 2014). We used the self-assignment tests to construct a confusion matrix to identify which collections had low self-assignment rates (<0.7) and which collections were "receiving" erroneously assigned individuals. Comparing the confusion matrix to pairwise F_{st} estimates indicated that self-assignment errors were often committed among geographically proximate collections that were poorly differentiated ($F_{st} < 0.01$). We therefore aggregated collections into reporting units if self-assignment confusion among collections was high, pairwise F_{st} was low, *and* the collections were made at different locations within the same tributary stream or catchment. We dropped six collections from our baseline because sample sizes were low ($n \leq 5$ per collection; 20 individuals total) and aggregation with other collections was not possible following the approach described above (excluding these collections did not affect GSI performance as indicated by z-scores, below).

We tested the accuracy and precision of our final baseline reporting units by simulating mainstem Snake River mixtures using baseline allele frequencies following the leave-one-out approach of Anderson et al. (2008). We used the "assess_reference_loo" function in *rubias* to simulate 500 mixtures of 1000 individuals (using flat Dirichlet priors among reporting units) and assigned those individuals back to baseline reporting units (*sensu* Hargrove et al. 2023, Horne et al. 2023). We then calculated residuals (the difference between the simulated true and estimated mixing proportions for each reporting unit and simulation) and compared the distribution of residuals to 0 to assess bias in estimated contributions to the mainstem Snake River for each reporting unit, independently.

Mixture Analysis

We quantified the contribution of reporting units to the mainstem Snake River using the "infer_mixture" function in *rubias* with parametric bootstrapping to account for bias as estimated above. We conducted separate mixture analyses for each combination of year and section to evaluate spatiotemporal variation in tributary contributions. *Rubias* functions in a Bayesian probabilistic framework, whereby each mixture sample (i.e., adult YCT) assigns to every reporting unit with a given probability. Reporting unit mixing proportions are thus calculated by summing individual probabilities over each unit. Bootstrap-corrected mixing proportions are then generated by multiplying uncorrected mixing proportions by mean bias as estimated using the leave-one-out approach implemented within the "infer_mixture" function (Moran and Anderson 2019). As an additional check on assignment accuracy, *rubias* computes z-scores for each fish, which represent how similar an individual is to samples in the baseline. To assess whether individuals in the mixture(s) originated from source populations not included in our baseline, we compared the distribution of z-scores to a normal distribution. We considered individuals with z-scores two standard deviations beyond the mean z-score to have originated from source populations not included in our baseline (Bowersox et al. 2023).

Covariate Generation

For each reporting unit, we derived a suite of covariates hypothesized to affect proportional contributions to the mainstem Snake River (objective 2) and carry-over effects on growth (objective 3). Covariates included distance to the mainstem, catchment area, and a metric describing relative groundwater influence on stream conditions. To derive covariates, we required a stream network spatial object that accurately represented flowlines in the USRW, particularly in areas where groundwater upwelling creates dense drainage networks where many of our collections were made and which we hypothesized would make large contributions to the mainstem Snake River. We delineated the stream network as in Baldock et al. (*in prep*), briefly described here. We used the WhiteboxTools library implemented in R (Lindsay 2016, Wu and Brown 2022) to delineate a stream network from a 1/3 arc-second (*ca.* 10 m) bare-earth digital elevation model (accessed 15 November 2023, https://apps.nationalmap.gov/downloader/). This approach tended to omit flowlines for streams originating from high-volume groundwater springs, as groundwater-fed stream catchments are often small and poorly defined (Whiting and Moog 2001). We therefore delineated flowlines for these streams by hand and merged these features to the stream network using ArcMap ver. 10.8 (ESRI, Redlands, CA).

Following standard practices, we then used WhiteboxTools to delineate catchments and calculate catchment area for each of the 52 reporting units. For reporting units composed of multiple collections, we delineated catchments for the collection located furthest downstream. It is likely that (1) source populations extend downstream of where we collected samples and (2) unsampled, genetically distinct populations exist upstream. Therefore, we interpreted catchment area as a metric of stream habitat availability within the vicinity of the reporting unit, rather than total habitat availability within the catchment. We also acknowledge that some of our reporting units were spatially nested (located upstream, within the same catchment). Thus, for a pair of reporting units that are flow connected, catchment area of the downstream unit is intended to represent habitat area in the immediate vicinity and should not be thought to include habitat area associated with the upstream unit.

We used the *riverdist* package in R (Tyers, 2024) to calculate pairwise flowline distance between each reporting unit (or location of the most downstream collection, for units composed of multiple collections) and the mid-point of each section of the mainstem Snake River. Thus, the flowline distance between a given reporting unit and the mainstem may be short relative to one section of the mainstem, but much longer relative to another section.

Following the approach detailed in Baldock et al. (Chapter 1 of this report), we derived a metric describing relative groundwater influence for each of our 52 reporting units. Relative to the prior study, we extended our study area to include the Greys River basin, where some of our reporting groups were located. We briefly describe our modeling efforts here and refer interested readers to Baldock et al. (*in prep*) for detailed methodology. We used MaxEnt version 3.4.4 (Phillips and Dudík 2008, Elith et al. 2011; https://biodiversityinformatics.amnh.org/open_source/maxent/, accessed on 17 July 2023) to predict the prevalence of groundwater springs using 219 spring locations as presence points and 11 geologic and topographic layers as predictors (*sensu* Gerlach et al. 2022). Geologic layers and the digital elevation model used to prepare topographic layers were accessed from the Wyoming Geospatial Hub on 17 July 2023 (https://data.geospatialhub.org/). Of the 219 spring locations, 70% (n = 154) were used for model training and 30% (n = 65) were used for model testing. We assessed model performance by calculating the area under the receiver operating curve: the probability that a randomly chosen presence point will be ranked above a randomly chosen background location (Phillips and Dudík 2008). From the MaxEnt model output (a raster of spring prevalence, where the value for each *ca.* 10 x 10 m cell represents the probability of the cell containing a groundwater spring), we derived a metric describing relative groundwater influence on overall stream conditions. From the spring prevalence raster (buffered to the stream network; 100 m radius), we calculated the inverse distance-weighted mean prevalence within contributing catchments, which assumes that springs located further upstream exert exponentially less influence on conditions at the location of interest. We used the distance-weighted mean spring prevalence to describe relative groundwater influence for each reporting unit.

Statistical Analyses

Objective 1 – Spatiotemporal Variation in Metapopulation Composition

We used a zero-and-one inflated Dirichlet regression model implemented in the R package *zoid* to understand spatiotemporal variation in mainstem Snake River metapopulation composition (Jensen et al. 2022). *Zoid* estimates mixture proportions as functions of covariates applied to the entire mixture in a Bayesian framework. We used *zoid* to formally test five hypotheses (Table 1): (1) tributary contributions are constant across sections of the Snake River and years (null), (2) contributions vary by section, (3) contributions vary by year, (4) contributions vary by section and year, and (5) contributions vary by section and year, but certain sections are more temporally variable than others. We built candidate models to represent each hypothesis and compared models using leave-one-out cross validation (LOO-CV) using the R package *loo* (Vehtari et al. 2022), in which the model with the greatest support is that with the lowest expected log pointwise predictive density (elpdloo; Vehtari et al. 2017).

Objective 2 – Riverscape Effects on Tributary Contributions

As the output of the GSI as implemented in *rubias* was (effectively) count-based compositional data, we used Dirichlet-multinomial regression (*sensu* Douma and Weedon 2019) to quantify the effects of reporting unit characteristics on proportional contributions to the mainstem Snake River. Bayesian Dirichlet-multinomial models have been shown to outperform alternative approaches to modeling compositional count data, such as likelihood and frequentist methods implemented in existing R packages (Harrison et al. 2020b). While Dirichlet regression is commonly used to model compositional data with more than two categories, we parameterized the model using the multinomial distribution because the Dirichlet distribution alone cannot handle zeros (Douma and Weedon 2019) or account for unequal sample sizes among compositions (i.e., mixtures: section and year-specific sampling events). Thus, as the multinomial distribution requires integer count data, we multiplied bootstrapped mixing proportions estimated in *rubias* by the sample size of each mixture, rounded these values to the nearest integer (hereafter, bootstrapped mixing counts), and summed bootstrapped mixing counts over each mixture to obtain a bootstrapped sample size (which was always ±1 of the true sample size).

Our Dirichlet-multinomial regression model is similar to multivariate count models used in prior studies (Chong and Spencer 2018, Harrison et al. 2020b, Averill et al. 2021), but was altered to account for the specifics of our data and overall objectives. Let the bootstrapped mixing counts in mixture i be a vector $\mathbf{y}_i = (y_{i,1}, y_{i,2}, \ldots, y_{i,52})$, where $y_{i,j}$ is the observed contribution from the reporting group j to mixture i; and let $n_i = \Sigma_{j=1}^{52} y_{i,j}$ be the bootstrapped sample size in mixture i. The model is specified as follows:

$$\boldsymbol{y}_i \sim Multinomial(\boldsymbol{\rho}_i, n_i) \quad (1)$$

$$\boldsymbol{\rho}_i \sim Dirichlet(\boldsymbol{\gamma}_i) \quad (2)$$

$$\log(\boldsymbol{\gamma}_i) = \alpha + \beta_1 \boldsymbol{D} + \beta_2 A_j + \beta_3 G_j \quad (3)$$

where the vector $\boldsymbol{\rho}_i$ is the expected relative abundance of each reporting group in mixture i; the vector $\boldsymbol{\gamma}_i$ is the Dirichlet-distributed linear predictor; α is the intercept shared across all mixtures; β_1, β_2, and β_3 are coefficients; $\boldsymbol{D}$ is an i by j matrix of centered and scaled pairwise flowline distances between reporting unit j and the section sampled for mixture i; A_j is a vector of centered and scaled reporting unit catchment areas; and G_j is a vector of centered and scaled reporting unit groundwater index values. Relative abundances $\boldsymbol{\rho}_i$ were mapped to the Dirichlet distribution using a log-link function (Douma and Weedon 2019). Our specification of covariates as matrices and vectors allowed us to estimate proportional contribution as a function of the characteristics of individual reporting units. This is different than what is common in composition data analysis, where covariates are common to the entire composition (e.g., Chong and Spencer 2018, Jensen et al. 2022).

As the parameters of Dirichlet regression are difficult to interpret, we produced plots of predicted values under a different covariate values to understand the marginal and additive effects of distance, area, and groundwater on proportional contribution (*sensu* Douma and Weedon 2019). First, we visualized the marginal effects of each covariate on proportional contribution by

predicting $\boldsymbol{\rho}$ from a sequence of 52 (the number of reporting units in our study) values for the covariate of interest, holding all other covariates at their mean (0). We converted between $\boldsymbol{\gamma}$ and $\boldsymbol{\rho}$ using the formula $\boldsymbol{\rho} = \boldsymbol{\gamma} / \sum_{j=1}^{52} \boldsymbol{\gamma}$, which enforces the sum to one constraint (Douma and Weedon 2019). Second, to assess the additive effects of covariates on contribution, we similarly predicted $\boldsymbol{\rho}$ for 52 hypothetical reporting units. However, rather than varying a single covariate over the range of observed values across all reporting units, we held all covariates at their mean (0) for 51 reporting units ("reference units") and set covariates according to one of eight scenarios for the final unit ("test unit"; Table S1). We subtracted the estimated contribution of the reference unit from that of the test unit to understand how distance, area, and groundwater additively affect proportional contribution relative to units characterized by average conditions. We did this for each MCMC sample retained in our model (n = 3000) to generate ranges of plausible values for each scenario.

Objective 3 – Riverscape Drivers of Carry-Over Effects

To address our third objective, we used mass-at-age as a measure of growth performance and evaluated the relationship between mass-at-age and reporting unit characteristics to quantify carry-over effects and their variability throughout ontogeny. We restricted our analysis to individuals that assigned to reporting units with high certainty by retaining only those with posterior assignment probabilities (to a single reporting group) greater than 0.7 and z-scores within two standard deviations of the mean z-score (Bowersox et al. 2023, Horne et al. 2023). We used historical measured mean length-at-age data (Haganbuck 1970) to parameterize a von Bertalanffy growth model and then estimated probabilistic ages for all adult YCT that assigned to reporting units with high certainty. Following Budy et al. (2020), we treated total length of individual *i* (L_i) as a normally distributed random variable that followed a von Bertalanffy growth function with a constant coefficient of variation (cv):

$$L_i \sim Normal(\mu_i, \sigma_a) \tag{4}$$

$$\sigma_a = cv * \mu_i \tag{5}$$

$$\mu_i = L_\infty \left[1 - e^{-K(a_i - t_0)}\right] \tag{6}$$

where μ_i is the predicted total length of individual *i*; σ_a is the standard deviation in length at age *a*; L_∞ is the asymptotic length; K is the Brody growth coefficient; t_0 is the theoretical age at which length is 0 (i.e., the x-intercept); and a_i is the age of individual *i* which was either known (mean length-at-age from Haganbuck, 1970; n = 52) or estimated probabilistically (mainstem fish that assigned to reporting groups with high certainty; n = 1166). For un-aged individuals, ages a_i were drawn from a categorical age composition $\boldsymbol{w}$:

$$a_i \sim Categorical(\boldsymbol{w}) \tag{7}$$

$$\boldsymbol{w} = [w_1, w_2, \ldots, w_A] \tag{8}$$

where the maximum number of age-classes A was assumed to be five as this was the maximum age found by Haganbuck (1970). The proportional contribution w of each age-class was drawn from a symmetric Dirichlet distribution:

$$\boldsymbol{w} \sim Dirichlet(\boldsymbol{c}) \tag{9}$$

$$\boldsymbol{c} = [c_1, c_2, \ldots, c_A] = [1,1, \ldots,1] \tag{10}$$

For each fish, the model provided S age estimates, where S is the number of MCMC sampling iterations retained after thinning and burn-in (see below). We calculated the probability that each fish belonged to each age-class by dividing the number of age estimates of each age-class by S. We used these probabilities S_A as weights in a hierarchical weighted linear regression to evaluate the effect of groundwater on mass-at-age $M_{i,j,k}$ of individual i in year j and section k:

$$M_{i,j,k} \sim Normal(\mu_{i,j,k}, \epsilon_A / S_A) \tag{11}$$

$$\mu_{i,j,k} = \boldsymbol{\upsilon}_A + \upsilon_j + \upsilon_k + \boldsymbol{\theta}_{1,A} D_i + \boldsymbol{\theta}_{2,A} A_i + \boldsymbol{\theta}_{3,A} G_i \tag{12}$$

where ϵ_A is the standard deviation of mass-at-age for age-class A; $\boldsymbol{\upsilon}_A$ is a vector of intercepts drawn independently for each age-class; υ_j is the year-specific offset to $\boldsymbol{\upsilon}_A$ (i.e., random intercept); υ_k is the section-specific offset to $\boldsymbol{\upsilon}_A$; $\boldsymbol{\theta}_{1A}$, $\boldsymbol{\theta}_{2A}$, and $\boldsymbol{\theta}_{3A}$ are vectors of coefficients drawn independently for each age-class; and D_i, A_i, and G_i are the centered and scaled distance, area, and groundwater values for the reporting group to which individual i was assigned. We visualized results by plotting the relative difference between mass-at-age calculated for the maximum and minimum covariate values across age-classes, for each covariate independently. We compared relative differences in mass across age-classes to understand how carry-over effects of groundwater input to tributaries on growth change throughout ontogeny.

Model Fitting and Evaluation

All models were analyzed in a Bayesian framework in the Just Another Gibbs Sampler MCMC sampling environment (JAGS; Plummer 2003), implemented through R (R Core Team 2021) using the HDInterval (Meredith and Kruschke 2020), lubridate (Grolemund and Wickham 2011), MCMCvis (Youngflesh 2018), R2jags (Su and Yajima 2021), and tidyverse (Wickham et al. 2019) packages. All JAGS models were fit with diffuse priors; JAGS code is available in the Supplementary Materials. Because models varied in their degree of complexity and data inputs, we ran models with different numbers of MCMC chains, burn-in iterations, evaluation iterations, and thinning rates (Table S2). We assessed model convergence based on large effective sample sizes, potential scale reduction factors ($\hat{R}$) being less than 1.01 for all parameters, and visual inspection of MCMC trace plots to ensure mixing of chains (Gelman and Hill 2007). We used posterior predictive checks to evaluate goodness of fit of each model (Gelman et al 2004, Kruschke 2014). To do so, we plotted observed data (e.g., proportional contribution) against predicted data generated during parameter estimation and inspected plots to ensure linearity (Gelman 2003). We also derived model residuals, which we inspected to ensure normality around 0, and calculated root mean square error (RMSE) as an index of error in model estimates.

Results

Baseline Reporting Units and GSI Accuracy

After filtering to remove potential hybrids, samples with low genotyping success, full-siblings, and collections with small sample sizes that could not reasonably be aggregated into reporting units, our baseline consisted of 1,710 juvenile YCT representing 63 different collections, i.e., 63 different locations within the USRW. We aggregated collections into 52 reporting units with 1-3 collections and 10-82 individuals per unit (Table S3). Self-assignment rates of our final set of reporting units ranged from 0.48 to 1.00 (weighted mean = 0.84, Figure S1), which is greater than or equivalent to baseline self-assignment rates reported in recent studies (Bradbury et al. 2018, Bekkevold et al. 2021, Hargrove et al. 2023). There was no relationship between self-assignment rate and reporting unit sample size. In general, there was strong genetic differentiation among reporting units: pairwise F_{st} ranged from 0.006-0.293 (Figure S2). Pairwise F_{st} among just four reporting units fell below the 0.01 threshold for accurate GSI (Araujo et al. 2014). These reporting units were all small, groundwater-fed tributaries located immediately adjacent to the Snake River and near each other (three of these tributaries were within 2.5 river kms of each other, with the maximum pairwise distance being 8.1 river kms). We did not aggregate samples from these locations as each represented a distinct tributary known to host high-density spawning aggregations (Kiefling 1997). Results from the mixture simulation indicated that estimated contributions from certain reporting units may be biased (Figure S3). However, the magnitude of bias was very small: mean residuals per reporting unit ranged from -0.013 to 0.017, suggesting proportional contributions could be estimated within 2% of the true value, on average. Furthermore, standard deviations for 40 (out of 52) reporting units overlapped 0, suggesting minimal bias for most units.

After filtering, we retained 1,507 adult YCT genotypes from six sections of the mainstem Snake River over three years (n = 487, 508, 512 for years 2020, 2021, and 2022, respectively). All sections were sampled in all years, except for the section A in 2020 as the primary access point was closed for construction at the time of sampling. Sampling occurred between 11 October and 3 November of each year. As expected from mixture simulations conducted with the baseline data, bootstrap-corrected mixing proportions were in close concordance with uncorrected mixing proportions, generally following a one-to-one relationship (Figure S4); 95% of bootstrap corrections (for each reporting unit in each year and section) were within the interval [-0.015, 0.017]. Visual inspection of the distribution of individual z-scores relative to a normal distribution indicated that our baseline sufficiently covered the most important source populations (Figure S5). However, 6.5% of mixture samples had z-scores two standard deviations beyond the mean z-score, suggesting these individuals originated from source populations other than those included in our baseline.

Objective 1

There was considerable variation in reporting group contributions to the mainstem Snake River (Figure 2). Visual inspection of bootstrap-corrected mixing proportions suggested strong spatial structuring of contributions, such that upstream sections of the Snake River received

contributions from more northerly reporting groups with high groundwater index values and downstream sections received contributions from more southerly reporting groups with lower groundwater index values. *Zoid* model selection provided the most support for our second hypothesis, that reporting group contributions varied across sections but not among years (Table 1). While models representing spatiotemporal variability were ranked second and third (hypotheses 4 and 5, respectively), neither performed as well as our top-ranked model.

Objective 2

Our model describing the effects of distance, area, and groundwater on reporting unit contributions to the mainstem Snake River performed well (Figure S6). Model residuals were normally distributed around 0 and an RMSE of 0.596 indicated very little error in predicted contributions. However, while the posterior predictive check showed a linear relationship between observed and predicted contributions, the model was slightly biased (indicated by a deviation from the 1:1 line) and tended to overpredict small contributions and underpredict large contributions. The effects of distance, area, and groundwater on proportional contribution were all strong as none of the 95% credible intervals of the parameter estimates overlapped 0. However, the magnitude of the effect sizes varied considerably (Figure 3). Distance had the largest effect on proportional contribution, with contributions declining precipitously as distance from the mainstem increased. Area had a moderate effect on contribution, with large catchments contributing more than smaller catchments. Finally, groundwater had the smallest effect on contribution: reporting units with high groundwater index values contributed approximately twice as much as those with low values. Simulating proportional contribution under distinct combinations of reporting unit conditions provided insight into how distance, area, and groundwater additively affect contributions (Figure 4). Reporting units located near the mainstem contributed considerably more than units characterized by average conditions. This effect was pronounced for large relative to small catchments. In contrast, reporting units located far from the mainstem contributed less than average, regardless of catchment area. Importantly, groundwater mediated the effects of distance and size on proportional contribution, such that reporting units with high groundwater index values contributed significantly more than units with low values (paired t-tests: $p < 0.05$ for all high-low groundwater comparisons).

Objective 3

After removing individuals that assigned to reporting units with low certainty, we retained 1,166 fish from the Snake River for our analysis of carry-over effects on growth. The von Bertalanffy growth function fit the historical length-at-age data well and provided probabilistic age estimates for all other fish (Figure 5): 99% of individuals assigned to a single age-class with >50% probability, while 60% assigned to a single age-class with >75% probability. Individuals were distributed approximately evenly across five age-classes, with a resulting age composition of 0.19 (0.16-0.22, mean and 95% credible interval), 0.23 (0.19-0.26), 0.18 (0.14-0.22), 0.30 (0.24-0.36), and 0.10 (0.04-0.18) for age-classes 1-5, respectively.

Carry-over effects of distance, area, and groundwater on growth varied throughout ontogeny (Table 2, Figure 6). There was a very strong negative effect of distance on mass for age-1 fish, but a positive effect of distance on weight for age-2 fish. The effect of distance on mass for older

age-classes was much smaller in magnitude or non-significant (indicated by 95% credible intervals overlapping 0). With respect to area, fish originating from larger catchments were heavier at age-4 and 5, while there was no effect of area on weight for younger age-classes. Finally, age-4 and 5 fish originating from reporting units with high groundwater values were considerably heavier than those originating from units with lower values. The effect of groundwater on mass for younger age-classes was much smaller in magnitude or non-significant. Collectively, our results suggest that older fish originating from large, groundwater-dominated tributaries were much heavier than those from smaller tributaries with less groundwater influence. Mass-at-age for younger fish was primarily driven by distance, but the direction of the effect varied among age-classes. Inspection of posterior distributions for the random effects terms indicated considerable residual variation in weight-at-age among sections and years. After accounting for the primary effects of distance, area, and groundwater, fish captured the two most upstream sections were much heavier at age than fish captured in the four most downstream sections (Figure S7). Additionally, weight-at-age declined between 2020 and 2022 (Figure S8).

Discussion

Evaluating the role of tributaries to supporting mainstem rivers is important for riverine fishes that couple spatially distinct habitats to complete their life cycles (Huntsman et al. 2016, Armstrong et al. 2021). In this study, we used genetic stock identification (GSI) to understand the effect of tributaries on the demographic structure of a metapopulation of Yellowstone cutthroat trout (YCT) occupying the mainstem Snake River, Wyoming, USA, a core distributional area with high conservation value (Al-Chokhachy et al. 2018). We found near complete reliance of the mainstem metapopulation on demographic support from tributaries, but contributions from specific tributaries were spatially variable. Distance between habitats, catchment area, and groundwater input acted in concert to determine the contribution of tributaries to the mainstem metapopulation of YCT. We also found evidence for carry-over effects of tributary characteristics on growth, but the direction and magnitude of carry-over effects changed throughout ontogeny. Collectively, our results highlight the importance of tributaries to structuring metapopulations of fish and illustrate how intact riverscapes support ecologically and economically important native trout. Our results can be used to design and prioritize conservation actions and provide insight into metapopulation dynamics under anticipated global climate change.

Biocomplexity of Native Trout in the Upper Snake River Watershed

Our results suggest considerable biocomplexity of the mainstem Snake River metapopulation of YCT as individuals were genetically assigned to a wide array of source populations (*sensu* Hilborn et al. 2003). Genetic stock identification indicated that the mainstem metapopulation is almost entirely reliant on demographic support from tributaries, as there was little evidence of a mainstem-spawning sub-population. Inspection of z-scores suggests that 6.5% of fish sampled in the mainstem originated from subpopulations other than those included in our baseline; this may include unsampled tributary subpopulations, a mainstem-spawning subpopulation, or both. Nevertheless, tributaries and mainstem rivers cannot be considered in isolation, but rather part of

a broader habitat network in which tributary-origin fish depend on and make extensive use of mainstem habitats (Petty et al. 2014, Huntsman et al. 2016, Armstrong et al. 2021).

Previous work estimated that 22-30% of YCT use side-channels of the mainstem Snake River for spawning (Homel et al. 2015). Many of the side-channels in which Homel et al. (2015) located fish during the summer spawning period desiccate in the autumn as both natural streamflow subsides and managed flow from Jackson Lake Dam is reduced (Annear 1989). Rapid flow reductions may render side-channels ecological traps that allow for limited reproductive success (Nislow and Armstrong 2012, Robertson et al. 2013). Alternatively, mainstem spawners may be genetically indistinguishable from nearby tributary reporting units. High rates of geneflow between a given reporting unit and a mainstem-spawning population would inflate the estimated contribution of that unit. However, this is unlikely given high correspondence (and low RMSE) between observed and model predicted contributions based on tributary characteristics. It is also important to note that Homel et al. (2015) inferred spawning location based on the location to which radio-tagged fish were tracked between April and July, however, YCT do not always spawn each year (Rideout et al. 2005, Gresswell 2011), so reported prevalence of mainstem spawning could be an overestimate.

Our study provides important insight into source-sink dynamics in large river networks. The lack of evidence for a large self-sustaining mainstem population suggests the mainstem Snake River is a sink, where local reproduction is insufficient to balance mortality (Pulliam 1988). In contrast, many smaller tributary streams appear to act as sources that maintain a large sink metapopulation via dispersal and immigration (Pulliam 1988). This is not to say that the Snake River and other large rivers are not productive or important habitat. Mainstem rivers can provide critical trophic subsidies to mobile fish (Petty et al. 2014, Huntsman et al. 2016) and migration between habitats can functionally extend growing seasons and allow fish to attain much larger body sizes than if restricted to a single habitat type (Armstrong et al. 2021). In fact, dispersal to reproductive sinks may benefit source subpopulations by relieving density-dependent constraints on survival and reproductive success (Pulliam 1988, Gundersen et al. 2001). Additionally, we found strong spatial structure of the mainstem metapopulation of YCT, where metapopulation composition shifted among sections of the Snake River to reflect distinct combinations of contributing source tributaries. Spatial metapopulation structure arises from heterogeneity among and interactions between dispersal and productivity across habitat patches, often regulated by density-dependence (Howe and Davis 1991, Pulliam and Danielson 1991). Our results indicate that the role of tributaries as source habitats varies spatially, which is likely a result of limited dispersal and mixing within the mainstem Snake River.

The spatial configuration of habitat conditions can vary tremendously across time (Stanford et al. 2005), with important effects on fish growth and production (Brennan et al. 2019, Walsworth et al. 2020), survival (Pregler et al. 2023), and subpopulation dynamics (Maitland and Latzka 2022). Therefore, the contribution of subpopulations to a metapopulation is expected to exhibit similar degrees of temporal variability (*sensu* Hilborn et al. 2003, Rogers and Schindler 2008). We did not find strong evidence for temporal variability in tributary contributions to the mainstem (although we did detect considerable interannual variation in mass-at-age; Figure S8). However, our study included just three years, less than a generation (Kiefling 1978), and therefore had limited power to detect interannual variation. Interannual variability in tributary

contributions, growth, and other life history characteristics are expected to provide portfolio effects that buffer metapopulations against environmental stochasticity (Schindler et al. 2010, 2015, Moore et al. 2014). Because groundwater input buffers local stream conditions against climate variability (Ward 1985, Sear et al. 1999, Lusardi et al. 2021), demographic support from groundwater-dominated tributaries to the mainstem Snake River may be more stable than that from tributaries with less groundwater influence. Long-term genetic monitoring would provide insight into the degree to which groundwater input to tributaries buffers against variability in recruitment subsidies to the mainstem Snake River metapopulation (*sensu* Harrison et al. 2020b).

Drivers of Tributary Contributions to the Mainstem Snake River

While tributary contributions to the mainstem Snake River were driven primarily by distance and size, groundwater-dominated tributaries contributed approximately twice that of tributaries with less groundwater influence. Previous work investigating growth and production dynamics of age-0 YCT in this system found that groundwater-dominated streams were nearly eight times as productive as streams with less groundwater input (i.e., snowmelt-dominated streams), which was driven in large part by an approximately 20-fold difference in age-0 density (Baldock et al. *in prep*). Variation in density-dependent resource limitation during the juvenile period may underlie differences in the prevalence of alternative migratory strategies (i.e., resident vs. migrant) among sub-populations, where juveniles spawned in groundwater-dominated habitats disperse at greater rates to larger, downstream habitats were constraints on growth and production may be relaxed (Fretwell and Lucas 1970, Einum et al. 2006). In this way, tributary streams may function similar to marine nursey habitats and protected areas, where density-dependent spillover and ontogenetic habitat shifts subsidize connected habitats and enhance metapopulation performance (Mumby et al. 2004, Abesamis and Russ 2005).

Our model describing the effects of distance, area, and groundwater on tributary contributions to the mainstem Snake River performed remarkably well as indicate by an RMSE of 0.596 (i.e., on average, predicted contributions were within 1 individual of the observed contribution). However, the model tended to overpredict contributions from reporting units that contributed little (i.e., contributions of zero or near-zero) and underpredict contributions from units contributing many individuals to the mainstem. Riverscape factors not included in our analysis may help explain bias in model predictions. For example, barriers to fish passage can negatively affect functional connectivity between tributaries and large mainstem environments (Sheer and Steel 2006, Fullerton et al. 2010). Additionally, lateral connectivity between the active stream channel and the floodplain can provide important foraging and thermal habitat diversity that fish exploit to maximize growth (Armstrong and Schindler 2013, Baldock et al. 2016). Future model development should aim to include barriers (e.g., SARP National Aquatic Barrier Inventory) and metrics of floodplain connectivity (Glassic et al. 2024) as covariates in proportional contribution modeling to reduce bias and error in model predictions.

Carry-Over Effects of Tributaries on Growth

We found substantial evidence for carry-over effects of natal tributary characteristics on growth of fish occupying the mainstem (*sensu* O'Connor et al. 2014); however, the magnitude and direction of effects varied across life stages. The negative effect of distance on mass at age-1

suggests an initial travel cost of dispersal from distant tributaries to the mainstem Snake River. Dispersal costs are well documents and typically associated with the movement phase of dispersal (Belichon et al. 1996), where individuals moving longer distances can experience temporarily reduced growth and survival due to the increased energetic demands. However, the positive effect of distance on mass at age-2 suggests that long-distance migrants may exhibit compensatory growth, where individuals in poor condition grow rapidly to catch up to (or in this case surpass) short-distance migrants heavier at age-1 (Al-Chokhachy et al. 2019). While the effect of distance was transient, the very strong effects of distance on growth for early life stages is important as juvenile body size can influence survival (Quinn and Peterson 1996, Carlson et al. 2008) and juvenile recruitment drives population dynamics of later life stages (Kanno et al. 2016).

For reproductive aged fish (ages 4 and 5), growth was positively associated with groundwater. Assuming fish display strong natal site fidelity and spawn in their tributary of origin (Quinn 1990), this suggests a growth benefit to spawning in groundwater-dominated streams. Depleted post-spawning nutritional condition is associated with high overwinter mortality and low probability of future reproduction (Bordeleau et al. 2019). Therefore, access to productive habitats that enable post-spawning recovery has important implications for lifetime reproductive success and fitness. Flow through organic-rich strata often enriches groundwater with nutrients and enhances secondary production of macroinvertebrates, which can increase salmonid growth relative to habitats with less groundwater input (Lusardi et al. 2016, Mejia et al. 2016). As fecundity increases with body size for salmonids (Bromage et al. 1990, Meyer et al. 2003), individuals spawning in groundwater-fed streams may experience greater reproductive success during subsequent life stages. Variation in per-capita reproductive success may thereby increase intrinsic rates of subpopulation growth along gradients of groundwater input (*sensu* Rodenhouse et al. 1997, McPeek et al. 2001). Carry-over effects of groundwater on growth and potential downstream effects on population-level productivity may in part explain the positive effect of groundwater on tributary contribution to the Snake River. Mass-at-age for reproductive aged fish was also associated with catchment area, although the magnitude of the effect was much less than that of groundwater. Increased growth of individuals originating from (and spawning in) larger habitats be a result of greater habitat diversity and thus increased availability of productive foraging stations (REF). Evaluating carry-over effects of tributaries on growth provides insight into the processes that structure metapopulation demography.

There are several important caveats to our analysis of carry-over effects. First, because we did not measure empirical age, uncertainty in age-estimates from the von Bertalanffy growth model contribute considerable uncertainty to our estimation of carry-over effects. However, we fully account for this uncertainty using the weighted hierarchical linear regression model. Second, the lower size cut-off for mainstem Snake River sampling (200 mm) resulted in a truncated first age-class. As a result, we do not know where the smallest age-1 individuals originated from, which may affect inferences for this age class. Third, like many studies, we do not know which fish lived to be sampled versus died prior to sampling. Therefore, this analysis is biased in that there is no way to assess the ultimate carry-over effect: mortality.

Conservation Applications

Distinct metapopulation composition across sections suggests limited dispersal and mixing once fish enter the mainstem Snake River. Monitoring programs using index sites or reaches to draw inferences about (meta)population dynamics in large rivers implicitly assume the fish sampled in one section are representative of those occupying other parts of the watershed (Rieman and McIntyre 1996). Our results suggest that such programs instead only capture the dynamics of a small subset of subpopulations. Long-term population dynamics of fishes occupying dendritic river network can be highly asynchronous across space and time (Isaak et al. 2003, Rogers and Schindler 2008, Valentine et al. 2023). Monitoring programs using index reaches could therefore fail to adequately describe the dynamics of subpopulations occupying other parts of the river network (Davis and Schindler 2021). Critically, monitoring at one location may fail to identify declines and vulnerability of component subpopulations. Our results contribute to a growing body of literature emphasizing the need for a continuous view of rivers to understand how patterns at broad spatial extents arise from processes acting at finer spatial scales (Fausch et al. 2002).

While aquatic habitat in the USRW is highly connected compared to many other watersheds, there are both natural and anthropogenic barriers that likely inhibit the expression of diverse migratory tactics and prohibit certain tributaries from contributing individuals to the mainstem. Assessing the impacts of barriers on tributary support of mainstem river metapopulations is important as habitat fragmentation can increase both climate change vulnerability and metapopulation extinction risk of fishes occupying river networks (Fagan 2002, Letcher et al. 2007, LeMoine et al. 2020). Indeed, enhancing and restoring connectivity within river networks is often a primary goal of many conservation programs (Neeson et al. 2015, Bouska et al. 2023). Unfortunately, evaluating the success of barrier removal and other restoration projects can be challenging (Bilby et al. 2024), particularly at the spatial scale at which fish complete their life history (e.g., 100s of kms; Chudnow et al. 2023) and given the coexistence of behaviorally cryptic life history forms within subpopulations (e.g., residents and migrants; Al-Chokhachy and Budy 2008). Genetic monitoring programs may prove useful for detecting the re-emergence of migratory life history forms following the restoration of connectivity between tributary and mainstem habitats. Genetic monitoring may be particularly successful as isolation above barriers often leads to strong genetic divergence from populations downstream (Wofford et al. 2005), thus increasing the accuracy of subpopulation assignment using GSI.

Our study provides strong evidence that tributary-origin fish make extensive use of mainstem river habitats and provide critical demographic support to large mainstem rivers, which often the target of culturally and economically valuable recreational fisheries (Cline et al. 2022). Importantly, many of the groundwater-dominated streams that made large contributions to Snake River are located on private land. Land-use change can influence stream biophysical processes and negatively affect salmonid populations (e.g., by increasing sedimentation rates which subsequently reduce juvenile recruitment; Jensen et al. 2009). Therefore, the actions of relatively few landowners may exert disproportionate influence on (and potentially threaten) the status of the Snake River fishery. Effective conservation efforts may therefore require coordination and cooperation with broad coalition of stakeholders, especially private landowners (Clancy et al. 2020).

Conclusions

Biocomplexity in many forms (e.g., habitat and life-history diversity) underpins the long-term productivity and stability of metapopulations and associated ecosystem services (Hilborn et al. 2003, Schindler et al. 2010). In free-flowing river networks, processes occurring in headwaters are aggregated as tributaries converge downstream, such that patterns observed in large mainstem rivers often reflect headwater environments (Moore 2015, French et al. 2020). Asynchrony in fish production among tributaries can stabilize metapopulations and mixed-stock fishery catches in larger mainstem rivers via portfolio effects (Moore et al. 2015, Schindler et al. 2015). Therefore, protecting and conserving tributaries will likely be necessary to ensure the long-term viability of mainstem river ecosystems (Bouska et al. 2023).

Here, we demonstrate the influence of tributary streams on the demography of a mainstem river metapopulation of native Yellowstone cutthroat trout. By investigating the influence of tributary characteristics on metapopulation demography, our results provide insight into the mechanisms that give rise to metapopulation behavior in riverine ecosystems. Our results illustrate how spatially discrete and distributed riverscape attributes influence patterns at broader spatial scales and levels of organization (*sensu* Heffernan et al. 2014, Terui et al. 2021). Our results have important implications for understanding how habitat fragmentation and the subsequent loss of habitat diversity may scale up to destabilize ecologically and economically important metapopulations of fish (Fagan 2002).

References

Abesamis, R. A., and G. R. Russ. 2005. Density-dependent spillover from a marine reserve: Long-term evidence. Ecological Applications 15:1798–1812.

Al-Chokhachy, R., R. P. Kovach, A. Sepulveda, J. Strait, B. B. Shepard, and C. C. Muhlfeld. 2019. Compensatory growth offsets poor condition in native trout populations. Freshwater Biology:1–11.

Al-Chokhachy, R., B. B. Shepard, J. C. Burckhardt, D. Garren, S. Opitz, T. M. Koel, L. Nelson, and R. E. Gresswell. 2018. A portfolio framework for prioritizing conservation efforts for Yellowstone Cutthroat Trout populations. Fisheries 43:485–496.

Al-Chokhachy, R., and P. Budy. 2008. Demographic Characteristics, Population Structure, and Vital Rates of a Fluvial Population of Bull Trout in Oregon. Transactions of the American Fisheries Society 137:1709–1722.

Anderson, E. C., R. S. Waples, and S. T. Kalinowski. 2008. An improved method for predicting the accuracy of genetic stock identification. Canadian Journal of Fisheries and Aquatic Sciences 65:1475–1486.

Annear, T. C. 1989. Snake River Instream Flow Studies. Cheyenne, WY.

Araujo, H. A., J. R. Candy, T. D. Beacham, B. White, and C. Wallace. 2014. Advantages and Challenges of Genetic Stock Identification in Fish Stocks with Low Genetic Resolution. Transactions of the American Fisheries Society 143:479–488.

Armstrong, J. B., A. H. Fullerton, C. E. Jordan, J. L. Ebersole, J. R. Bellmore, I. Arismendi, B. E. Penaluna, and G. H. Reeves. 2021. The importance of warm habitat to the growth regime of cold-water fishes. Nature Climate Change.

Armstrong, J. B., and D. E. Schindler. 2013. Going with the Flow: Spatial Distributions of Juvenile Coho Salmon Track an Annually Shifting Mosaic of Water Temperature. Ecosystems 16:1429–1441.

Averill, C., Z. R. Werbin, K. F. Atherton, J. M. Bhatnagar, and M. C. Dietze. 2021. Soil microbiome predictability increases with spatial and taxonomic scale. Nature Ecology & Evolution 5:747–756.

Baldock, J. R., R. K. Al-Chokhachy, M. R. Campbell, and A. Walters. 2023. Timing of reproduction underlies fitness tradeoffs for a salmonid fish. Oikos:1–13.

Baldock, J. R., J. B. Armstrong, D. E. Schindler, and J. L. Carter. 2016. Juvenile coho salmon track a seasonally shifting thermal mosaic across a river floodplain. Freshwater Biology:1–12.

Beacham, T. D., C. Wallace, K. Jonsen, B. J. G. Sutherland, C. Gummer, and E. B. Rondeau. 2020. Estimation of conservation unit and population contribution to chinook salmon mixed-stock fisheries in british columbia, canada, using direct dna sequencing for single nucleotide polymorphisms. Canadian Journal of Fisheries and Aquatic Sciences 77:1302–1315.

Bekkevold, D., A. Piper, R. Campbell, P. Rippon, R. M. Wright, C. Crundwell, K. Wysujack, J. R. Stevens, R. Andrew King, K. Aarestrup, and A. Maltby. 2021. Genetic stock identification of sea trout (Salmo trutta L.) along the British North Sea Coast shows prevalent long-distance migration. ICES Journal of Marine Science 78:952–966.

Belichon, S., J. Clobert, and M. Massot. 1996. Are there differences in fitness components between philopatric and dispersing individuals? Acta Oecologica 17:503–517.

Benda, L., N. L. Poff, D. Miller, T. Dunne, G. Reeves, G. Pess, and M. Pollock. 2004. The network dynamics hypothesis: How channel networks structure riverine habitats. BioScience 54:413–427.

Bilby, R. E., K. P. Currens, K. L. Fresh, D. B. Booth, R. R. Fuerstenberg, and G. L. Lucchetti. 2024. Why Aren't Salmon Responding to Habitat Restoration in the Pacific Northwest? Fisheries 49:16–27.

Bordeleau, X., B. G. Hatcher, S. Denny, F. G. Whoriskey, D. A. Patterson, and G. T. Crossin. 2019. Nutritional correlates of the overwintering and seaward migratory decisions and long-term survival of post-spawning Atlantic salmon. Conservation Physiology 7:1–13.

Bouska, K. L., B. D. Healy, M. J. Moore, C. G. Dunn, J. J. Spurgeon, and C. P. Paukert. 2023. Diverse portfolios: Investing in tributaries for restoration of large river fishes in the Anthropocene. Frontiers in Environmental Science.

Bowersox, B. J., J. S. Hargrove, T. Copeland, and M. R. Campbell. 2023. The Genetic Composition of Wild Steelhead Based on Spatial Proximity to a Hatchery. North American Journal of Fisheries Management 43:431–450.

Bradbury, I. R., B. F. Wringe, B. Watson, I. Paterson, J. Horne, R. Beiko, S. J. Lehnert, M. Clément, E. C. Anderson, N. W. Jeffery, S. Duffy, E. Sylvester, M. Robertson, and P. Bentzen. 2018. Genotyping-by-

sequencing of genome-wide microsatellite loci reveals fine-scale harvest composition in a coastal Atlantic salmon fishery. Evolutionary Applications 11:918–930.
Brennan, S. R., D. E. Schindler, T. J. Cline, T. E. Walsworth, G. Buck, and D. P. Fernandez. 2019. Shifting habitat mosaics and fish production across river basins. Science 364:783–786.
Bromage, N. R., P. Hardiman, J. Jones, J. Springate, and V. Bye. 1990. Fecundity, egg size and total egg volume differences in 12 stocks of rainbow trout, Oncorhynchus mykiss Richardson. Aquaculture and Fisheries Management 21:269–284.
Budy, P., P. D. Thompson, M. D. McKell, G. P. Thiede, T. E. Walsworth, and M. M. Conner. 2020. A multifaceted reconstruction of the population structure and life history expressions of a remnant metapopulation of Bonneville cutthroat trout: implications for maintaining intermittent connectivity. Transactions of the American Fisheries Society 149:443–461.
Campbell Grant, E. H., W. H. Lowe, and W. F. Fagan. 2007. Living in the branches: Population dynamics and ecological processes in dendritic networks. Ecology Letters 10:165–175.
Campbell, N. R., S. A. Harmon, and S. R. Narum. 2015. Genotyping-in-Thousands by sequencing (GT-seq): A cost effective SNP genotyping method based on custom amplicon sequencing. Molecular Ecology Resources 15:855–867.
Carlson, S. M., E. M. Olsen, and L. A. Vøllestad. 2008. Seasonal mortality and the effect of body size: A review and an empirical test using individual data on brown trout. Functional Ecology 22:663–673.
Chezik, K. A., S. C. Anderson, and J. W. Moore. 2017. River networks dampen long-term hydrological signals of climate change. Geophysical Research Letters 44:7256–7264.
Chong, F., and M. Spencer. 2018. Analysis of relative abundances with zeros on environmental gradients: A multinomial regression model. PeerJ 2018:1–26.
Chudnow, R., B. van Poorten, R. Pillipow, I. Spendlow, N. Gantner, and S. Hinch. 2023. Modelling migratory behaviour and habitat use of fish in a large, uninterrupted river network: A case study of a migratory salmonid. Ecology of Freshwater Fish:1–16.
Clancy, N. G., J. P. Draper, J. M. Wolf, U. A. Abdulwahab, M. C. Pendleton, S. Brothers, J. Brahney, J. Weathered, E. Hammill, and T. B. Atwood. 2020. Protecting endangered species in the USA requires both public and private land conservation. Scientific Reports 10:1–8.
Cline, T. J., C. C. Muhlfeld, R. Kovach, R. Al-Chokhachy, D. Schmetterling, D. Whited, and A. J. Lynch. 2022. Socioeconomic resilience to climatic extremes in a freshwater fishery. Science advances 8:eabn1396.
Cordoleani, F., C. C. Phillis, A. M. Sturrock, A. M. Fitzgerald, A. Malkassian, G. E. Whitman, P. K. Weber, and R. C. Johnson. 2021. Threatened salmon rely on a rare life history strategy in a warming landscape. Nature Climate Change 11:982–988.
Crozier, W. W., P. J. Schön, G. Chaput, E. C. E. Potter, N. Ó Maoiléidigh, and J. C. MacLean. 2004. Managing Atlantic salmon (Salmo salar L.) in the mixed stock environment: Challenges and considerations. ICES Journal of Marine Science 61:1344–1358.
Davis, B. M., and D. E. Schindler. 2021. Effects of variability and synchrony in assessing contributions of individual streams to habitat portfolios of river basins. Ecological Indicators 124:107427.
Dobrowski, S. Z. 2011. A climatic basis for microrefugia: The influence of terrain on climate. Global Change Biology 17:1022–1035.
Douma, J. C., and J. T. Weedon. 2019. Analysing continuous proportions in ecology and evolution: A practical introduction to beta and Dirichlet regression. Methods in Ecology and Evolution 10:1412–1430.
Einum, S., L. Sundt-Hansen, and K. H. Nislow. 2006. The partitioning of density-dependent dispersal, growth and survival throughout ontogeny in a highly fecund organism. Oikos 113:489–496.
Elith, J., S. J. Phillips, T. Hastie, M. Dudík, Y. E. Chee, and C. J. Yates. 2011. A statistical explanation of MaxEnt for ecologists. Diversity and Distributions 17:43–57.
Fagan, W. F. 2002. Connectivity, fragmentation, and extinction risk in dendritic metapopulations. Ecology 83:3243–3249.
Fausch, K. D., C. E. Torgersen, C. V. Baxter, and H. W. Li. 2002. Landscapes to Riverscapes: Bridging the Gap between Research and Conservation of Stream Fishes. BioScience 52:483.
Fisher, S. G. 1997. Creativity, idea generation, and the functional morphology of streams. Journal of the North American Benthological Society 16:305–318.
Forseth, T., T. F. Næsje, B. Jonsson, and K. Hårsaker. 1999. Juvenile migration in brown trout: A consequence of energetic state. Journal of Animal Ecology 68:783–793.

French, D. W., D. E. Schindler, S. R. Brennan, and D. Whited. 2020. Headwater Catchments Govern Biogeochemistry in America's Largest Free-Flowing River Network. Journal of Geophysical Research: Biogeosciences 125:1–20.
Fretwell, S. D., and H. L. J. Lucas. 1970. On territorial behavior and other factors influencing habitat distribution in birds. Acta Biotheoretica 19:16–36.
Frissell, C. A., W. J. Liss, C. E. Warren, and M. D. Hurley. 1986. A hierarchical framework for stream habitat classification: Viewing streams in a watershed context. Environmental Management 10:199–214.
Fullerton, A. H., K. M. Burnett, E. A. Steel, R. L. Flitcroft, G. R. Pess, B. E. Feist, C. E. Torgersen, D. J. Miller, and B. T. Sanderson. 2010. Hydrological connectivity for riverine fish: Measurement challenges and research opportunities. Freshwater Biology 55:2215–2237.
Gerlach, M. E., K. C. Rains, E. J. Guerrón-Orejuela, W. J. Kleindl, J. Downs, S. M. Landry, and M. C. Rains. 2022. Using remote sensing and machine learning to locate groundwater discharge to salmon-bearing streams. Remote Sensing 14.
Glassic, H. C., K. C. McGwire, W. W. Macfarlane, C. Rasmussen, N. Bouwes, J. M. Wheaton, and R. Al-Chokhachy. 2024. From pixels to riverscapes: How remote sensing and geospatial tools can prioritize riverscape restoration at multiple scales. WIREs Water:1–22.
Gresswell, R. E. 2011. Biology, status, and management of the Yellowstone cutthroat trout. North American Journal of Fisheries Management 31:782–812.
Griffiths, J. R., D. E. Schindler, and L. W. Seeb. 2013. How stock of origin affects performance of individuals across a meta-ecosystem: an example from sockeye salmon. PloS ONE 8:e58584.
Gundersen, G., E. Johannesen, H. P. Andreassen, and R. A. Ims. 2001. Source-sink dynamics: How sinks affect demography of sources. Ecology Letters 4:14–21.
Haganbuck, W. W. 1970. A study of the age and growth of the cutthroat trout from the Snake River, Teton County, Wyoming. University of Wyoming.
Hanski, I. 1999. Habitat connectivity, habitat continuity, and metapopulations in dynamic landscapes. Oikos 87:209–219.
Hanski, I., and M. Gilpin. 1991. Metapopulation dynamics: brief history and conceptual domain. Biological Journal of the Linnean Society 42:3–16.
Hargrove, J. S., T. A. Delomas, J. H. Powell, J. E. Hess, S. R. Narum, and M. R. Campbell. 2023. Efficient population representation with more genetic markers increases performance of a steelhead (Oncorhynchus mykiss) genetic stock identification baseline. Evolutionary Applications:1–16.
Harrison, H. B., M. Bode, D. H. Williamson, M. L. Berumen, and G. P. Jones. 2020a. A connectivity portfolio effect stabilizes marine reserve performance. Proceedings of the National Academy of Sciences 117:25595–25600.
Harrison, J. G., W. J. Calder, V. Shastry, and C. A. Buerkle. 2020b. Dirichlet-multinomial modelling outperforms alternatives for analysis of microbiome and other ecological count data. Molecular Ecology Resources 20:481–497.
Harrison, X. A., J. D. Blount, R. Inger, D. R. Norris, and S. Bearhop. 2011. Carry-over effects as drivers of fitness differences in animals. Journal of Animal Ecology 80:4–18.
Healy, B. D., and E. O. Smith. 2023. Quantifying the contributions of tributaries to large-river fish populations through mark-recapture modeling. North American Journal of Fisheries Management:1–20.
Heffernan, J. B., P. A. Soranno, M. J. Angilletta, L. B. Buckley, D. S. Gruner, T. H. Keitt, J. R. Kellner, J. S. Kominoski, A. V. Rocha, J. Xiao, T. K. Harms, S. J. Goring, L. E. Koenig, W. H. McDowell, H. Powell, A. D. Richardson, C. A. Stow, R. Vargas, and K. C. Weathers. 2014. Macrosystems ecology: Understanding ecological patterns and processes at continental scales. Frontiers in Ecology and the Environment 12:5–14.
Hilborn, R., T. P. Quinn, D. E. Schindler, and D. E. Rogers. 2003. Biocomplexity and fisheries sustainability. Proceedings of the National Academy of Sciences of the United States of America 100:6564–8.
Homel, K. M., R. E. Gresswell, and J. L. Kershner. 2015. Life history diversity of Snake River finespotted cutthroat trout: Managing for persistence in a rapidly changing environment. North American Journal of Fisheries Management 35:789–801.
Horne, J. B., S. E. Roden, E. L. LaCasella, A. Frey, S. L. Martin, T. T. Jones, S. Murakawa, S. Brunson, G. H. Balazs, and P. H. Dutton. 2023. Origins of green turtle fishery bycatch in the central pacific revealed by mixed genetic markers. Frontiers in Marine Science 10:1–13.
Hostetler, S. W., C. Whitlock, B. Shuman, D. Liefert, C. W. Drimal, and S. Bischke. 2021. Greater Yellowstone climate assessment: past, present, and future climate change in greater Yellowstone watersheds. Bozeman, MT.

Howe, R. W., and G. J. Davis. 1991. The demographic significance of “sink” populations. Biological Conservation 57:239–255.
Huntsman, B. M., J. T. Petty, S. Sharma, and E. R. Merriam. 2016. More than a corridor: use of a main stem stream as supplemental foraging habitat by a brook trout metapopulation. Oecologia 182:463–473.
Hutchinson, W. F. 2008. The dangers of ignoring stock complexity in fishery management: the case of the North Sea cod. Biology Letters 4:693–695.
Isaak, D. J., R. F. Thurow, B. E. Rieman, and J. B. Dunham. 2003. Temporal variation in synchrony among chinook salmon (Oncorhynchus tshawytscha) redd counts from a wilderness area in central Idaho. Canadian Journal of Fisheries and Aquatic Sciences 60:840–848.
Isaak, D. J., M. K. Young, D. L. Horan, D. Nagel, M. K. Schwartz, and K. S. McKelvey. 2022. Do metapopulations and management matter for relict headwater bull trout populations in a warming climate? Ecological Applications.
Jensen, A. J., R. P. Kelly, E. C. Anderson, W. H. Satterthwaite, A. O. Shelton, and E. J. Ward. 2022. Introducing zoid: A mixture model and R package for modeling proportional data with zeros and ones in ecology. Ecology 103:1–8.
Jensen, D. W., E. A. Steel, A. H. Fullerton, and G. R. Pess. 2009. Impact of fine sediment on egg-to-fry survival of pacific salmon: A meta-analysis of published studies. Reviews in Fisheries Science 17:348–359.
Källo, K., K. Birnie-Gauvin, H. Baktoft, D. Bekkevold, C. Lesher, P. Grønkjær, G. H. Barfod, R. Johnson, G. Whitman, M. Willmes, J. Glessner, and K. Aarestrup. 2023. Otolith microchemistry combined with genetics reveal patterns of straying and population connectivity in anadromous brown trout (Salmo trutta). Ecology of Freshwater Fish.
Kanno, Y., K. C. Pregler, N. P. Hitt, B. H. Letcher, D. J. Hocking, and J. E. B. Wofford. 2016. Seasonal temperature and precipitation regulate brook trout young-of-the-year abundance and population dynamics. Freshwater Biology 61:88–99.
Kanno, Y., J. C. Vokoun, and B. H. Letcher. 2011. Sibship reconstruction for inferring mating systems, dispersal and effective population size in headwater brook trout (Salvelinus fontinalis) populations. Conservation Genetics 12:619–628.
Kiefling, J. 1978. Studies on the ecology of the Snake River Cutthroat Trout. Cheyenne, WY.
Kiefling, J. 1997. A history of the Snake River spring creek spawning tributaries. Cheyenne, WY.
Koel, T. M., L. M. Tronstad, J. L. Arnold, K. A. Gunther, D. W. Smith, J. M. Syslo, and P. J. White. 2019. Predatory fish invasion induces within and across ecosystem effects in Yellowstone National Park. Science Advances 5:1–11.
Kovach, R. P., R. Al-Chokhachy, and T. Stephens. 2018. Proactive Rainbow Trout Suppression Reduces Threat of Hybridization in the Upper Snake River Basin. North American Journal of Fisheries Management 38:811–819.
Kovach, R. P., L. A. Eby, and M. P. Corsi. 2011. Hybridization between Yellowstone cutthroat trout and rainbow trout in the upper Snake River basin, Wyoming. North American Journal of Fisheries Management 31:1077–1087.
Kraemer, P., and G. Gerlach. 2017. Demerelate: calculating interindividual relatedness for kinship analysis based on codominant diploid genetic markers using R. Molecular Ecology Resources 17:1371–1377.
LeMoine, M. T., L. A. Eby, C. G. Clancy, L. G. Nyce, M. J. Jakober, and D. J. Isaak. 2020. Landscape resistance mediates native fish species distribution shifts and vulnerability to climate change in riverscapes. Global Change Biology 26:5492–5508.
Letcher, B. H., K. H. Nislow, J. A. Coombs, M. J. O’Donnell, and T. L. Dubreuil. 2007. Population response to habitat fragmentation in a stream-dwelling brook trout population. PLoS ONE 2.
Letcher, B. H., P. Schueller, R. D. Bassar, K. H. Nislow, J. A. Coombs, K. Sakrejda, M. Morrissey, D. B. Sigourney, A. R. Whiteley, M. J. O’Donnell, and T. L. Dubreuil. 2015. Robust estimates of environmental effects on population vital rates: An integrated capture-recapture model of seasonal brook trout growth, survival and movement in a stream network. Journal of Animal Ecology 84:337–352.
Lusardi, R. A., M. T. Bogan, P. B. Moyle, and R. A. Dahlgren. 2016. Environment shapes invertebrate assemblage structure differences between volcanic springfed and runoff rivers in northern California. Freshwater Science 35:1010–1022.
Lusardi, R. A., A. L. Nichols, A. D. Willis, C. A. Jeffres, A. H. Kiers, E. E. Van Nieuwenhuyse, and R. A. Dahlgren. 2021. Not All Rivers Are Created Equal: The Importance of Spring-Fed Rivers Under a Changing Climate. Water 13:1–22.

Magnuson, J. J., L. B. Crowder, and P. A. Medvick. 1979. Temperature as an ecological resource. American Zoologist 19:331–343.
Maitland, B. M., and A. W. Latzka. 2022. Shifting climate conditions affect recruitment in Midwestern stream trout, but depend on seasonal and spatial context. Ecosphere 13:1–19.
McPeek, M. A., N. L. Rodenhouse, R. T. Holmes, and T. W. Sherry. 2001. A general model of site-dependent population regulation: Population-level regulation without individual-level interactions. Oikos 94:417–424.
Mejia, F. H., C. V. Baxter, E. K. Berntsen, and A. K. Fremier. 2016. Linking groundwater – surface water exchange to food production and salmonid growth. Canadian Journal of Fisheries and Aquatic Sciences 73:1650–1660.
Meyer, K. A., D. J. Schill, F. S. Elle, and J. A. J. Lamansky. 2003. Reproductive demographics and factors that influence length at sexual maturity of Yellowstone Cutthroat Trout in Idaho. Transactions of the American Fisheries Society 132:183–195.
Moilankn, A., and I. Hanski. 1998. Metapopulation dynamics: Effects of habitat quality and landscape structure. Ecology 79:2503–2515.
Moore, J. W. 2015. Bidirectional connectivity in rivers and implications for watershed stability and management. Can. J. Fish. Aquat. Sci 72:1–11.
Moore, J. W., M. P. Beakes, H. K. Nesbitt, J. D. Yeakel, D. A. Patterson, L. A. Thompson, C. C. Phillis, D. C. Braun, C. Favaro, D. Scott, C. Carr-Harris, and W. I. Atlas. 2015. Emergent stability in a large, free-flowing watershed. Ecology 96:340–347.
Moore, J. W., J. D. Yeakel, D. Peard, J. Lough, and M. Beere. 2014. Life-history diversity and its importance to population stability and persistence of a migratory fish: Steelhead in two large North American watersheds. Journal of Animal Ecology 83:1035–1046.
Moran, B. M., and E. C. Anderson. 2019. Bayesian inference from the conditional genetic stock identification model. Canadian Journal of Fisheries and Aquatic Sciences 76:551–560.
Morita, K., T. Tamate, M. Kuroki, and T. Nagasawa. 2014. Temperature-dependent variation in alternative migratory tactics and its implications for fitness and population dynamics in a salmonid fish. Journal of Animal Ecology 83:1268–1278.
Mumby, P. J., A. J. Edwards, J. E. Arias-Gonzalez, K. C. Lindeman, P. G. Blackwell, A. Gall, M. I. Gorczynska, A. R. Harborne, C. L. Pescod, H. Renken, C. C. C. Wabnitz, and G. Llewellyn. 2004. Mangroves enhance the biomas of coral reef fish communities in the Caribbean. Nature 427:533–536.
Neeson, T. M., M. C. Ferris, M. W. Diebel, P. J. Doran, J. R. O'Hanley, and P. B. McIntyre. 2015. Enhancing ecosystem restoration efficiency through spatial and temporal coordination. Proceedings of the National Academy of Sciences of the United States of America 112:6236–6241.
Nislow, K. H., and J. D. Armstrong. 2012. Towards a life-history-based management framework for the effects of flow on juvenile salmonids in streams and rivers. Fisheries Management and Ecology 19:451–463.
Nolan, B. T., and K. A. Miller. 1995. Water resources of Teton County, Wyoming, exclusive of Yellowstone National Park: U.S. Geological Survey Water-Resources Investigations Report 95–4204.
Novak, M. A., and M. L. Sadak. 2003. Movement patterns of stream-resident Snake River and Yellowstone cutthroat trout. Jackson, Wyoming.
O'Connor, C. M., D. R. Norris, G. T. Crossin, and S. J. Cooke. 2014. Biological carryover effects: Linking common concepts and mechanisms in ecology and evolution. Ecosphere 5:1–11.
Östergren, J., S. Palm, J. Gilbey, and J. Dannewitz. 2020. Close relatives in population samples: Evaluation of the consequences for genetic stock identification. Molecular Ecology Resources 20:498–510.
Peakall, R., and P. E. Smouse. 2006. GENALEX 6: Genetic analysis in Excel. Population genetic software for teaching and research. Molecular Ecology Notes 6:288–295.
Peterson, E. E., J. M. Ver Hoef, D. J. Isaak, J. A. Falke, M. J. Fortin, C. E. Jordan, K. McNyset, P. Monestiez, A. S. Ruesch, A. Sengupta, N. Som, E. A. Steel, D. M. Theobald, C. E. Torgersen, and S. J. Wenger. 2013. Modelling dendritic ecological networks in space: An integrated network perspective. Ecology Letters 16:707–719.
Petty, J. T., D. Thorne, B. M. Huntsman, and P. M. Mazik. 2014. The temperature-productivity squeeze: Constraints on brook trout growth along an Appalachian river continuum. Hydrobiologia 727:151–166.
Phillips, S. J., and M. Dudík. 2008. Modeling of species distributions with Maxent: new extensions and a comprehensive evaluation. Ecography 31:161–175.
Poff, N. L., J. D. Allan, M. B. Bain, J. R. Karr, K. L. Prestegaard, B. D. Richter, R. E. Sparks, and J. C. Stromberg. 1997. The Natural Flow Regime. BioScience 47:769–784.

Pollux, B. J. A., A. Korosi, W. C. E. P. Verberk, P. M. J. Pollux, and G. van der Velde. 2006. Reproduction, growth, and migration of fishes in a regulated lowland tributary: Potential recruitment to the river Meuse. Hydrobiologia 565:105–120.
Pregler, K. C., X. Lu, G. P. Valentine, S. Kim, and Y. Kanno. 2023. Temperature variation generates interspecific synchrony but spatial asynchrony in survival for freshwater fish communities. Ecology and Evolution 13:1–14.
Pritchard, V. L., N. R. Campbell, S. R. Narum, M. M. Peacock, and J. C. Garza. 2013. Discovery and characterization of novel genetic markers for use in the management of Lahontan cutthroat trout (Oncorhynchus clarkii henshawi). Molecular Ecology Resources 13:276–288.
Pulliam, H. R. 1988. Sources, sinks, and population regulation. The American Naturalist 132:652–661.
Pulliam, H. R., and B. J. Danielson. 1991. Sources, sinks, and habitat selection: a landscape perspective on population dynamics. The American Naturalist 137:S50–S66.
Quinn, T. P. 1990. Current controversies in the study of salmon homing. Ethology Ecology and Evolution 2:49–63.
Quinn, T. P., and N. P. Peterson. 1996. The influence of habitat complexity and fish size on over-winter survival and growth of individually marked juvenile coho salmon (Oncorhynchus kisutch) in Big Beef Creek, Washington. Canadian Journal of Fisheries and Aquatic Sciences 53:1555–1564.
Rideout, R. M., G. A. Rose, and M. P. M. Burton. 2005. Skipped spawning in female iteroparous fishes. Fish and Fisheries 6:50–72.
Rieman, B. E., and J. D. McIntyre. 1996. Spatial and Temporal Variablilty in Bull Trout Redd Counts. North American Journal of Fisheries Management 16:132–141.
Robertson, B. A., J. S. Rehage, and A. Sih. 2013. Ecological novelty and the emergence of evolutionary traps. Trends in Ecology and Evolution 28:552–560.
Rodenhouse, N. L., T. W. Sherry, and R. T. Holmes. 1997. Site-dependent regulation of population size: A new synthesis. Ecology 78:2025–2042.
Roff, D. A. 1991. Life history consequences of bioenergetic and biomechanical constraints on migration. American Zoologist 31:205–216.
Rogers, L. A., and D. E. Schindler. 2008. Asynchrony in population dynamics of sockeye salmon in southwest Alaska. Oikos 117:1578–1586.
Sanderson, T. B., and W. A. Hubert. 2009. Movements by adult cutthroat trout in a lotic system: implications for watershed-scale management. Fisheries Management and Ecology 16:329–336.
Satterthwaite, W. H., J. Ciancio, E. Crandall, M. L. Palmer-Zwahlen, A. M. Grover, M. R. O'Farrell, E. C. Anderson, M. S. Mohr, and J. C. Garza. 2015. Stock composition and ocean spatial distribution inference from California recreational Chinook salmon fisheries using genetic stock identification. Fisheries Research 170:166–178.
Schindler, D. E., J. B. Armstrong, and T. E. Reed. 2015. The portfolio concept in ecology and evolution. Frontiers in Ecology and the Environment 13:257–263.
Schindler, D. E., R. Hilborn, B. Chasco, C. P. Boatright, T. P. Quinn, L. A. Rogers, and M. S. Webster. 2010. Population diversity and the portfolio effect in an exploited species. Nature 465:609–12.
Schlosser, I. J. 1991. Stream fish ecology: A landscape perspective. BioScience 41:704–712.
Sear, D. A., P. D. Armitage, and F. H. Dawson. 1999. Groundwater dominated rivers. Hydrological Processes 13:255–276.
Seeb, L. W., A. Antonovich, M. A. Banks, T. D. Beacham, M. R. Bellinger, S. M. Blankenship, M. R. Campbell, N. A. Decovich, J. C. Garza, C. M. Guthrie, T. A. Lundrigan, P. Moran, S. R. Narum, J. J. Stephenson, K. J. Supernault, D. J. Teel, W. D. Templin, J. K. Wenburg, S. F. Young, and C. T. Smith. 2007. Development of a standardized DNA database for Chinook salmon. Fisheries 32:540–552.
Sheer, M. B., and E. A. Steel. 2006. Lost Watersheds: Barriers, Aquatic Habitat Connectivity, and Salmon Persistence in the Willamette and Lower Columbia River Basins. Transactions of the American Fisheries Society 135:1654–1669.
Sloat, M. R., and G. H. Reeves. 2014. Individual condition, standard metabolic rate, and rearing temperature influence steelhead and rainbow trout (Oncorhynchus mykiss) life histories. Canadian Journal of Fisheries and Aquatic Sciences 71:491–501.
Stanford, J. A., M. S. Lorang, and F. R. Hauer. 2005. The shifting habitat mosaic of river ecosystems. Internationale Vereinigung für theoretische und angewandte Limnologie: Verhandlungen 29:123–136.
Taylor, E. B., R. Chudnow, R. Pillipow, I. Spendlow, and B. van Poorten. 2021. Microsatellite DNA analysis of overwintering bull trout (Salvelinus confluentus) and its implications for harvest regulation and habitat management. Fisheries Management and Ecology 28:219–229.

Terui, A., N. Ishiyama, H. Urabe, S. Ono, J. C. Finlay, and F. Nakamura. 2018. Metapopulation stability in branching river networks. Proceedings of the National Academy of Sciences 115:E5963–E5969.
Terui, A., S. Kim, C. L. Dolph, T. Kadoya, and Y. Miyazaki. 2021. Emergent dual scaling of riverine biodiversity. Proceedings of the National Academy of Sciences 118.
Thorson, J. T., M. D. Scheuerell, E. R. Buhle, and T. Copeland. 2014. Spatial variation buffers temporal fluctuations in early juvenile survival for an endangered Pacific salmon. Journal of Animal Ecology 83:157–167.
Tsuboi, J., K. Morita, Y. Koseki, S. Endo, G. Sahashi, D. Kishi, T. Kikko, D. Ishizaki, M. Nunokawa, and Y. Kanno. 2022. Small giants: tributaries rescue spatially structured populations from extirpation in a highly fragmented stream. Journal of Applied Ecology:1–13.
Vähä, J.-P., J. Erkinaro, M. Falkegård, P. Orell, and E. Niemelä. 2017. Genetic stock identification of Atlantic salmon and its evaluation in a large population complex. Canadian Journal of Fisheries and Aquatic Sciences 74:327–338.
Valentine, G. P., X. Lu, K. C. Pregler, and M. B. Hooten. 2023. Spatial asynchrony and cross-scale climate interactions in populations:1–17.
Vannote, R. L., G. W. Minshall, K. W. Cummins, J. R. Sedell, and C. E. Cushing. 1980. The River Continuum Concept. Canadian Journal of Fisheries and Aquatic Sciences 37:130–137.
Vehtari, A., A. Gelman, and J. Gabry. 2017. Practical Bayesian model evaluation using leave-one-out cross-validation and WAIC. Statistics and Computing 27:1413–1432.
Vincenzi, S., A. J. Crivelli, D. Jesensek, and G. A. De Leo. 2008. The role of density-dependent individual growth in the persistence of freshwater salmonid populations. Oecologia 156:523–534.
Vincenzi, S., A. J. Crivelli, D. Jesensek, and G. A. De Leo. 2010. Individual growth and its implications for the recruitment dynamics of stream-dwelling marble trout (Salmo marmoratus). Ecology of Freshwater Fish 19:477–486.
Walsworth, T. E., J. R. Baldock, C. E. Zimmerman, and D. E. Schindler. 2020. Interaction between watershed features and climate forcing affects habitat profitability for juvenile salmon. Ecosphere 1.
Wang, J. 2002. An estimator for pairwise relatedness using molecular markers. Genetics 160:1203–1215.
Waples, R. S., and E. C. Anderson. 2017. Purging putative siblings from population genetic data sets: A cautionary view. Molecular Ecology 26:1211–1224.
Ward, J. V. 1985. Thermal characteristics of running waters. Hydrobiologia 125:31–46.
Weir, B. S., and C. C. Cockerham. 1984. Estimating F-Statistics for the Analysis of Population Structure. Evolution 38:1358–1370.
Wenger, S. J., D. J. Isaak, C. H. Luce, H. M. Neville, K. D. Fausch, J. B. Dunham, D. C. Dauwalter, M. K. Young, M. M. Elsner, B. E. Rieman, A. F. Hamlet, and J. E. Williams. 2011. Flow regime, temperature, and biotic interactions drive differential declines of trout species under climate change. Proceedings of the National Academy of Sciences 108:14175–14180.
Whiting, P. J., and D. B. Moog. 2001. The geometric, sedimentologic and hydrologic attributes of spring-dominated channels in volcanic areas. Geomorphology 39:131–149.
Wilson, K. L., A. C. Sawyer, A. Potapova, C. J. Bailey, D. LoScerbo, E. K. Sweeney-Bergen, E. E. Hodgson, K. J. Pitman, K. M. Seitz, L. K. Law, L. Warkentin, S. M. Wilson, W. I. Atlas, D. C. Braun, M. R. Sloat, M. T. Tinker, and J. W. Moore. 2023. The role of spatial structure in at-risk metapopulation recoveries. Ecological Applications 33:1–22.
Wofford, J. E. B., R. E. Gresswell, and M. A. Banks. 2005. Influence of barriers to movement on within-watershed genetic variation of coastal cutthroat trout. Ecological Applications 15:628–637.
Wu, F. 2000. Modeling embryo survival affected by sediment deposition into salmonid spawning gravels: Application to flushing flow prescriptions. Water Resources Research 36:1595–1603.
Wyoming Game and Fish Department. 2019. Annual Fisheries Progress Report on the 2019 Work Schedule. Cheyenne, WY.
Yamada, T., H. Urabe, and F. Nakamura. 2024. Pink salmon productivity is driven by catchment hydrogeomorphology and can decline under a changing climate. Freshwater Biology:1–11.

Tables

Table 1 Summary of *zoid* model selection results investigating spatiotemporal variability in proportional contribution of reporting groups to the mainstem Snake River. *ID* refers to the numbered hypotheses outlines in the text. *Model* represents the linear predictor. Leave-one-out cross-validation diagnostics are defined as follows: *elpdloo* = expected log pointwise predictive density, *SE(elpdloo)* = standard error of *elpdloo*, *elpddiff* = estimated difference of *elpdloo* of the candidate model and top model, and *SE(elpddiff)* = standard error of *elpddiff*. Candidate models are ordered according to minimum *elpdloo*.

ID	Model	$elpd_{loo}$	$SE(elpd_{loo})$	$elpd_{diff}$	$SE(elpd_{diff})$
2	Section	-1199.48	53.62	0.00	0.00
4	Section + Year	-1228.01	51.52	-28.53	16.12
5	Section * Year	-1294.45	47.58	-94.97	25.34
3	Year	-1807.41	98.08	-607.93	73.72
1	Null	-3272.92	137.00	-2073.44	128.25

Table 2 Age-specific posterior probability estimates of the effects of distance, catchment area, and groundwater index on weight-at-age. Estimates are given as the posterior median and 95% credible interval (in parentheses). Significant effects (in which the 95% credible interval does not overlap 0) are in **bold**.

Age	Distance	Area	Groundwater
1	**-0.0151 (-0.0192, -0.0111)**	-0.0013 (-0.0031, 0.0006)	-0.0006 (-0.0031, 0.0019)
2	**0.0162 (0.0108, 0.0213)**	0.0017 (-0.0004, 0.0041)	**-0.0032 (-0.0062, -0.0003)**
3	-0.002 (-0.008, 0.0041)	0.0027 (-0.0008, 0.0061)	**-0.0055 (-0.0096, -0.0015)**
4	**-0.0121 (-0.0214, -0.0027)**	**0.0076 (0.0023, 0.0132)**	**0.0157 (0.0098, 0.0217)**
5	-0.0078 (-0.0242, 0.0085)	**0.0135 (0.006, 0.0208)**	**0.042 (0.0326, 0.0509)**

Figures

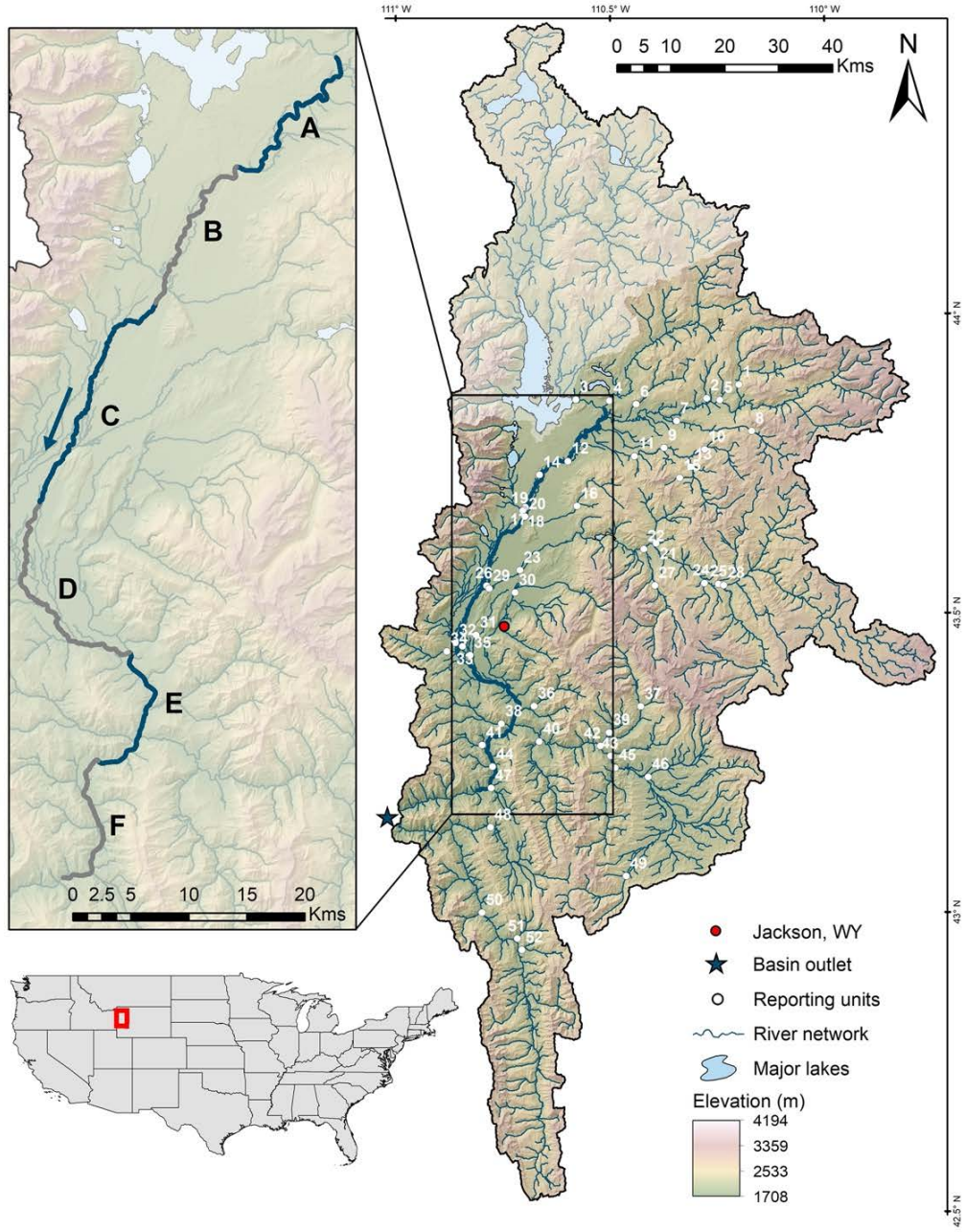

Figure 1 Map of the upper Snake and Greys River watershed (USRW). *Thin flowlines* represent tributaries streams. *Thick flowlines* represent the mainstem Snake River where mixture tissue samples were collected. Distinct mainstem sections are depicted in the inset map (*alternating colors* and *lettered* as referenced in the main text). *White points* mark the most downstream sampling location for reporting units, *numbered* as in Table S3. *Star* marks the confluence of the Snake and Greys Rivers (i.e., basin outlets), which flow into Palisades Reservoir. Flow direction is denoted by the *blue arrow*. *Opaque region* in the northern portion of the USRW is excluded from our study as it is upstream of Jackson Lake Dam, which is a complete barrier to fish passage. *Red point* marks the town of Jackson, Wyoming, and the *red box* in the U.S. map marks the location of the USRW, for visual reference.

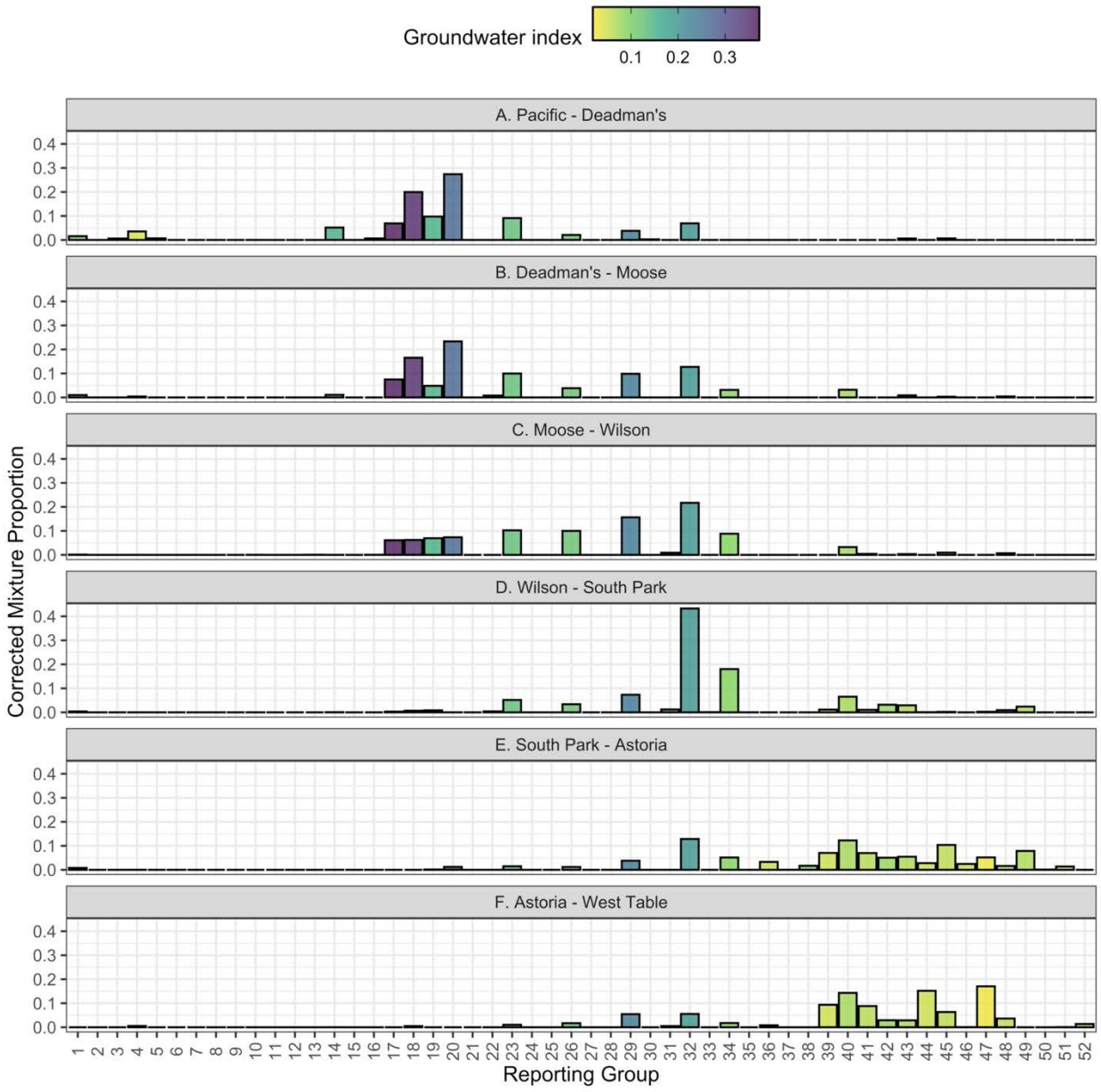

Figure 2 Bootstrap-corrected mixing proportional contribution of 52 reporting units (*bars*, numbered as in Table S3) to six sections of the mainstem Snake River (*panels*). Reporting groups are ordered by latitude from north to south; sections are ordered from upstream (north) to downstream (south). *Bar color* represents the groundwater index value calculated for each reporting group.

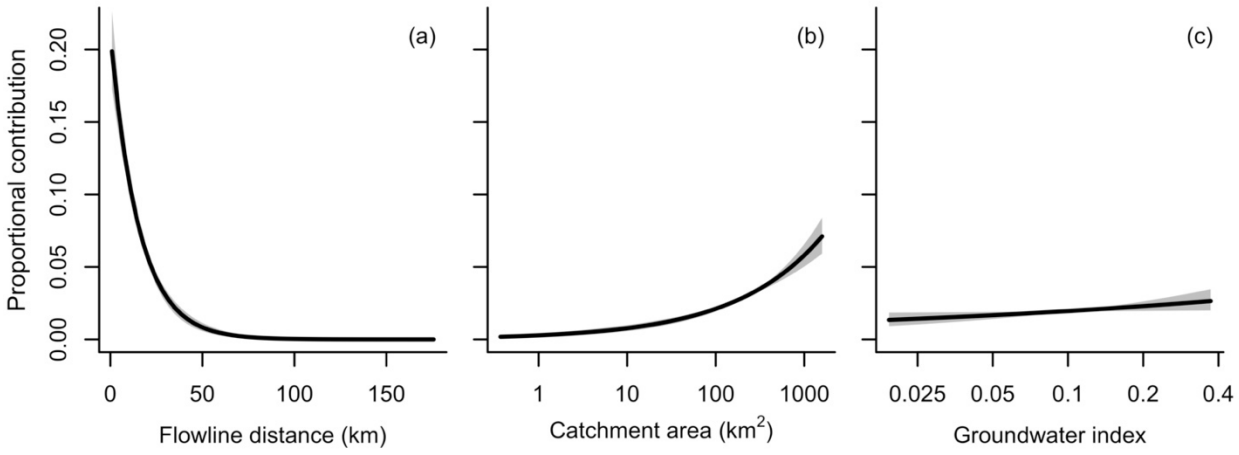

Figure 3 Predicted marginal effects of (a) flowline distance (km), (b) catchment area (km^2), and (c) groundwater index on proportional contribution of reporting groups to the mainstem Snake River.

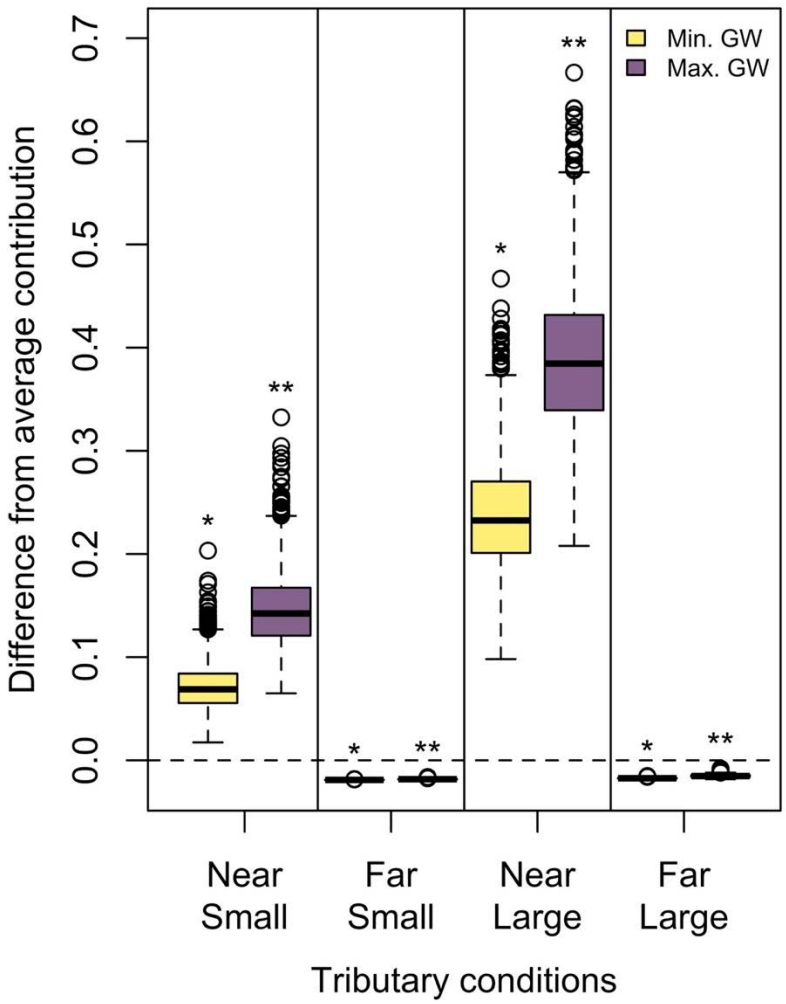

Figure 4 Additive effects of distance, area, and groundwater on proportional contribution of reporting groups relative to average conditions. For each scenario, distance was altered to reflect reporting groups located near (-1 SD) or far (+1 SD) from the Snake River, area was altered to reflect small (-1 SD) or large (+1 SD) catchments, and groundwater index was altered to reflect minimum or maximum observed values (*colors*). Points falling above 0 indicate test reporting groups that contributed more than the reference group, while points below 0 indicate test groups that contributed less than the reference group. *Horizontal dashed line* indicates no difference between test and reference groups (0). *Asterisks* represent statistically significant differences between groundwater conditions for each scenario (paired t-test, alpha = 0.05).

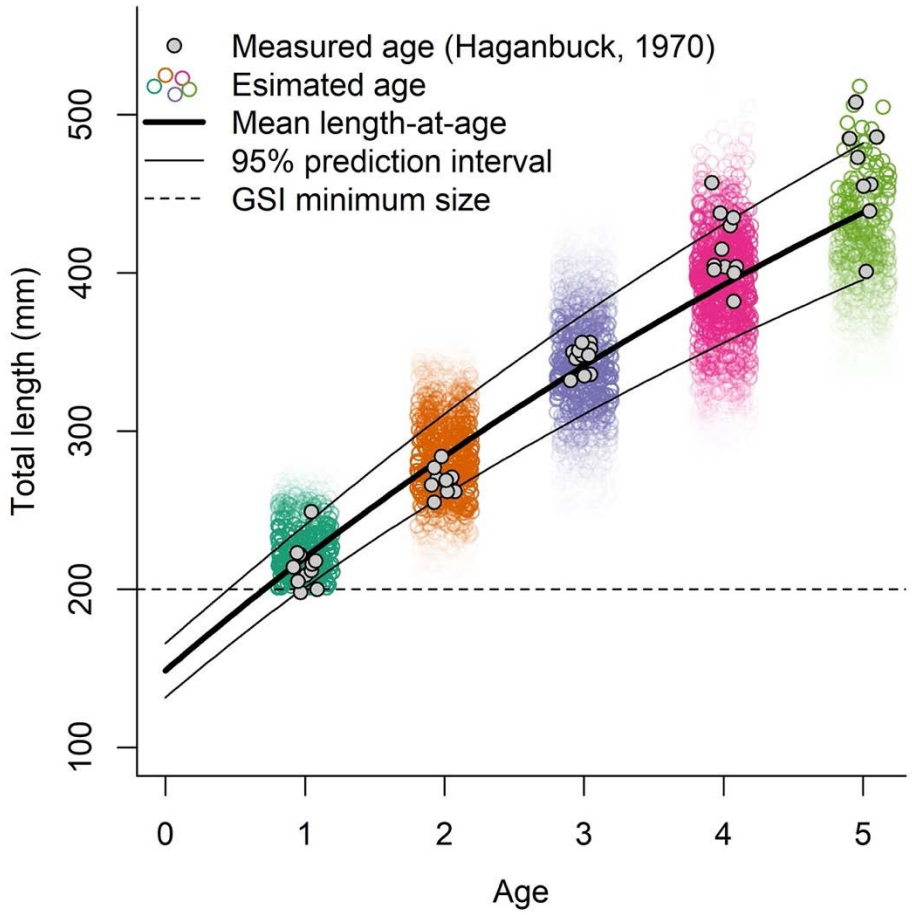

Figure 5 Model estimated von Bertalanffy growth relationships for YSC captured in the mainstem Snake River. *Thick line* represents the median predicted length-at-age; *thin lines* represent the 95% prediction interval. *Grey points* represents historical measured length-at-age from Haganbuck (1970). *Colored points* represent estimated ages of individuals in this study, where the transparency of each point indicates the probability that each individual belongs to a given age-class. Points are jittered around age to aid visual interpretation. *Horizontal dashed line* represents the minimum size of fish sampled for GSI (200 mm total length).

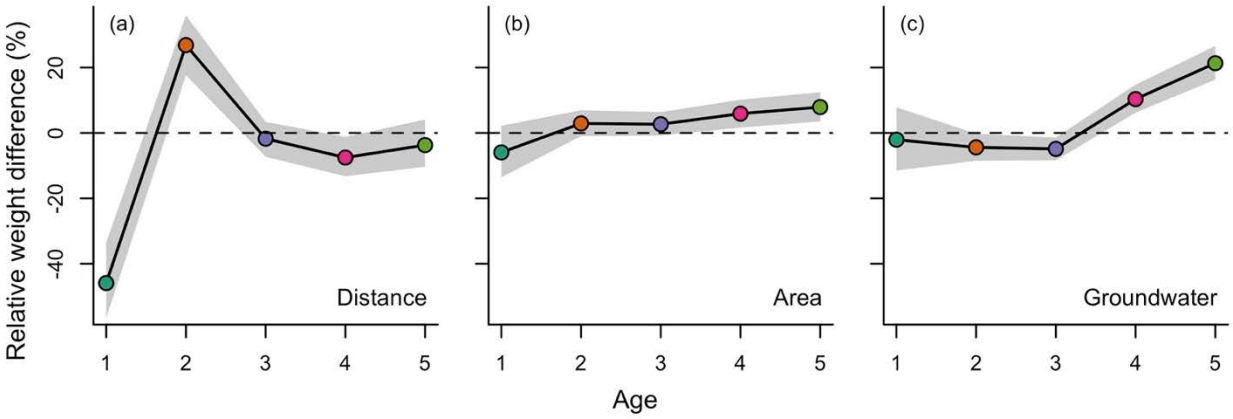

Figure 6 Age-specific effects (a) distance, (b) area, and (c) groundwater on body mass. Plots depict the relative difference between mass-at-age calculated for the maximum and minimum covariate values, for each age-class independently. For example, in panel (a), points above the dashed line (0) indicate that individuals from distant tributaries were heavier than individuals from nearby tributaries; conversely, points below the dashed line indicate that individuals from nearby tributaries were heavier than individuals from distant tributaries.

Supporting Information

Table S1 Scenarios used to evaluate additive effects of distance, area, and groundwater on proportional contribution of reporting units to the mainstem Snake River.

Scenario	Alias	Distance	Area	Groundwater
1	Near/Small	-1	-1	Minimum
2	Near/Small	-1	-1	Maximum
3	Far/Small	1	-1	Minimum
4	Far/Small	1	-1	Maximum
5	Near/Large	-1	1	Minimum
6	Near/Large	-1	1	Maximum
7	Far/Large	1	1	Minimum
8	Far/Large	1	1	Maximum

Table S2 Bayesian model fitting specifications. *Objective* refers to the numbered objective as referenced in the main text and *model description* is a brief description of the model in question. *Platform* refers to the Bayesian model fitting platform used (note that the R package *zoid* runs on the Stan platform; all other models were specified in JAGS). *Chains* represent the number of independent MCMC chains; *Burn-in iterations* is the number of iterations to initialize each mode, which were discarded prior to model interpretation; *evaluation iterations* is the total number of sampling iterations; *thinning rate* is the rate at which evaluations were retained; and *retained iterations* is the total number of sampling iterations after burn-in and thinning across all MCMC chains.

Objective	**Model description**	**Platform**	**Chains**	**Burn-in iterations**	**Evaluation iterations**	**Thinning rate**	**Retained iterations**
1	Spatiotemporal variability in composition	*zoid* (Stan)	3	2,000	2,000	NA	6,000
2	Tributary contribution	JAGS	10	10,000	160,000	1/500	3,000
3	von Bertalanffy growth	JAGS	10	200,000	1,700,000	1/1500	10,000
3	Carry-over effects	JAGS	3	2,000	12,000	1/20	1,500

Table S3 Reporting unit details. Fields are defined as follows: *Code* = numeric code as specified in Figure 1, *Alias* = local stream name(s), *Lat.* = latitude, *Long.* = longitude, N_c = number of collections, *N* = sample size (number of fish), *Self-assign.* = self-assignment rate (Figure S1), *Mean resid.* = mean residuals from simulated mixtures (mean and standard deviation, Figure S3), *Area* = catchment area in square kilometers, *GW* = groundwater index.

Code	Alias	Lat.	Long.	N_c	N	Self-assign.	Mean resid.	Area	GW
1	northbuffalofork_NA	43.885	-110.208	1	40	0.66	0.006 (0.007)	211.728	0.109
2	box_NA	43.863	-110.282	1	16	1	-0.006 (0.006)	29.141	0.025
3	spring_nps	43.862	-110.584	1	25	0.96	-0.001 (0.004)	4.013	0.092
4	pacific_NA	43.86	-110.506	2	62	0.895	0 (0.004)	415.057	0.042
5	clear_NA	43.859	-110.251	1	37	0.914	0.001 (0.006)	16.604	0.029
6	lava_NA	43.853	-110.444	1	34	1	0 (0.004)	65.334	0.037
7	blackrock_lower	43.825	-110.352	1	29	0.962	-0.002 (0.005)	124.922	0.044
8	blackrock_upper	43.807	-110.179	1	27	1	0 (0.004)	80.686	0.069
9	spread_uppermainstem	43.78	-110.381	1	33	0.818	0.002 (0.006)	202.609	0.045
10	spreadnf_flagstaff	43.777	-110.287	2	14	0.889	-0.008 (0.007)	62.106	0.077
11	rock_NA	43.767	-110.449	1	20	1	0 (0.004)	11.986	0.019
12	deadmansbar_NA	43.759	-110.603	1	25	0.955	-0.003 (0.005)	11.761	0.123
13	spread_southfork	43.748	-110.319	1	36	0.895	0.003 (0.006)	98.903	0.033
14	cowboycabin_NA	43.736	-110.669	2	23	0.692	-0.013 (0.008)	6.639	0.151
15	leidy_NA	43.73	-110.346	1	16	1	0 (0.004)	10.736	0.045
16	ditch_NA	43.684	-110.583	1	23	1	0 (0.004)	67.691	0.038
17	snakeriversidechannel	43.683	-110.701	1	31	0.667	-0.003 (0.006)	18.81	0.372
18	upperbarbc_NA	43.678	-110.705	1	39	0.619	0.004 (0.007)	5.737	0.352
19	cottonwood_nps	43.677	-110.707	1	40	0.796	0.007 (0.006)	187.153	0.152
20	blacktail_NA	43.667	-110.703	1	42	0.559	0.017 (0.011)	61.145	0.266
21	slate_NA	43.621	-110.401	2	34	1	-0.001 (0.003)	97.257	0.033
22	crystal_lower	43.612	-110.429	1	30	0.862	0.002 (0.006)	185.115	0.053
23	grosventre_lower	43.577	-110.715	1	38	0.571	0.013 (0.007)	1589.647	0.128
24	goosewing_NA	43.554	-110.29	1	10	0.833	-0.009 (0.009)	40.396	0.045
25	cottonwood_grosventre	43.552	-110.259	1	34	0.892	0.006 (0.007)	89.178	0.074
26	threechannel_NA	43.551	-110.791	2	39	0.667	-0.005 (0.006)	32.365	0.118
27	crystal_upper	43.551	-110.404	1	29	0.839	0.001 (0.005)	155.612	0.035
28	fish_grosventre	43.55	-110.246	1	17	0.917	-0.005 (0.006)	587.876	0.057
29	lowerbarbc_NA	43.547	-110.786	1	40	0.574	0.005 (0.007)	6.397	0.238
30	flat_NA	43.54	-110.726	1	30	1	-0.003 (0.005)	173.369	0.237
31	spring_tss	43.469	-110.815	1	15	1	-0.003 (0.004)	24.858	0.2
32	fish_NA	43.456	-110.863	2	82	0.68	0.017 (0.006)	233.374	0.193
33	fordspring_NA	43.45	-110.847	1	13	0.75	-0.01 (0.008)	0.371	0.308
34	mosquito_NA	43.442	-110.883	1	40	0.865	-0.003 (0.004)	61.641	0.088
35	cody_bluecrane	43.436	-110.829	2	18	1	-0.001 (0.003)	18.512	0.297
36	horse_NA	43.35	-110.683	1	24	1	-0.002 (0.004)	63.204	0.054
37	granite_upper	43.349	-110.439	1	17	1	-0.006 (0.006)	131.175	0.051
38	fall_coburn	43.321	-110.758	3	75	1	0 (0.008)	116.532	0.106
39	boulder_NA	43.306	-110.512	1	29	0.8	-0.001 (0.005)	53.7	0.05
40	willow_NA	43.291	-110.672	1	40	0.483	0.015 (0.008)	185.703	0.072
41	dog_NA	43.285	-110.803	1	46	0.953	0 (0.005)	31.09	0.062
42	granite_lower	43.283	-110.532	1	38	0.842	0.001 (0.005)	220.383	0.079
43	shoal_NA	43.266	-110.509	1	40	0.795	0.002 (0.005)	82.65	0.066
44	cabin_NA	43.249	-110.779	1	37	0.816	0.001 (0.005)	23.51	0.05
45	cliff_NA	43.247	-110.499	1	38	0.81	0.003 (0.005)	158.381	0.06
46	dell_NA	43.231	-110.423	1	31	1	-0.003 (0.005)	118.157	0.051
47	bailey_NA	43.214	-110.782	1	29	0.737	-0.009 (0.008)	41.571	0.028
48	littlegreys_steer	43.148	-110.783	3	77	0.939	0.004 (0.005)	179.346	0.057
49	hoback_upper	43.066	-110.474	1	38	0.895	0.001 (0.005)	114.078	0.067
50	white_NA	43.006	-110.803	1	14	1	-0.009 (0.008)	32.672	0.064
51	deadman_greys	42.962	-110.723	1	26	0.864	-0.003 (0.006)	42.607	0.042
52	blindbull_NA	42.943	-110.713	1	30	0.821	0.001 (0.006)	36.352	0.07

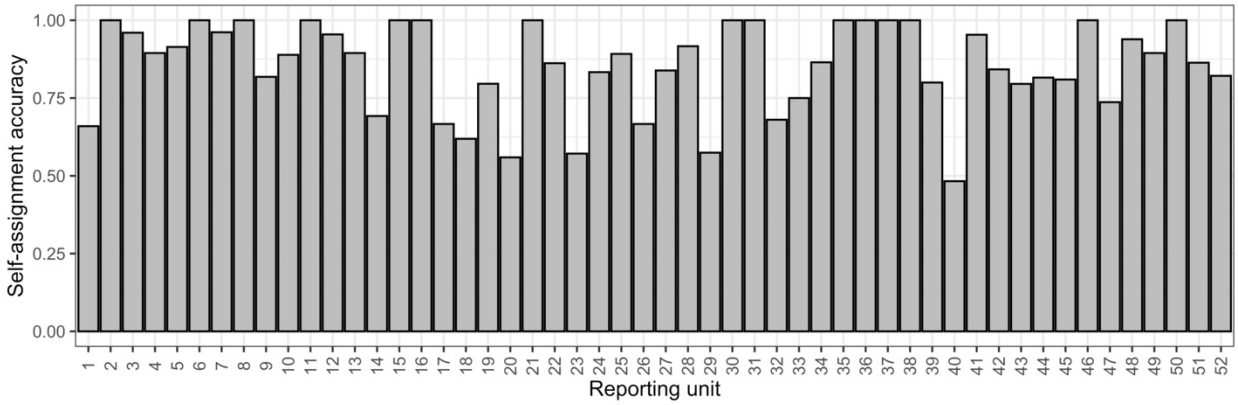

Figure S1 Self-assignment rates for each reporting unit (numbered as in Table S3) obtained from the "self_assign" function in the R package *rubias*. Self-assignment rates refer to the proportion of individuals that correctly assigned to their reporting unit of origin.

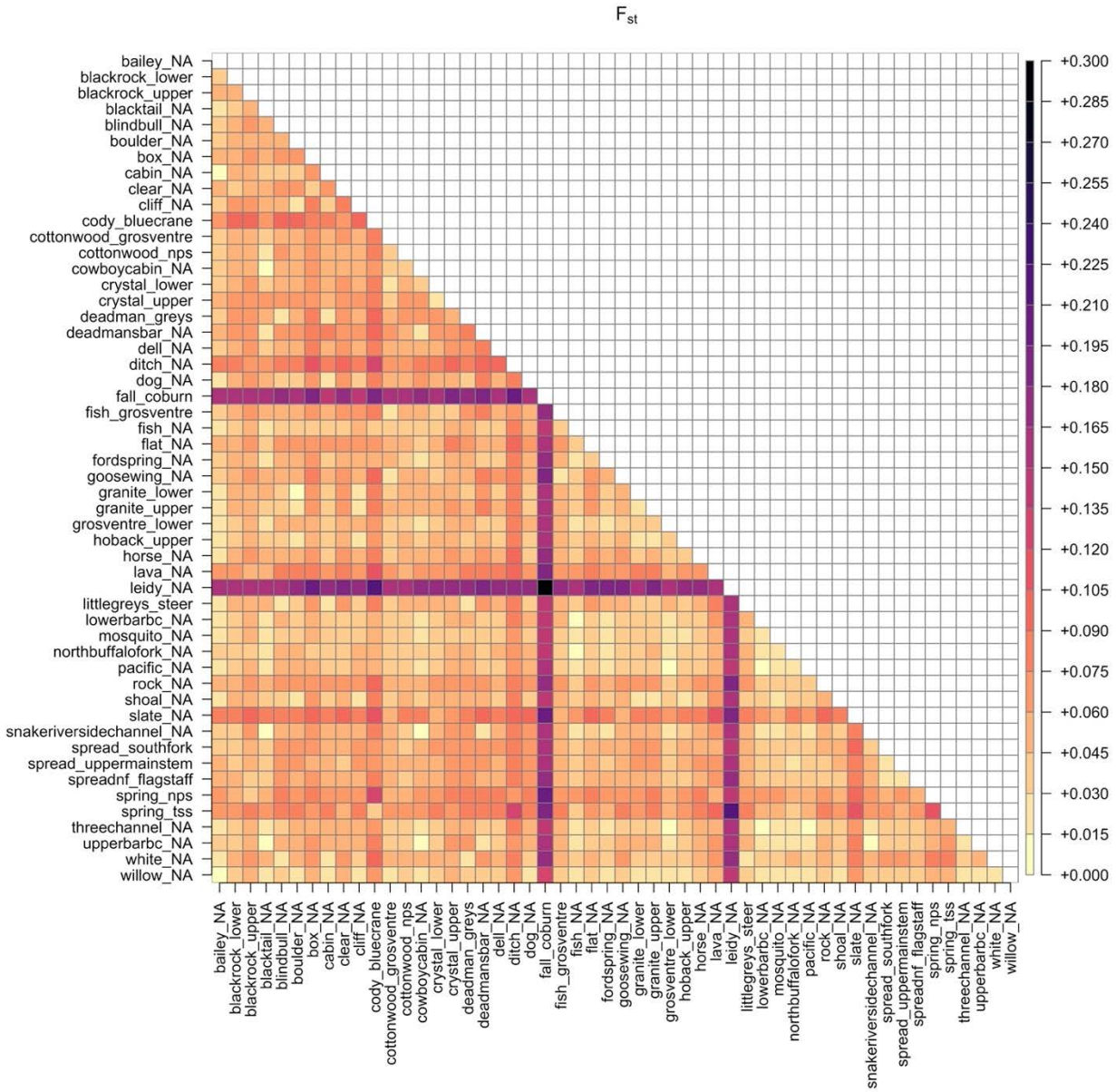

Figure S2 Pairwise measures of genetic differentiation among reporting units, F_{st} (Weir and Cockerham 1984). Note that reporting unit names, rather than numeric codes, are given, as specified in Table S3.

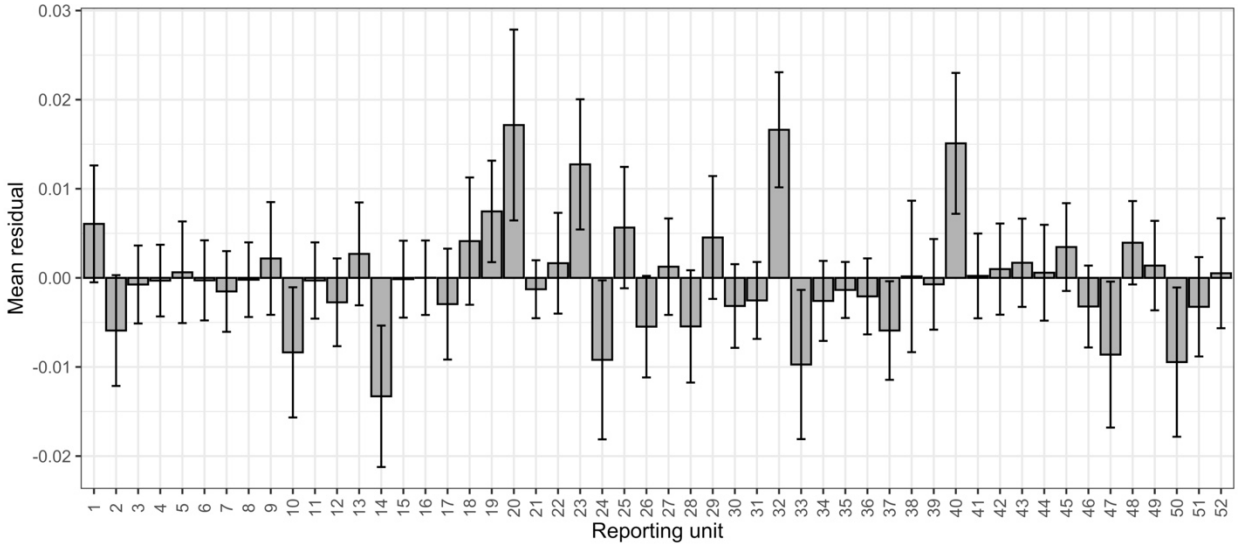

Figure S3 Reporting unit-specific mean residuals from 500 simulated mixtures calculated using the "assess_reference_loo" function in the R package *rubias*. *Error bars* represent standard deviations.

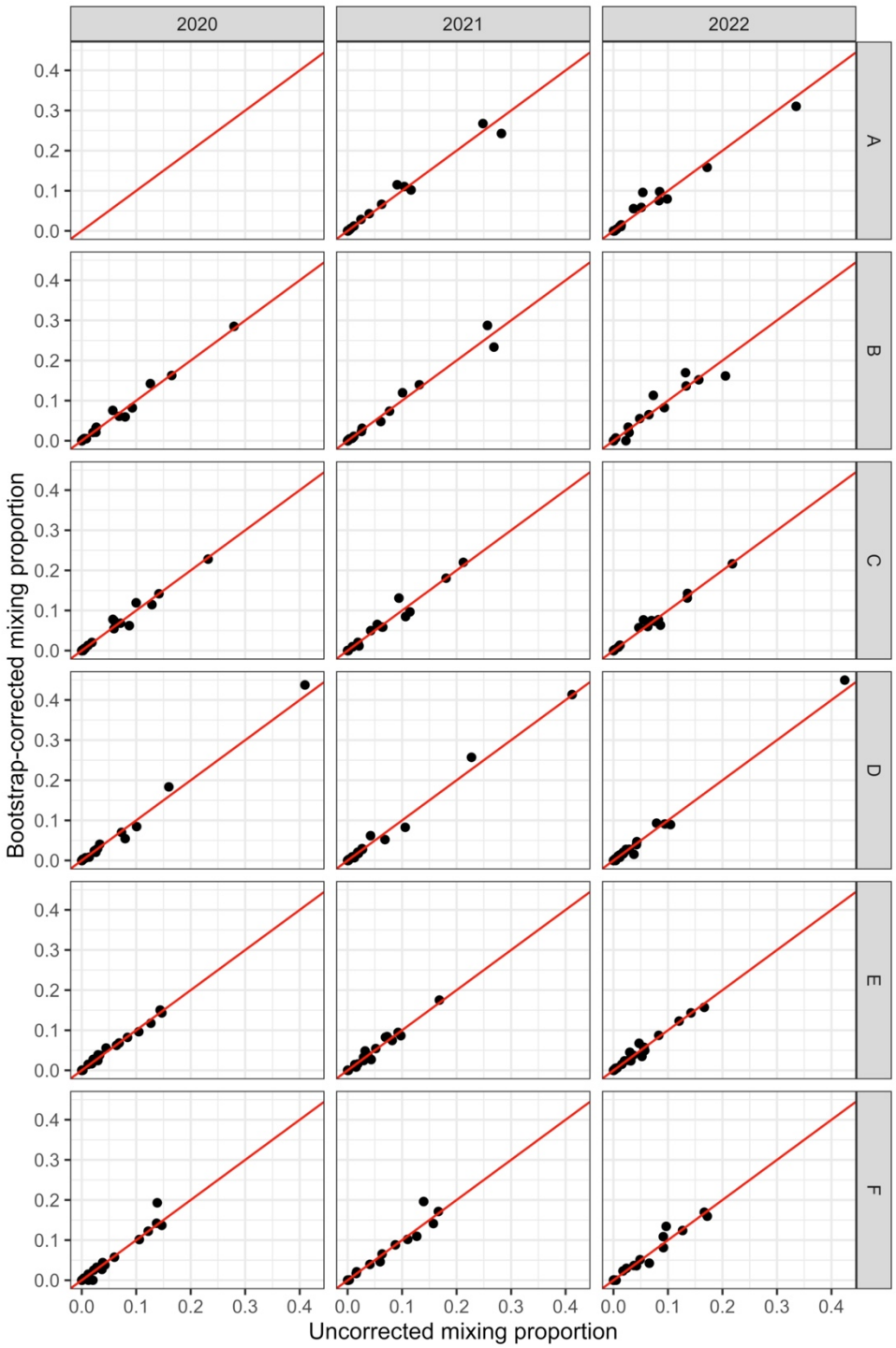

Figure S4 Relationship between uncorrected and bootstrap-corrected mixing proportions across six sections of the Snake River (*rows*) and three years (*columns*). *Red lines* represent 1:1 relationships.

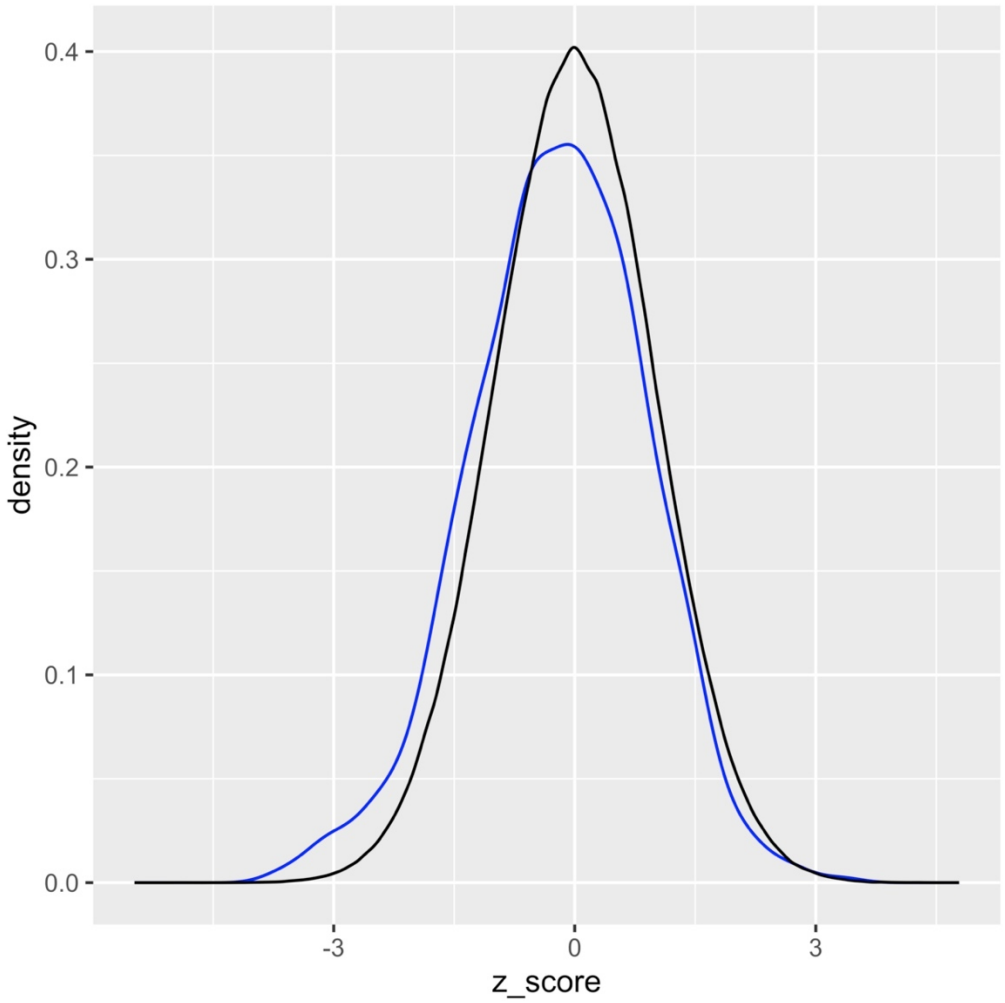

Figure S5 Distribution of z-scores (*blue line*) relative to a normal distribution (*black line*; expected outcome if all mixture samples assigned with high certainty to source populations in the baseline dataset).

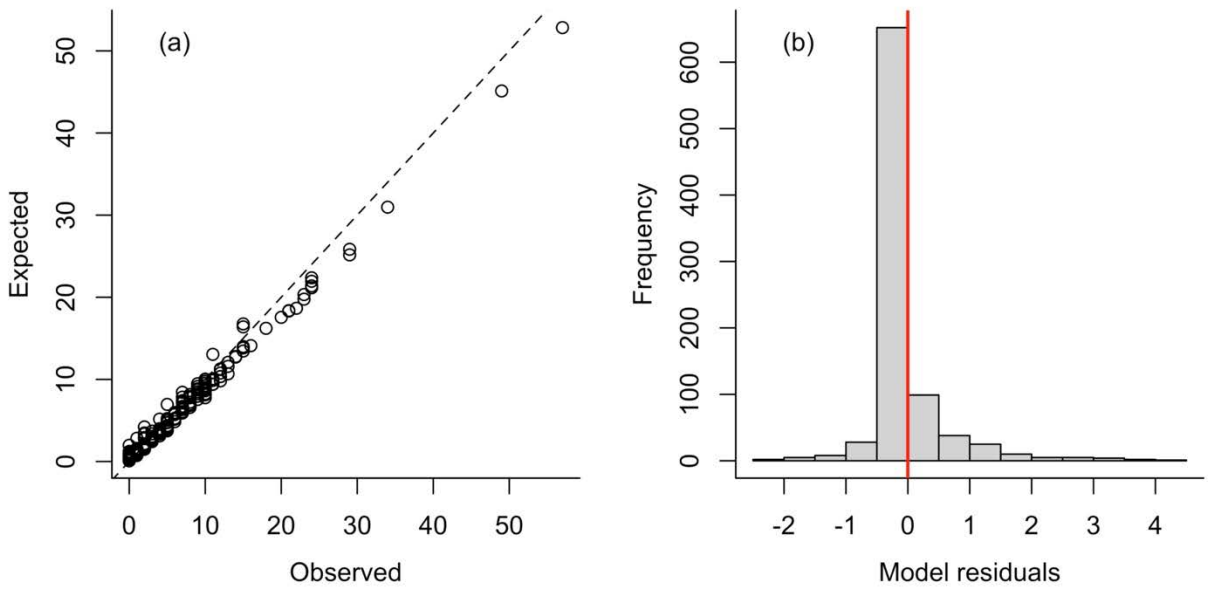

Figure S6 Model diagnostic plots for the Dirichlet-multinomial model describing the effect of tributary characteristics on contribution to the mainstem Snake River. (a) Posterior predictive check showing the relationship between model-predicted ("expected") and observed contributions ("bootstrapped numbers of fish", as described in the main text). *Dashed line* represents the 1:1 line. (b) Histogram of model residuals; *red line* denotes 0 for visual reference.

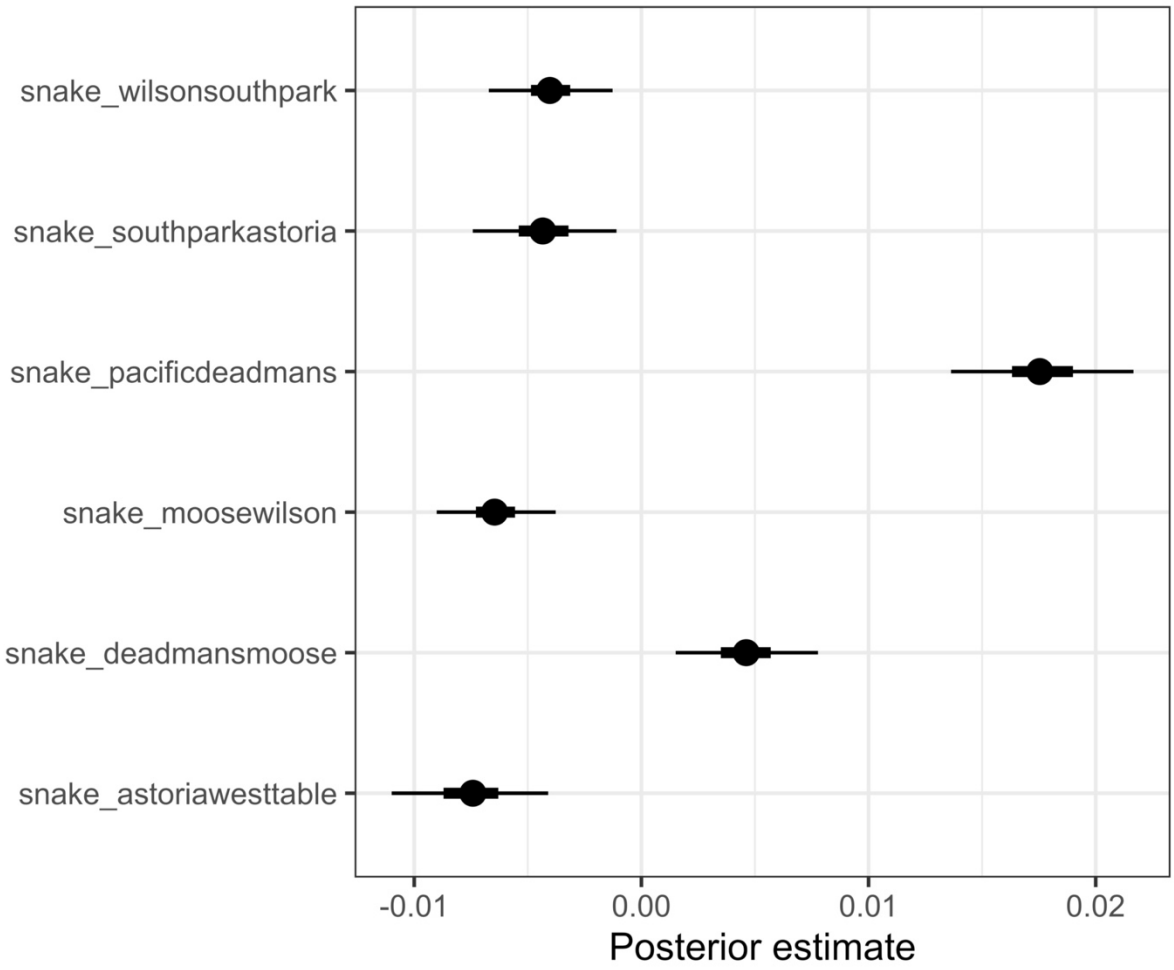

Figure S7 Posterior estimates of random intercept terms for Snake River section in the hierarchical weighted linear regression evaluating carry-over effects of tributary characteristics on mass-at-age. *Points* represent median posterior estimates and *thick and thin error bars* represent 50% and 95% credible intervals, respectively.

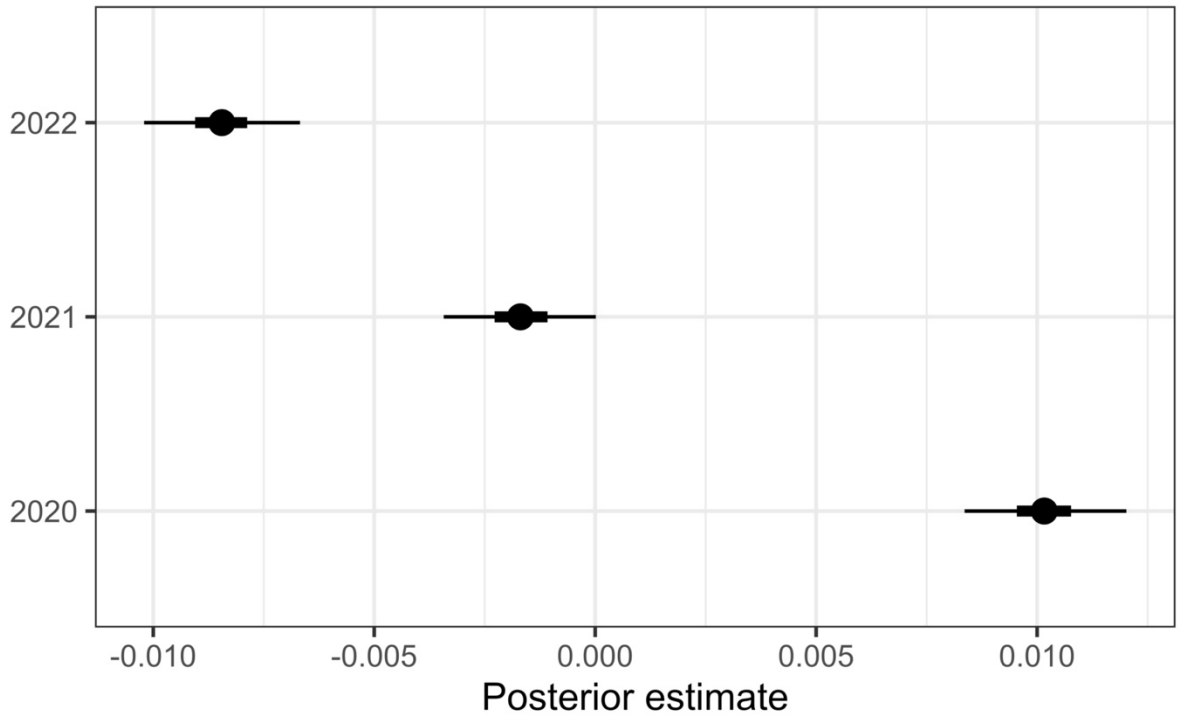

Figure S8 Posterior estimates of random intercept terms for year in the hierarchical weighted linear regression evaluating carry-over effects of tributary characteristics on mass-at-age. *Points* represent median posterior estimates and *thick and thin error bars* represent 50% and 95% credible intervals, respectively.

CHAPTER 3

Integrating groundwater into riverscape approaches to fisheries management

Jeffrey R. Baldock[1]

[1]Wyoming Cooperative Fish and Wildlife Research Unit, Department of Zoology and Physiology and Program in Ecology and Evolution, University of Wyoming, Laramie, Wyoming, USA.

Introduction

Both within the upper Snake River watershed (USRW) and across the Greater Yellowstone Area, Yellowstone cutthroat trout (*Oncorhynchus virginalis bouvieri*; YCT) are an integral component of aquatic and terrestrial food webs (Koel et al. 2019) and support economically and culturally valuable recreational fisheries. Habitat degradation and hybridization and competition with non-native species has led to widespread declines (Gresswell 2011) and anticipated climate warming further threatens many extant populations (Wenger et al. 2011). However, YCT in the USRW display successful natural reproduction (Baldock et al. 2023), negligible genetic introgression by non-natives (Kovach et al. 2018), and stable or increasing trends in population abundance (Wyoming Game and Fish Department 2019). These features, in combination with high habitat connectivity and life-history diversity, make the USRW a high priority for YCT conservation efforts (Al-Chokhachy et al. 2018).

Understanding the factors that support robust populations of YCT in the USRW will help guide local conservation efforts. Furthermore, in other parts of the range where YCT populations do not fare as well, this understanding can be used as a baseline when designing management programs aimed at mitigating population declines or re-establishing populations following local extirpation. However, conservation needs for species such as YCT are often immense relative to the capacity for management actions (e.g., funding, public support, and personnel time), such as stream habitat restoration. These constraints also limit the ability of managers to monitor the effects of management actions on intended outcomes (Bilby et al. 2024). Therefore, data and tools and that can be used to prioritize the implementation of and monitor the impacts of conservation efforts are needed to maximize the effectiveness of species-level management plans (Glassic et al. 2024, Kiser et al. 2024).

In this chapter, we expand upon how the results of our research can be used to guide the of conservation and management of YCT in the USRW. Specifically, the results of Chapter 1 can be used to prioritize the implementation of stream habitat protection and restoration projects intended to bolster YCT recruitment. The results of Chapter 2 have similar implications for prioritization schemes, but with respect to later life stages. Furthermore, Chapter 2 illustrates an approach for monitoring the effectiveness of restoration projects using genetic tools. Throughout this chapter, we discuss how the results of our research affect the interpretation of current population monitoring and highlight potentially fruitful areas for future work not already described in previous chapters.

Managing Habitat for Recruitment

Key Results from Chapter 1

In Chapter 1, we found that geologic and topographic variables explained spatial heterogeneity in groundwater discharge to streams, which stabilized temperature regimes and was associated with high YOY densities. Temperature and density, in turn, interacted to influence YOY growth rates: growth increased strongly with temperature, but this effect was reduced when density was high. Accordingly, variation in groundwater influence among stream reaches diversified trends in growth and production. At the riverscape scale, this diversity tended to reduce spatial variation in growth capacity but led to the formation of distinct hotspots of production. Collectively, our results demonstrate how groundwater, an important factor driving aquatic ecosystem heterogeneity, structures YCT recruitment dynamics across a riverscape.

Prioritization Tools for Habitat Management

Applying the results of ecological research to conservation efforts can be challenging given mismatches between the spatial extent and resolution at which research is conducted relative to that at which fish complete their life-history and management actions are applied (Fausch et al. 2002, Torgersen et al. 2021). In Chapter 1, we sought to negotiate these mismatches by projecting growth and production at both large spatial scales (across the entire USRW) and fine spatial resolutions (300 m reaches). Our results (i.e., maps of groundwater influence and YOY growth and production) can therefore be used to prioritize locations for habitat restoration and protection and to identify where such efforts may have the greatest impact on conservation outcomes. For example, if the management goal is to increase recruitment, managers may opt to place a restoration project in reaches with high groundwater index values, given the positive effects of groundwater on juvenile production.

The spatial distribution of groundwater can be compared to the spatial distribution of other known stressors (e.g., land-use change, water diversions for agriculture) to further prioritize conservation efforts. For example, a diversion dam that entrains juveniles in agricultural ditches may have a much more harmful effect on *basin-wide* population dynamics if that dam is located within a groundwater-dominated reach where YOY densities and productivity are high, relative to reaches with less groundwater influence where densities and productivity are much lower. Alternatively, if the management goal is to bolster *local* population persistence, diversion dams (or any other stressor) located in reaches with low groundwater influence may be a higher priority for managers as entrainment may threaten to eliminate an already small local population.

As highlighted in the examples above, different management goals can lead to differences in how the results of Chapter 1 are used to prioritize habitat management projects. This point underscores the need for thoughtful development of intended outcomes when designing and implementing conservation plans, as is standard practice. Ultimately, our results are just one of many factors that should be considered when deciding when and where to conduct costly restoration and protection projects. Additional factors may include the habitat needs of later life

stages (e.g., sub-adults and spawners), the opinions of professionals with complementary expertise, and existing relationships with private landowners. Nevertheless, the distribution of groundwater is an important landscape attribute with large effects on physical habitat conditions and ecological processes and should be considered when making consequential fisheries management decisions.

The Spatial Distribution of Groundwater in the USRW

The spatial distribution of groundwater discharge to streams generally matched *a priori* expectations: groundwater springs were most prevalent at toe slopes formed by stream channel incision into unconsolidated alluvium and colluvium. Past studies suggest that conservation efforts should focus on *high-elevation* headwater streams because these habitats have historically been least responsive to climate variability (Isaak et al. 2016, 2017). Our results suggest this may not be generally applicable. In the USRW, groundwater springs were most likely to occur at relatively *low elevations* (*ca.* 1800-2100 meters), which likely reflects the sub-surface flow paths of glaciated basins. Stream reaches with the greatest groundwater index values were often located immediately adjacent to larger mainstem rivers that offer contrasting, but complementary environmental conditions. The stark spatial juxtaposition of habitat conditions may in part underlie the long-term resilience of YCT in the USRW, as exploiting spatial heterogeneity in habitat conditions would require short-distance movements, relative to other river basins in which variation in water temperature and other habitat variables are arranged along elevational gradients. Importantly, applying a headwaters-focused management plan in the USRW may fall short of meeting conservation goals as this would largely overlook spatial habitat diversity imposed by groundwater.

The results of our groundwater model can help guide future research and other work as the model identified groundwater-dominated stream reaches that were not previously known to fisheries managers or other local experts. Specifically, we identified a hotspot of groundwater activity in the South Fork of Fish Creek of the Gros Ventre River basin, comparable to that of the dense, low-elevation drainage networks in and around the town of Jackson, WY. Our research would benefit from exploratory sampling trips to determine if this region is a hotspot of adult YCT spawning and YOY production, as predicted by our models. Integrated spatial modelling exercises, as detailed in Chapter 1, may prove to be a valuable tool for discovering previously unknown critical habitat and candidate locations for habitat remediation efforts.

Managing Habitat for Diversity and Resilience

Groundwater-dominated habitats are expected to become increasingly important to YCT recruitment under future climate scenarios in which regional air temperatures rise and hydrologic extremes (e.g., flooding and drought) occur more frequently (Hostetler et al. 2021, Queen et al. 2021). We discuss these topics at length in the Discussion section of Chapter 1. Additionally, there is evidence that groundwater-dominated habitats can serve as climate refugia for later life stages. For YCT in the USRW, Homel et al. (2015) found extended post-spawning residency in groundwater-dominated habitats relative to other stream types, prior to returning to overwintering habitat in the mainstem Snake River. Cool summer temperatures may enhance post-spawning recovery, whereas warmer temperatures in habitats less affected by groundwater

may threaten survival as energy stores are largely depleted (*sensu* Bordeleau et al. 2019). Additionally, salmonids congregate in cooler, groundwater-dominated habitats when temperatures elsewhere exceed tolerance thresholds, presumably to mitigate negative effects of high temperature on survival (Torgersen et al. 1999, O'Sullivan et al. 2023, Sullivan and Vokoun 2023). As climate change pushes stream conditions beyond historical baselines, access to a diversity of habitats will be necessary for salmonids seeking to both complete their life history and mitigate physiological stress (Brewitt and Danner 2014, Armstrong et al. 2021).

Conservation and management plans for YCT should specifically account for groundwater when designating critical habitat and mapping out future habitat protection and restoration efforts (Mejia et al. 2023). For example, the National Park Service currently allows outfitting companies to operate horse riding trips in the vicinity of key, groundwater-dominated spawning streams (e.g., Upper Bar BC spring and Deadman's Bar spring). On multiple occasions, we have observed guides leading clients on horseback through high-density spawning areas, trampling redds and disrupting actively spawning fish. More stringent regulations on outfitter operations or area closures may be warranted to protect critical spawning and recruitment habitat. Additionally, angling closures in and around cold, groundwater-dominated habitats may help ameliorate the physiological stress fish experience during warm periods. In the Housatonic River, CT, fisheries managers have identified cold-water refuges and close these areas to angling when temperatures in the mainstem river approach pre-defined temperature thresholds, as fish congregate in these areas to mitigate thermal stress (Sullivan et al. 2021, Mejia et al. 2023). Most groundwater-dominated streams in the USRW are close to angling until August 1 to protect spawning. However, as water temperatures continue to rise due to climate change, managers might consider extending closures to protect fish that use groundwater-dominated habitats for thermoregulatory purposes or fish that are attempting to recover critical energy stores following spawning.

While groundwater is a key component of climate refugia for stream fishes (Ebersole et al. 2020, Mejia et al. 2023), adaptation to climate change may be most successful under strategies that protect and maintain habitat heterogeneity (Walsworth et al. 2019, Moore and Schindler 2022). For example, as snowmelt often contributes most to aquifer recharge (Winograd et al. 1998), groundwater contributions to streamflow may decline as snowpack is lost under future climate scenarios (Godsey et al. 2014, Hostetler et al. 2021). Therefore, groundwater habitats may instead act as transient "stepping stones" that temporarily relieve climate impacts, assisting longer term adaptation (Hannah et al. 2014). An improved understanding of subsurface hydrology would enable predictions of where and over what time scales groundwater-dominated habitats will be resistant to climate change. Furthermore, locally adapted populations currently occupying warm and dynamic riverine habitats may harbor the genetic diversity needed for species-level adaptation to novel climate regimes (Jensen et al. 2008, Walsworth et al. 2019). Conserving habitats that span the complete range of groundwater influence is likely necessary to maximize adaptive capacity of YCT, and management plans should reflect this.

Managing Tributaries to Support the Mainstem Snake River

Key Results from Chapter 2

In Chapter 2, we found near complete reliance of the mainstem metapopulation of YCT on demographic support from tributaries, but contributions from specific tributaries varied along the length of the Snake River. Distance between habitats, catchment area, and groundwater input acted in concert to determine the contribution of tributaries to the mainstem metapopulation of YCT. Specifically, large, groundwater-dominated tributaries located near the Snake River contributed most to the mainstem YCT metapopulation. We also found evidence for carry-over effects of tributaries on growth, where metapopulation size structure was a function of natal tributaries characteristics and life stage. Importantly, weight-at-age was positively associated with groundwater for reproductive aged fish (ages 4 and 5), suggesting growth benefits for fish spawning in groundwater-dominated streams. Collectively, our results highlight the importance of tributaries to structuring metapopulations of fish and illustrate how intact riverscapes support ecologically and economically important native trout.

The Role of Tributaries to Mainstem River Fisheries

Our results indicate that the mainstem metapopulation is almost entirely reliant on demographic support from tributaries, as there was little evidence of a mainstem-spawning sub-population. This is not to say that the Snake River is not productive or unimportant. Mainstem rivers can provide critical trophic subsidies to mobile fish (Petty et al. 2014, Huntsman et al. 2016) and migration between habitats can extend growing seasons and allow fish to attain much larger body sizes than if restricted to a single habitat type (Armstrong et al. 2021). Therefore, tributaries and the mainstem Snake River cannot be considered in isolation, but rather part of a broader habitat network in which tributary-origin fish depend on and make extensive use of mainstem habitats as habitat needs change throughout their life cycle (Petty et al. 2014, Huntsman et al. 2016, Armstrong et al. 2021). We discuss these topics in greater detail in the Discussion section of Chapter 2, where we also compare our results to past work that came to somewhat different conclusions with respect to spawning in the Snake River (Homel et al. 2015).

Our analysis of carry-over effects indicates that groundwater-dominated streams disproportionately support trophy fisheries. Relative to snowmelt-dominated streams, fish originating from groundwater-dominated streams were 10.2% heavier at age-4 (1.19 vs. 1.32 lbs) and 21.4% heavier at age-5 (1.52 vs. 1.85 lbs), on average. Protecting access to groundwater-dominated spawning streams may therefore be important to maintaining trophy status of the Snake River fishery and ensuring angler satisfaction.

Implications for Population Monitoring

The very strong effect of distance on proportional contributions and variation in metapopulation composition among sections suggests limited dispersal and mixing once fish enter the mainstem Snake River. Monitoring programs using index sites or reaches to draw inferences about (meta)population dynamics in large rivers implicitly assume the fish sampled in one section are representative of those occupying other parts of the watershed (Rieman and McIntyre 1996). Our

results suggest that such programs instead only capture the dynamics of a small subset of subpopulations. The Wyoming Game and Fish Department (WGFD) conducts annual population estimates on three sections of the Snake River: Deadman's-Moose, Moose-Wilson, and Wilson-South Park. Metapopulation composition in these sections was overwhelmingly dominated by contributions from a small number of groundwater-fed streams (e.g., Upper Bar BC, Blacktail Springs, Lower Bar BC, and Fish Creek). In contrast, the metapopulation in the two most downstream sections (South Park-Astoria and Astoria-West Table) received contributions from a much greater number of tributaries, most of which had very low groundwater index values. Historical Snake River population estimates conducted on upstream sections are therefore not applicable to downstream sections. These results suggest a considerable gap in the WGFD population monitoring program. We suggest WGFD consider expanding their monitoring to include a downstream section (Astoria-West Table), which would provide critical insight into metapopulation dynamics in a section of river that bears most of the angling effort at times of year when floating the Snake River through Grand Teton National Park is prohibited. In 2022, the WGFD conducted a population estimate in the Astoria-West Table section to determine feasibility. Our results provide direct support for expanding the Snake River population monitoring program.

Prioritization Tools for Habitat Management

Robust population monitoring programs are difficult to implement across large riverscapes. Integrating multiple data sources may extend the applicability of current monitoring programs to unmonitored locations and help diagnose or locate sources of population change. Our results indicate that contributions from a relatively small number of tributaries comprise a large majority of the mainstem Snake River metapopulation of YCT. Therefore, to maximize the effectiveness of management goals seeking to bolster Snake River YCT abundance, conservation efforts might focus on the tributaries making the greatest contributions. For example, approximately 45% of the fish captured in the Wilson-South Park section originated from Fish Creek. Thus, efforts to protect and restore habitat in Fish Creek would be expected to lead to increases in YCT abundance in the Wilson-South Park section of the Snake River. Conversely, if monitoring showed persistent population declines in the Wilson-South Park section, managers might look to sudden or large changes to Fish Creek habitat to explain such declines. It is important to note that the role of any single tributary depends on the Snake River section in question. Fish Creek is far less well-represented in other sections of the Snake River (e.g., Pacific-Deadman's and Astoria-West Table). As a result, conservation efforts might instead focus on Blacktail Springs and Upper Bar BC to bolster Pacific-Deadman's YCT abundance, or on Bailey and Cabin Creeks to bolster Astoria-West Table YCT abundance. Our results will likely have broad relevance for managers seeking to understand which tributaries may be driving observed changes to the Snake River metapopulation.

The results of Chapter 2 indicate that groundwater-dominated tributaries make disproportionate contributions to the mainstem Snake River metapopulation of YCT, supporting findings from Chapter 1. Specifically, relative to snowmelt-dominated tributaries, groundwater-dominated tributaries were expected to contribute approximately twice as many fish to Snake River. These results suggest that disproportionately allocating resources to groundwater-dominated streams may have the greatest impact on intended conservation outcomes. However, it is important to

note that the effects of tributary distance (to the Snake River) and catchment area were far larger than the effect of groundwater, implying key roles of dispersal ability and total habitat availability on metapopulation structure. Indeed, conserving groundwater-dominated streams alone would appear to do little to bolster the Snake River metapopulation in the two most downstream sections, where fish primarily originated from snowmelt-dominated streams. Prioritization schemes for habitat protection and restoration must be based on clearly defined management goals. When those management goals change, under alternative or complementary management plans, we should expect the highest priority streams or reaches to change as well. Ultimately, adaptation to climate change may be most successful under strategies that protect and maintain habitat heterogeneity (Walsworth et al. 2019, Moore and Schindler 2022), as discussed above.

Ongoing Work

Our model describing the effects of distance, area, and groundwater on tributary contributions to the mainstem Snake River performed well. However, the model tended to overpredict contributions from reporting units that contributed little (i.e., contributions of zero or near-zero) and underpredict contributions from units contributing many individuals to the mainstem. Riverscape factors not included in our analysis may help explain bias in model predictions. For example, barriers to fish passage can negatively affect functional connectivity between tributaries and large mainstem environments (Sheer and Steel 2006, Fullerton et al. 2010). While aquatic habitat in the USRW is highly connected compared to many other watersheds, there are both natural and anthropogenic barriers that likely inhibit the expression of diverse migratory tactics and prohibit certain tributaries from contributing individuals to the mainstem. Ongoing work seeks to evaluate the effects of barriers on tributary contributions to the mainstem Snake River. As of this writing (June 2024), Trout Unlimited is working to update and expand the Aquatic Barrier Inventory (Southeast Aquatic Resources Partnership) in the USRW (Leslie Steen, *personal communication*). Future modelling will include covariates describing the presence of barriers between tributaries and the Snake River and the number of barriers within tributary catchments to understand to degree to which barriers limit contributions to the Snake River and, ultimately, the expression of migratory life-histories. Based on model results, we may be able to identify specific barriers for which removal or restoration would have the greatest effect on increasing contributions to the Snake River.

Developing Tools to Support Fisheries and Fish Habitat Management

Throughout the course of our research, we have sought to develop tools to support fisheries and fish habitat management in the USRW and beyond. Riverscape (i.e., spatially continuous) approaches to understanding groundwater influence in streams have been particularly challenging. Because groundwater inflow decouples stream and air temperature regimes (Caissie 2006), temperature sensitivity is often used as a proxy for groundwater influence (O'Driscoll and DeWalle 2006, Adelfio et al. 2019, Gallagher and Fraser 2023). However, using temperature sensitivity alone to infer groundwater contributions to streams is not recommended at broad spatial extents given the many landscape factors that influence sensitivity (Lisi et al. 2015, Beaufort et al. 2020). Therefore, metrics of groundwater that are independent of stream

temperature are needed to inform aquatic ecosystem research and management (Letcher et al. 2016, Mejia et al. 2023). In Chapter 1, we combined remote sensing and machine learning techniques to estimate the degree of groundwater influence continuously across the river network. Our approach is relatively simple, requiring easy-to-obtain field observations, publicly available spatial data, and modest computing power, making it tractable to apply to other watersheds where increased understanding of groundwater dynamics is needed. We have already had discussions with WGFD biologists about how such a model could be built and used to locate groundwater-dominated habitats in watersheds across Wyoming. Our novel approach represents an important development in the field of ecohydrology and provides a solution for obtaining high-resolution data describing groundwater activity at broad spatial scales.

Enhancing and restoring connectivity within river networks is often a primary goal of many fish conservation programs (Neeson et al. 2015, Bouska et al. 2023). Unfortunately, evaluating the success of barrier removal and other restoration projects can be challenging (Bilby et al. 2024), particularly at the spatial scale at which fish complete their life history (e.g., 100s of kms; Chudnow et al. 2023) and given the coexistence of resident and migrant life-history forms (Al-Chokhachy and Budy 2008). Genetic monitoring programs (i.e., genetic stock identification, GSI, Chapter 2) may prove useful for detecting the re-emergence of migratory life-histories following the restoration of connectivity between tributary and mainstem habitats. Genetic monitoring may be particularly successful as isolation above barriers often leads to strong genetic divergence from populations downstream (Wofford et al. 2005), thereby increasing assignment accuracy. Our study demonstrates how GSI could be incorporated into existing population monitoring programs to evaluate the success of barrier removal projects and other restoration efforts. For example, if a barrier to fish passage was removed from stream X, that project might be deemed successful if a greater number of fish originating from (i.e., genetically assigned to) stream X were captured in the Snake River following project completion. Our research demonstrates how low-cost, high throughput genetic sequencing tools can be used to answer pressing management questions, motivating development of similar tools to address concerns in other basins where YCT are at greater risk of extirpation. However, the state of Wyoming does not currently have the genetic sequencing capabilities to establish such a program and would be reliant on outside expertise to do so (e.g., University of Wyoming or Idaho Department of Fish and Game – Eagle Fish Genetics Lab). Investments in novel technologies (such as genetic sequencing and associated techniques) is likely necessary for efficient and effective fisheries management under global change.

Conclusions

Across the range of YCT, the USRW is a top priority for species conservation efforts (Al-Chokhachy et al. 2018) and is the crown jewel for anglers targeting native trout. While threats to YCT may be more imminent in other parts of the range, understanding how healthy riverine ecosystems function is of utmost importance as it provides a standard by which to evaluate other populations and a goal to aim for when restoring more degraded systems. With this body of research, we have (1) provided insight into the ecology of healthy metapopulations of YCT and (2) developed tools to guide the design and implementation of YCT conservation and management plans. Over the past six years, we have worked closely with representatives of the

Wyoming Game and Fish Department, National Park Service, US Forest Service, and Trout Unlimited to ensure that our research addresses critical information needs for YCT in the USRW. We strive to maintain these collaborative relationships and hope our collective action goes far to ensure the long-term success of native trout.

References

Adelfio, L. A., S. M. Wondzell, N. J. Mantua, and G. H. Reeves. 2019. Warm winters reduce landscape-scale variability in the duration of egg incubation for coho salmon (Oncorhynchus kisutch) on the Copper River Delta, Alaska. Canadian Journal of Fisheries and Aquatic Sciences 76:1362–1375.

Al-Chokhachy, R., B. B. Shepard, J. C. Burckhardt, D. Garren, S. Opitz, T. M. Koel, L. Nelson, and R. E. Gresswell. 2018. A portfolio framework for prioritizing conservation efforts for Yellowstone Cutthroat Trout populations. Fisheries 43:485–496.

Al-Chokhachy, R., and P. Budy. 2008. Demographic Characteristics, Population Structure, and Vital Rates of a Fluvial Population of Bull Trout in Oregon. Transactions of the American Fisheries Society 137:1709–1722.

Armstrong, J. B., A. H. Fullerton, C. E. Jordan, J. L. Ebersole, J. R. Bellmore, I. Arismendi, B. E. Penaluna, and G. H. Reeves. 2021. The importance of warm habitat to the growth regime of cold-water fishes. Nature Climate Change.

Baldock, J. R., R. K. Al-Chokhachy, M. R. Campbell, and A. Walters. 2023. Timing of reproduction underlies fitness tradeoffs for a salmonid fish. Oikos:1–13.

Beaufort, A., F. Moatar, E. Sauquet, P. Loicq, and D. M. Hannah. 2020. Influence of landscape and hydrological factors on stream–air temperature relationships at regional scale. Hydrological Processes 34:583–597.

Bilby, R. E., K. P. Currens, K. L. Fresh, D. B. Booth, R. R. Fuerstenberg, and G. L. Lucchetti. 2024. Why Aren't Salmon Responding to Habitat Restoration in the Pacific Northwest? Fisheries 49:16–27.

Bordeleau, X., B. G. Hatcher, S. Denny, F. G. Whoriskey, D. A. Patterson, and G. T. Crossin. 2019. Nutritional correlates of the overwintering and seaward migratory decisions and long-term survival of post-spawning Atlantic salmon. Conservation Physiology 7:1–13.

Bouska, K. L., B. D. Healy, M. J. Moore, C. G. Dunn, J. J. Spurgeon, and C. P. Paukert. 2023. Diverse portfolios: Investing in tributaries for restoration of large river fishes in the Anthropocene. Frontiers in Environmental Science.

Brewitt, K. S., and E. M. Danner. 2014. Spatio-temporal temperature variation influences juvenile steelhead (Oncorhynchus mykiss) use of thermal refuges. Ecosphere 5.

Caissie, D. 2006. The thermal regime of rivers: a review. Freshwater Biology 51:1389–1406.

Chudnow, R., B. van Poorten, R. Pillipow, I. Spendlow, N. Gantner, and S. Hinch. 2023. Modelling migratory behaviour and habitat use of fish in a large, uninterrupted river network: A case study of a migratory salmonid. Ecology of Freshwater Fish:1–16.

Ebersole, J. L., R. M. Quiñones, S. Clements, and B. H. Letcher. 2020. Managing climate refugia for freshwater fishes under an expanding human footprint. Frontiers in Ecology and the Environment 18:271–280.

Fausch, K. D., C. E. Torgersen, C. V. Baxter, and H. W. Li. 2002. Landscapes to Riverscapes: Bridging the Gap between Research and Conservation of Stream Fishes. BioScience 52:483.

Fullerton, A. H., K. M. Burnett, E. A. Steel, R. L. Flitcroft, G. R. Pess, B. E. Feist, C. E. Torgersen, D. J. Miller, and B. T. Sanderson. 2010. Hydrological connectivity for riverine fish: Measurement challenges and research opportunities. Freshwater Biology 55:2215–2237.

Gallagher, B. K., and D. J. Fraser. 2023. Stream groundwater inputs generate fine-scale variation in brook trout phenology and growth across a warming landscape. Freshwater Biology:1–16.

Glassic, H. C., K. C. McGwire, W. W. Macfarlane, C. Rasmussen, N. Bouwes, J. M. Wheaton, and R. Al-Chokhachy. 2024. From pixels to riverscapes: How remote sensing and geospatial tools can prioritize riverscape restoration at multiple scales. WIREs Water:1–22.

Godsey, S. E., J. W. Kirchner, and C. L. Tague. 2014. Effects of changes in winter snowpacks on summer low flows: Case studies in the Sierra Nevada, California, USA. Hydrological Processes 28:5048–5064.

Gresswell, R. E. 2011. Biology, status, and management of the Yellowstone cutthroat trout. North American Journal of Fisheries Management 31:782–812.

Hannah, L., L. Flint, A. D. Syphard, M. A. Moritz, L. B. Buckley, and I. M. McCullough. 2014. Fine-grain modeling of species' response to climate change: Holdouts, stepping-stones, and microrefugia. Trends in Ecology and Evolution 29:390–397.

Homel, K. M., R. E. Gresswell, and J. L. Kershner. 2015. Life history diversity of Snake River finespotted cutthroat trout: Managing for persistence in a rapidly changing environment. North American Journal of Fisheries Management 35:789–801.

Hostetler, S. W., C. Whitlock, B. Shuman, D. Liefert, C. W. Drimal, and S. Bischke. 2021. Greater Yellowstone

climate assessment: past, present, and future climate change in greater Yellowstone watersheds. Bozeman, MT.
Huntsman, B. M., J. T. Petty, S. Sharma, and E. R. Merriam. 2016. More than a corridor: use of a main stem stream as supplemental foraging habitat by a brook trout metapopulation. Oecologia 182:463–473.
Isaak, D. J., S. J. Wenger, E. E. Peterson, J. M. Ver Hoef, D. E. Nagel, C. H. Luce, S. W. Hostetler, J. B. Dunham, B. B. Roper, S. P. Wollrab, G. L. Chandler, D. L. Horan, and S. Parkes-Payne. 2017. The NorWeST summer stream temperature model and scenarios for the Western U.S.: A crowd-sourced database and new geospatial tools foster a user community and predict broad climate warming of rivers and streams. Water Resources Research 53:9181–9205.
Isaak, D. J., M. K. Young, C. H. Luce, S. W. Hostetler, S. J. Wenger, E. E. Peterson, J. M. Ver Hoef, M. C. Groce, D. L. Horan, and D. E. Nagel. 2016. Slow climate velocities of mountain streams portend their role as refugia for cold-water biodiversity. Proceedings of the National Academy of Sciences 113:4374–4379.
Jensen, L. F., M. M. Hansen, C. Pertoldi, G. Holdensgaard, K. L. D. Mensberg, and V. Loeschcke. 2008. Local adaptation in brown trout early life-history traits: Implications for climate change adaptability. Proceedings of the Royal Society B: Biological Sciences 275:2859–2868.
Kiser, A. H., C. A. Craig, T. H. Bonner, B. Littrell, C. H. Smith, C. R. Robertson, H. H. Wang, W. E. Grant, M. S. Johnson, R. Lopez, and C. R. Randklev. 2024. Creating a systematic prioritization of stream reaches for conservation of aquatic species. Ecosphere 15:1–17.
Koel, T. M., L. M. Tronstad, J. L. Arnold, K. A. Gunther, D. W. Smith, J. M. Syslo, and P. J. White. 2019. Predatory fish invasion induces within and across ecosystem effects in Yellowstone National Park. Science Advances 5:1–11.
Kovach, R. P., R. Al-Chokhachy, and T. Stephens. 2018. Proactive Rainbow Trout Suppression Reduces Threat of Hybridization in the Upper Snake River Basin. North American Journal of Fisheries Management 38:811–819.
Letcher, B. H., D. J. Hocking, K. O'Neil, A. R. Whiteley, K. H. Nislow, and M. J. O'Donnell. 2016. A hierarchical model of daily stream temperature using air-water temperature synchronization, autocorrelation, and time lags. PeerJ 2016:1–26.
Lisi, P. J., D. E. Schindler, T. J. Cline, M. D. Scheuerell, and P. B. Walsh. 2015. Watershed geomorphology and snowmelt control stream thermal sensitivity to air temperature. Geophysical Research Letters 42:3380–3388.
Mejia, F. H., V. Ouellet, M. A. Briggs, S. M. Carlson, R. Casas-Mulet, M. Chapman, M. J. Collins, S. J. Dugdale, J. L. Ebersole, D. M. Frechette, A. H. Fullerton, A. Carole-Gillis, Z. C. Johnson, C. Kelleher, B. L. Kurylyk, R. Lave, B. H. Letcher, K. M. Myrvold, T.-L. Nadeau, H. Neville, H. Piégay, K. A. Smith, D. Tonolla, and C. E. Torgersen. 2023. Closing the gap between science and management of water refuges in rivers and streams. Global Change Biology:1–27.
Moore, J. W., and D. E. Schindler. 2022. Getting ahead of climate change for ecological adaptation and resilience. Science 376:1421–1426.
Neeson, T. M., M. C. Ferris, M. W. Diebel, P. J. Doran, J. R. O'Hanley, and P. B. McIntyre. 2015. Enhancing ecosystem restoration efficiency through spatial and temporal coordination. Proceedings of the National Academy of Sciences of the United States of America 112:6236–6241.
O'Driscoll, M. A., and D. R. DeWalle. 2006. Stream-air temperature relations to classify stream-ground water interactions in a karst setting, central Pennsylvania, USA. Journal of Hydrology 329:140–153.
O'Sullivan, A. M., E. M. Corey, E. N. Collet, J. Helminen, R. A. Curry, C. MacIntyre, and T. Linnansaari. 2023. Timing and frequency of high temperature events bend the onset of behavioural thermoregulation in Atlantic salmon (Salmo salar). Conservation Physiology 11:1–16.
Petty, J. T., D. Thorne, B. M. Huntsman, and P. M. Mazik. 2014. The temperature-productivity squeeze: Constraints on brook trout growth along an Appalachian river continuum. Hydrobiologia 727:151–166.
Queen, L. E., P. W. Mote, D. E. Rupp, O. Chegwidden, and B. Nijssen. 2021. Ubiquitous increases in flood magnitude in the Columbia River basin under climate change. Hydrology and Earth System Sciences 25:257–272.
Rieman, B. E., and J. D. McIntyre. 1996. Spatial and Temporal Variablilty in Bull Trout Redd Counts. North American Journal of Fisheries Management 16:132–141.
Sheer, M. B., and E. A. Steel. 2006. Lost Watersheds: Barriers, Aquatic Habitat Connectivity, and Salmon Persistence in the Willamette and Lower Columbia River Basins. Transactions of the American Fisheries Society 135:1654–1669.
Sullivan, C. J., and J. C. Vokoun. 2023. Disentangling effects of habitat on salmonid abundance in thermal refuges

while accounting for imperfect detection. Ecosphere 14:1–19.
Sullivan, C. J., J. C. Vokoun, A. M. Helton, M. A. Briggs, and B. L. Kurylyk. 2021. An ecohydrological typology for thermal refuges in streams and rivers. Ecohydrology 14:1–15.
Torgersen, C. E., C. Le Pichon, A. H. Fullerton, S. J. Dugdale, J. J. Duda, F. Giovannini, E. Tales, J. Belliard, P. Branco, N. E. Bergeron, M. L. Roy, D. Tonollo, N. Lamouroux, H. Capra, and C. V. Baxter. 2021. Riverscape approaches in practice: perspectives and applications. Biological Reviews:1–24.
Torgersen, C. E., D. M. Price, H. W. Li, and B. a. McIntosh. 1999. Multiscale thermal refugia and stream habitat associations of chinook salmon in northeastern Oregon. Ecological Applications 9:301–319.
Walsworth, T. E., D. E. Schindler, M. A. Colton, M. S. Webster, S. R. Palumbi, P. J. Mumby, T. E. Essington, and M. L. Pinsky. 2019. Management for network diversity speeds evolutionary adaptation to climate change. Nature Climate Change 9:632–636.
Wenger, S. J., D. J. Isaak, C. H. Luce, H. M. Neville, K. D. Fausch, J. B. Dunham, D. C. Dauwalter, M. K. Young, M. M. Elsner, B. E. Rieman, A. F. Hamlet, and J. E. Williams. 2011. Flow regime, temperature, and biotic interactions drive differential declines of trout species under climate change. Proceedings of the National Academy of Sciences 108:14175–14180.
Winograd, I. J., A. C. Riggs, and T. B. Coplen. 1998. The relative contributions of summer and cool-season precipitation to groundwater recharge, Spring Mountains, Nevada, USA. Hydrogeology Journal 6:77–93.
Wofford, J. E. B., R. E. Gresswell, and M. A. Banks. 2005. Influence of barriers to movement on within-watershed genetic variation of coastal cutthroat trout. Ecological Applications 15:628–637.
Wyoming Game and Fish Department. 2019. Annual Fisheries Progress Report on the 2019 Work Schedule. Cheyenne, WY.

Appendix 1

Total project funds awarded

Table 1 Total funds awarded for this project, by organization

Organization	Grant number	Start date	End date	Award total
Jackson Hole One Fly Foundation	2021-050	8/1/2021	6/1/2024	$32,000
Wyoming Wildlife and Natural Resource Trust	03-21-023	8/30/2021	7/1/2024	$25,000
Boyd Evison Fellowship, Grand Teton Association	NA	4/4/2022	5/31/2024	$10,000
Graduate Student Research Enhancement Grant, Biodiversity Institute, University of Wyoming	NA	8/3/2021	6/30/2022	$10,000
UW-NPS Small Grants Program	NA	5/1/2022	12/31/2023	$5,000